

https://dspace.org/

Synthesis and spectroscopic characterization of soluble mixed-ligand diruthenium complexes: potential application as anti-cancer agents.

Mashiloane, Karabo

2018

https://hdl.handle.net/10539/24928

Mashiloane, Karabo Concious (2018) Synthesis and spectroscopic characterization of soluble mixed-ligand diruthenium complexes: potential application as anti-cancer agents, University of the Witwatersrand, Johannesburg, https://hdl.handle.net/10539/24928

Downloaded from a DSpace repository. https://dspace.org/

Synthesis and Spectroscopic Characterization of Soluble Mixed-ligand Diruthenium Complexes; Potential Application as Anti-Cancer Agents.

By
Karabo Mashiloane
455905

A dissertation submitted to the faculty of science, in partial fulfilment of the requirements for the award of Master of Science degree.



School of Chemistry
Faculty of Science

Supervisors: Dr Juanita Van Wyk
University of the Witwatersrand

Dr Siyabonga Ngubane
University of Cape Town

Declaration

I declare that the thesis, **Synthesis and Spectroscopic Characterization of Soluble Mixed-ligand Diruthenium Complexes; Potential Application as Anti-cancer Agents**, is my work and that all the information sources used have been referenced and that this work has not previously been submitted to another institution for examination.

_____on this_____ day of _____

Candidate

Acknowledgements

- I would like to thank God, the creator of it all for giving me the spirit of resilience, wisdom and understanding. This research would have been impossible without him.
- Dr Juanita Van Wyk and Dr Siyabonga Ngubane, thank you for your professional guidance and support throughout the research project and advice that shaped this dissertation.
- Thato Medupe, thank you for doing anti-cancer screening of the ruthenium complexes for me, your help is greatly appreciated.
- To mom and dad, Lindah and Calvin Mashiloane, thank you for your prayers, encouragement, love and support.
- Thankful for my beautiful sisters Kgomotso and Lerato Mashiloane, your love and support kept me going.
- To Dr Lerato Hlekelele, thank you for taking time out of your busy schedule to proof-read my work, I am grateful.
- To the Wits inorganic chemistry research group, thank you for the positive criticism during presentations and for the useful discussions.
- Lastly, to the National research foundation (NRF) for funding this project.

Presentations

The work presented in this dissertation has been presented at a conference as shown below:

- Mashiloane, K. C. **Synthesis and Spectroscopic Characterization of Soluble Mixed-ligand Diruthenium Complexes**. *Oral presentation*, held at the PerkinElmer offices in Midrand, Johannesburg, 15 November 2016.

List of abbreviations and symbols

OAc	Acetate
Hap	Anilinopyridinate
ATO	Arsenic trioxide
λ	Chemical shift
CV	Cyclic voltammetry
°C	Degree Celsius
DNA	Deoxyribonucleic acid
$CDCl_3$	Deuterated chloroform
DMSO	Dimethyl sulfoxide
e^-	Electron
eV	Electron Volt
EtOH	Ethanol
H(Fap)	Fluoroanilinopyridinate
FTIR	Fourier transform infrared spectroscopy
g	Grams
$E_{1/2}$	Half potential
Hz	Hertz
HOMO	Highest occupied molecular orbital
i-PrOH	Iso-propanol
LUMO	Lowest unoccupied molecular orbital
L	Ligand
MS	Mass spectrometry
m/z	Mass to charge ratio
H(Meap)	Methylanilinopyridinate
MeOH	Methanol
µs	Micro siemens
ml	Millilitre
mV	Millivolts
M	Molar
M_w	Molecular weight
nm	Nanometre

NMR	Nuclear magnetic resonance
ppm	Parts per million
AgCl	Silver(I) chloride
$AgBF_4$	Silver(I) tetrafluoroborate
TBACl	Tetrabutylammonium chloride
TBAP	Tetrabutylammonium perchlorate
TEABr	Tetraethylammonium bromide
THF	Tetrahydrofuran
TLC	Thin layer chromatography
UV/Vis	Ultra Violet Visible Spectroscopy
V	Volts

Contents

Section Page

Declaration i

Acknowledgements ii

Presentations iii

List of abbreviations and symbols iv

List of figures ixx

List of schemes and tables xii

Abstract xii

CHAPTER 1: LITERATURE REVIEW……...1

1.1 Introduction 1

1.2 Platinum-based metallodrugs 4

1.3 Ruthenium based metallodrugs 6

1.4 Dinuclear ruthenium complexes 11

1.5 Mixed-ligand diruthenium complexes. 15

1.6 Aims and objectives 20

1.7 References 21

CHAPTER 2: RESULTS & DISCUSSION……25

2.1 Introduction 25

2.2 Results and discussion 27

2.2.1 Synthesis and characterization of substituted anilinopyridinate ligands. 27

2.2.1.1 Nuclear magnetic resonance of anilinopyridinate ligands. 28

2.2.1.2 Characterization of substituted anilinopyridinate ligands with FTIR. 30

2.2.1.3 Mass spectrometry and elemental analysis of anilinopyridinate ligands. 32
2.2.2 Synthesis and characterization of mixed-ligand diruthenium complexes. 33
2.2.2.1 Characterization of mixed-ligand diruthenium complexes with FTIR. 38
2.2.2.2 Mass spectrometry + CHN analysis of diruthenium complexes. 39
2.2.2.3 UV/Visible spectroscopy of diruthenium complexes. 41
2.3 $Ru_2(OAc)_3(L)Cl$ with excess halides 43
2.4 Halide abstraction experiments 46
2.4.1 UV/Visible spectroscopy of cationic diruthenium complexes. 47
2.5 Conductivity studies 49
2.6 Conclusions 49
2.7 Experimental 50
2.7.1 Materials and instrumentation 50
2.7.2 Ligand synthesis 51
2.7.2.1 Synthesis of Hap 51
2.7.2.2 Synthesis of H(2-Meap) 51
2.7.2.3 Synthesis of H(2-Fap) 52
2.7.3 Complex synthesis 52
2.7.3.1 Synthesis of $Ru_2(OAc)_4Cl$ 52
2.7.3.2 Synthesis of $Ru_2(OAc)_3(ap)Cl$ 53
2.7.3.3 Synthesis of $Ru_2(OAc)_3(2\text{-Meap})Cl$ 53
2.7.3.4 Synthesis of $Ru_2(OAc)_3(2\text{-Fap})Cl$ 53
2.8 References 55

CHAPTER 3: ELECTROCHEMISTRY……57

3.1 Introduction 57
3.2 Results and discussion 58
3.2.1 Redox activity of $Fe(C_5H_5)_2$ at electrode surface 58
3.2.2 Electrochemistry analysis of Ru_2^{5+} diruthenium complexes. 60
3.2.3 Characterization of $Ru_2(OAc)_3(2\text{-Fap})Cl$ by cyclic voltammogram 61

3.3 Conclusions 65
3.4 Experimental 65
3.4.1 Material and instrumentation 65
3.5 References 67

CHEMISTRY: APPLICATION……69

4.1 Introduction 68
4.2 Cytotoxicity studies of mono-substituted diruthenium complexes 69
4.3 Conclusions 72
4.4 Experimental 73
4.4.1 Material and instrumentation 73
4.4.2 Cytotoxicity assays 73
4.4.2.1 24-hour treatment 73
4.4.2.2 Statistical analysis 74
4.5 References 75

CHAPTER 5: SUMMARY & FUTURE WORK ……...77

6.1 Appendix 78

List of figures

Figure 1.1:	Structure of Arsenic trioxide (ATO).....	2
Figure 1.2:	Chemical structures of Cisplatin, Carboplatin and Oxaliplatin.....	5
Figure 1.3:	The ligand exchange rates of selected transition metals.....	6
Figure 1.4:	The oxidation state modifications of ruthenium in cancerous and healthy cell…….	7
Figure 1.5:	Description of the selective uptake by the cancer cells…….	8
Figure 1.6:	Illustration of modes of binding, intercalation, groove binding and threading binding……...	9
Figure 1.7:	Chemical structures of NAMI-A and KP1019.....	11
Figure 1.8:	Examples of symmetrical or unsymmetrical ionic bridging ligands with varied donor groups…….	12
Figure 1.9:	The structural representation of a diruthenium tetracarboxylate $[Ru_2(OAc)_4Cl]$	13
Figure 1.10:	Diagram of the molecular orbitals of a Ru_2^{5+}dimetal core.....	14
Figure 2.1:	Possible geometric isomers of mixed-ligand diruthenium complexes…….....	26
Figure 2.2:	Substituted anilinopyridinate ligand systems investigated in this study……	27
Figure 2.3:	^{1}H NMR spectrum of H(2-Meap) in $CDCl_3$	29
Figure 2.4:	^{13}C NMR spectrum of H(2-Meap) in $CDCl_3$.....	30
Figure 2.5:	FTIR spectrum of H(2-Meap)	31
Figure 2.6:	Mass spectrum of H(2-Meap)	32
Figure 2.7:	UV/Visible spectrum of $Ru_2(OAc)_x(Fap)_{4-x}Cl$ in CH_2Cl_2.....	34

Figure 2.8: Monitoring of $Ru_2(OAc)_3(2\text{-Fap})Cl$ by UV/Visible spectroscopy at room temperature…….. 36

Figure 2.9: Structures of the synthesized complexes, $Ru_2(OAc)_3(ap)Cl$, $Ru_2(OAc)_3(2\text{-Meap})Cl$ and $Ru_2(OAc)_3(2\text{-Fap})Cl$……..... 38

Figure 2.10: FTIR spectra of free ligand, Hap and mixed-ligand complex, $Ru_2(OAc)_3(ap)Cl$..... 39

Figure 2.11: Mass spectrum of $Ru_2(OAc)_3(2\text{-Meap})Cl$..... 40

Figure 2.12: UV/Visible spectra of $Ru_2(OAc)_3(ap)Cl$ and $Ru_2(OAc)_3(2\text{-Meap})Cl$, $Ru_2(OAc)_3(2\text{-Fap})Cl$ in neat CH_2Cl_2……..…… 43

Figure 2.13: UV/Visible spectra of $Ru_2(OAc)_3(ap)Cl$, $Ru_2(OAc)_3(2\text{-Meap})Cl$ and $Ru_2(OAc)_3(2\text{-Fap})Cl$ in neat CH_2Cl_2 (black), TBACl (red) and TEABr (blue)..... 45

Figure 2.14: UV/Visible spectra of $Ru_2(OAc)_3(ap)Cl$ in i-prOH, $Ru_2(OAc)_3(2\text{-Meap})Cl$ in *i*-prOH and $Ru_2(OAc)_3(2\text{-Fap})Cl$ in etOH after reacting with $AgBF_4$..... 48

Figure 3.1: Cyclic voltammogram of Ferrocene..... 59

Figure 3.2: An anodic current vs scan rate straight-line graph of ferrocene..... 60

Figure 3.3: Oxidation cyclic voltammograms of $Ru_2(OAc)_3(2\text{-Fap})Cl$ in CH_2Cl_2 containing 0.10 M TBAP at 0.10 V/s scan rate..... 62

Figure 3.4: Reduction cyclic voltammogram of $Ru_2(OAc)_3(2\text{-Fap})Cl$ in CH_2Cl_2 containing 0.10 M TBAP at 0.10 V/s scan rate..... 63

Figure 4.1 Survival rate of MCF7 cell lines treated with Ru_2 metallodrugs (5 µM) for 24 & 48 hours……. 72

Figure 4.2: Survival rate of MCF7 cell lines treated with Ru_2 metallodrugs (10 µM) for 24 & 48 hours……. 72

List of schemes and tables

Scheme1.1: Diagram indicating the structures of the complexes in the $Ru_2(OAc)_x(Fap)_{4-x}Cl$, (x = 0-3) series..... 16

Table 1.1: UV/Visible Spectral Data of the (4,0) and (3,1) Isomers of $Ru_2(L)_4Cl$, Where L Is 2-CH_3ap, ap, 2-Fap, 2,5-F_2ap, 2,4,6-F_3ap, 2,6-F_2ap, and F_5ap, in CH_2Cl_2 Containing 0.2 M TBAP..... 18

Scheme 2.1: General synthetic route of the anilinopyridinate ligands..... 28

Scheme 2.2: Stepwise metathesis displacement..... 33

Table 2.1: UV/Visible peaks of the synthesized complexes..... 43

Scheme 2.3: Modification of a substituted diruthenium complex..... 47

Scheme 3.1: Reaction mechanism of $Ru_2(OAc)_3$(2-Fap)Cl…… 64

Abstract

Three mixed-ligand metal-metal bonded complexes containing one unsymmetrical anionic bridging ligand were successfully synthesized and characterized as to their electrochemical and spectroscopic properties. The investigated mono-substituted diruthenium complexes have the general formula, $Ru_2(OAc)_3(L)Cl$, where OAc = acetate anion and L = anilinopyridinate bridging ligand (ap, 2-Meap, 2-Fap). UV/Visible spectroscopy studies reveal that the investigated diruthenium complexes exist in the forms $Ru_2(OAc)_3(L)Cl$ and $[Ru_2(OAc)_3(L)]^+$ in solution. The two forms are observed as a split band in the 500 – 700 nm visible region. A collapse of one band is seen upon reaction of the complexes with excess halide (Cl^-, Br^-) indicating an equilibrium shift towards the neutral species in solution, whereas a reaction with $AgBF_4$ precipitates the chloride as the AgCl salt, leaving only the cationic species in solution. Electrochemical characterization of the mixed-ligand diruthenium complexes conclusively reveals a stable Ru_2^{5+} oxidation state in all three complexes. Upon an applied potential in a non-coordinating solvent, each complex undergoes a reversible one-electron oxidation and reduction process accessing the Ru_2^{6+}, and Ru_2^{4+} oxidation states respectively. The treatment of human breast adenocarcinoma MCF-7 cells with these water-soluble complexes results in a less than 50 % cell survival. This demonstrates significance of solubility in the development of metallodrugs for cancer treatment.

Chapter 1

Review of metal compounds; potential applications as anti-cancer agents

1.1 Introduction

The search for an organometallic compound with improved biological properties gained momentum since the discovery of a precious metal, platinum in the 1960s.[1] Included in the search were metals such as gold (Au), which was used in the treatment of cancer, as well as rheumatoid arthritis; silver (Ag) useful as anti-microbial agents.[1]At the time, the platinum metal was very rare and therefore was believed to benefit health related issues.[2]

With time and in-depth research on the metal, medical properties of platinum compounds were then linked to specific biological properties.[3] The explanation of the mode of action of the platinum metal is however complex, therefore, the exact route activity for most drugs is still unknown.[2] Scientists have now resorted to solving the mechanism of action of these drugs step by step and the results are then used to design an anti-cancer drug with improved potency and little to no side effects.[3]

The most studied and well knownorganometallic complexes consist of metals that belong to the platinum group metals, as they displayed anti-cancer activities.[4] The unpremeditated discovery of anti-cancer properties of cisplatin paved a way for research into other platinum complexes to be used in cancer therapy.[4] Platinum drugs are still used in clinics and more drugs are still undergoing clinical trials not just to treat cancer but other diseases such as parasitic and bacterial infections.[5] Although some of the compounds have not been clinically approved, uses of other metals of the platinum, gold and silver group in medicine include; anti-cancer, dental alloys, microbial, anti-HIV, bronchial asthma and rheumatoidarthritis.[5]

Applications of metal drugs as anti-cancer agents stems from 1965, when Rosenberg accidentally discovered the activity of a platinum compound cisplatin, [(cis-$Pt(NH_3)_2Cl_2$].[6] Since then, metal based compounds became an area of research due to their material, catalysis and optical properties which led to applications in medicinal fields.[7]In medicine, interest in metal compounds arises from the remarkable

effectiveness of the platinum-based compound cisplatin, [(cis-Pt(NH_3)$_2$$Cl_2$] and its analogues for the treatment of testicular, ovarian, head and lung cancer, of which the cure rate was found to be greater than 90% in testicular cancer cases.[8] Cancer remains chronic because in spite of current medical interventions, no cure has been found and some anti-cancer drugs are not effective over a wide range of cancers.[9,10] In 2012, the globocan project of the world health organization (WHO) reported that cancer had resulted in about 8.8 million deaths world-wide.[11]Furthermore, it is amongst the top twenty causes of deaths in South Africa claiming about 14 % of the population.[11]

Although cisplatin is effective over a wide range of cancers, it is limited by its toxicity, poor solubility and the fact that it targets normal cells over those of cancerous cells.[12] In addition; it was found that cancer had become resistant towards the cisplatin drug; this was due to the changes in cellular uptake, efflux and increased detoxification of the drug.[13]

Metals such as arsenic, cadmium and lead were also found to be highly reactive and used as therapeutic agents; however, they were limited by their high toxicity.[13,14,15] Arsenic trioxide (ATO) (figure1.1) is the only non-platinum compound that has been approved for clinical use thus far.[13] This drug was used before and was re-discovered in 1997 when there were reports on complete remissions in Acute Promyelocytic leukaemia (APL) patients.[14,15] The compound as an anti-tumour drug was approved in 2000 by the FDA for the treatment of APL. Evaluation of ATO for the therapy of other cancers is still taking place.[16]

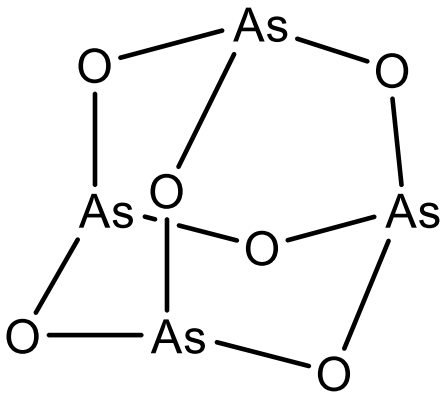


Figure 1.1: Structure of Arsenic trioxide (ATO).[13]

The arsenic trioxide compound works on particular proteins within the cell which speeds up the death of leukaemia cells at the same time encouraging normal blood cells to develop properly.[17] This drug is administered through a drip into the arm and the drip lasts for about 1-2 hours. Its mode of action is not fully understood but speculations are that it causes cell death of leukaemia cells via DNA fragmentation.[18] Furthermore, it damages the fusion promyelocytic leukaemia (PML).[17,18] The function of arsenic trioxide is therefore to treat acute promyelocytic leukaemia by stopping the growth of cancer cells.[18]

Side effects of the compound include QT prolongation, meaning that the heart muscles take longer to recharge between beats due to an electrical disturbance and this is capable of causing serious heart rhythm problems.[17] This compound may also result in unusual bruising or bleeding, decreased urination, hives and seizures, swelling of the arms and headaches.[17]

This has compelled the development of new effective metal compounds as anti-cancer agents. Various non-platinum antitumor agents such as dinuclear carboxylate species of rhodium (Rh),[19] rhenium (Ir)[20] and ruthenium (Ru)[21] have been reported over the past few years. Rh(III) and Ir(III) complexes containing bidentate aromatic ligands have shown that high cytotoxicity in cancer cells can be achieved by selection of a prudent ligand.[22] The exact mechanism of how the compound targets the cells is not known, however, these compounds have been reported to induce cell death through an intrinsic mitochondrial pathway.[23]

In spite of the fact that the octahedral rhodium and iridium complexes show promise as anti-cancer agents, the cytotoxicity of these complexes strongly depend on the type of ligand coordinated to the dimetal unit.[24] The rate of ligand exchange, accessible oxidation states, as well as the ability of ruthenium to mimic iron during binding to certain biological molecules are what makes ruthenium useful in drug design.[25]

Ruthenium containing complexes that offer reduced toxicity is an area of research that is gaining momentum towards identifying suitable drugs that are highly soluble, and selectively target cancerous cells over normal cells.[19,21] Investigations of anti-cancer agents have suggested DNA as a primary intracellular target.[13]

Recent findings claim that ruthenium complexes have displayed anti-cancer properties *in-vivo* such that by simply changing the ligand environment around the dimetal core, stimulates mechanism of action that does not result in the damage of normal cells.[26]

This chapter is a review of previously investigated metallodrugs and their suggested mode of action. Ruthenium complexes undergoing clinical trials will be discussed as well as dinuclear ruthenium complexes, together with the introduction of anilinopyridinate ligands which were used as substituents in the synthesis of mixed-ligand diruthenium complexes.

1.2 Platinum-based metallodrugs

Platinum is an inert transition metal in Group 10 of the periodic table and is considered a precious metal because it is rare and desirable.[27] The neighbours of this metal include iridium, palladium, ruthenium, osmium and rhodium, hence they are sometimes called platinum group metals.[27] The five metals are best known for their catalytic properties and are used to make compounds that end up as drugs, synthetic fibers and used in pharmaceuticals.[27]

The metallodrugs research was incited by the discovery of anti-cancer properties of platinum by Rosenberg, where running the electric current using the platinum electrode killed *E-coli*.[28,29] This observation sparked interest in the precious metal platinum and led to the synthesis and testing of a series of platinum based compounds such as, [(cis-$Pt(NH_3)_2Cl_2$], known as cisplatin.[29] In all the effort throughout the years, there has only been 2 world-wide drug approvals for platinum containing drugs which are carboplatin, discovered in 1992 and oxaliplatin, discovered in 2002 (figure 1.2).[7] The approved drugs are both direct analogues of cisplatin.

Pt(II) is a soft metal ion with a strong affinity for soft ligands such as sulfur.[30] Once cisplatin is administered, the Pt metal gets removed by sulphur containing ligands such as (N-acetyl-L-cysteine)glutathione in the system.[30] The suggested mode of action of cisplatin (figure 1.2 (1)) is that the chloride ligands get hydrolyzed within the cell and this generates a bis-aqua species which then irreversibly binds to DNA.[8]

This action inhibits cell replication resulting in controlled cell death, known as apoptosis.[8] This compound forms inter and intra strand cross links in the DNA which in turn prevents DNA replication and transcription, resulting in cell death.[31]

Carboplatin differs from cisplatin as it has a bidentate dicarboxylate instead of two chloride ligands which exchange with water molecules *in-vitro*.[31] Carboplatin (figure 1.2(2)) forms the same products as cisplatin *in-vitro*, even though it was found to exhibit lower and slower reaction DNA binding kinetics.[31] Oxaliplatin contains bidentate ligands, 1,2-diaminocyclohexane in place of the monodentate aniline ligands (figure 1.2 (3)).

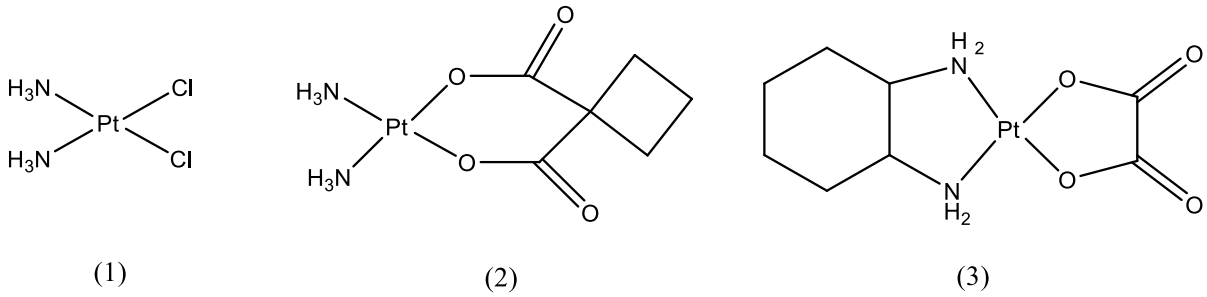


Figure 1.2: Chemical structures of Cisplatin (**1**), Carboplatin (**2**) and Oxaliplatin (**3**).[7]

The side effects of previously investigated anti-cancer drugs and their unknown mechanism of action necessitated the search for improved compounds as anti-cancer drugs. Members of the platinum group such as ruthenium, rhodium, palladium, osmium and iridium have since been investigated.

Platinum-based compounds are still regarded as the most successful chemotherapy agents, with an estimated 70 % of patients receiving the compound as part of the treatment.[32] While cisplatin is effective over a wide range of cancers, the clinical application of cisplatin is hampered by its high toxicity and poor solubility *in-vivo*.[33] Moreover; it was impeded by side effects such as nerve damage, hair loss and nausea.[7] Platinum–based drugs used in chemotherapy are now known to also target normal cells resulting in normal cell damage.[32,33] These shortcomings along with other disadvantages of the use of cisplatin has driven research towards different strategies in the development of new metal based anti-cancer agents with different modes of action.[34]

1.3 Ruthenium based metallodrugs

During the evaluation of ruthenium complexes as anti-cancer drugs, it was discovered that they exhibit similar ligand exchange kinetics as Pt(II) complexes.[34] The interaction of the metal drug with macromolecules such as proteins and H_2O is an important factor.[34] This is because it induces the desired therapeutic properties of the complex.[34] The rate of ligand exchange of ruthenium compounds depends on the concentration of exchanging ligands in the media.[35]

Ruthenium metal, amongst the platinum group, has oxidation states Ru(II), Ru(III) and Ru(IV) which are all accessible under physiological conditions.[36] In addition, there is a low energy barrier between the accessible oxidation states making it easier to interconvert between the oxidation states when inside the cell.[36] Ruthenium also displays a relatively slow ligand exchange rate between $10^{-4}/10^{-2}$ S^{-1} in water (figure 1.3).[36] The kinetics of ruthenium is on the timescale of cellular reproduction, this means that when ruthenium binds to a bio-molecule in the cell, there is a high chance that it remains bound for the remainder of the cells lifetime.[36]

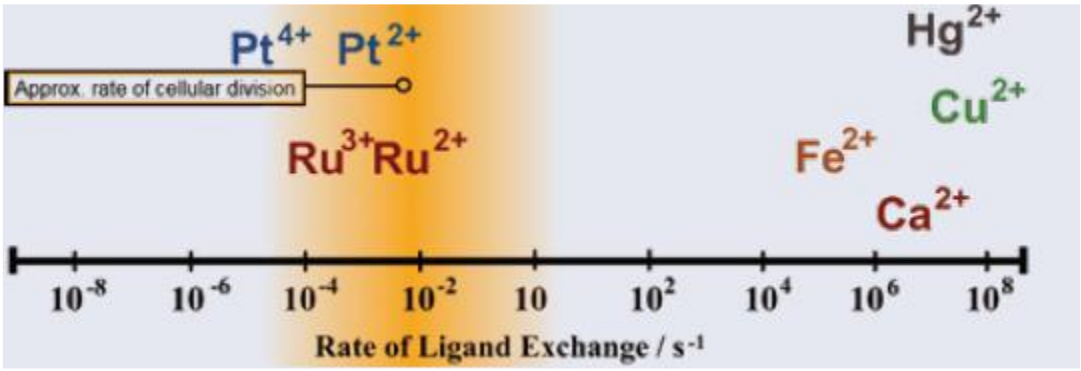


Figure 1.3: The ligand exchange rates of selected transition metals.[36]

The molecular geometry of ruthenium metal complexes have an octahedral geometry and Ru(III) complexes are more biologically inert than Ru(II) and Ru(IV) complexes.[35] Furthermore, the redox potential of ruthenium complexes can be changed by varying ligands.[35] Once the ruthenium compound is administered, ascorbates and other single electron transfer proteins can reduce Ru(III) and Ru(IV) or oxidise Ru(IV) by cytochrome oxidases (figure 1.4).[1] These are important properties of ruthenium

compounds because effective and improved drugs in clinic can be designed by exploiting the redox potentials of the ruthenium complexes.

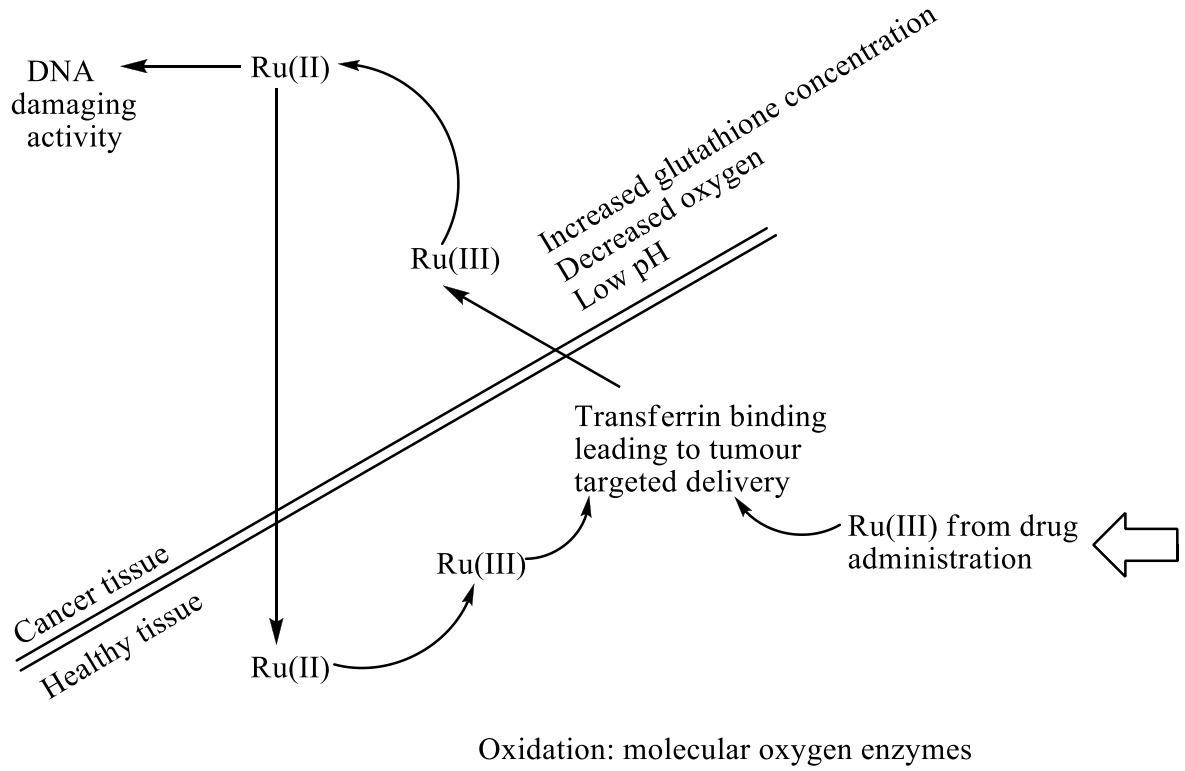


Figure 1.4: The oxidation state modifications of ruthenium in cancerous and healthy cells.[1]

Ruthenium compounds promise to exhibit less to no toxicity properties and this can be attributed to its ability to mimic iron in binding to biomolecules such as serum transferrin and albumin.[37] Cancerous cells have a greater requirement for iron; therefore, they increase the number of transferrin receptors in the cell surface, in that way segregating the circulating metal-loaded transferrins as shown in figure 1.5.[37]

Figure 1.5 shows a schematic representation of selective uptake of transferrin by cancer cells and because the drug is designed to target cancerous cells, its toxicity gets reduced as only a small amount of it reaches healthy cells.[1,37] This is due to the fact that metal-loaded transferrin gets delivered according to the number of transferrin receptors on their surfaces.[1]

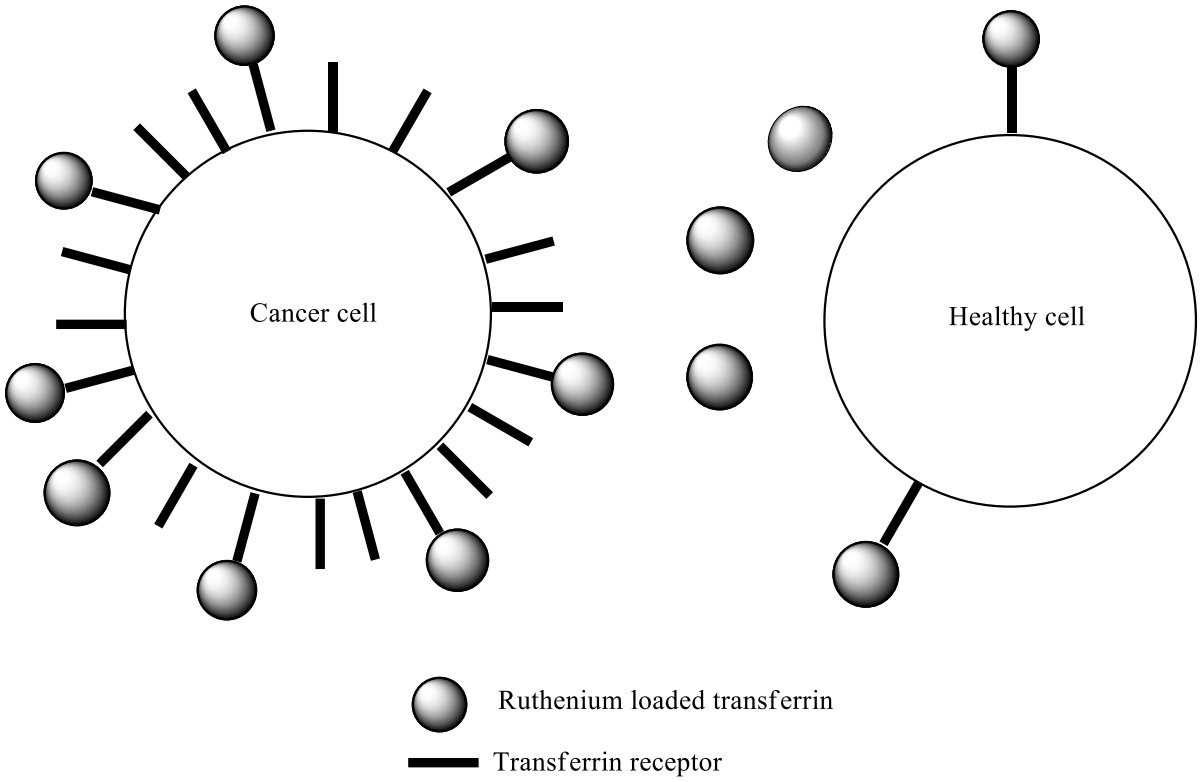
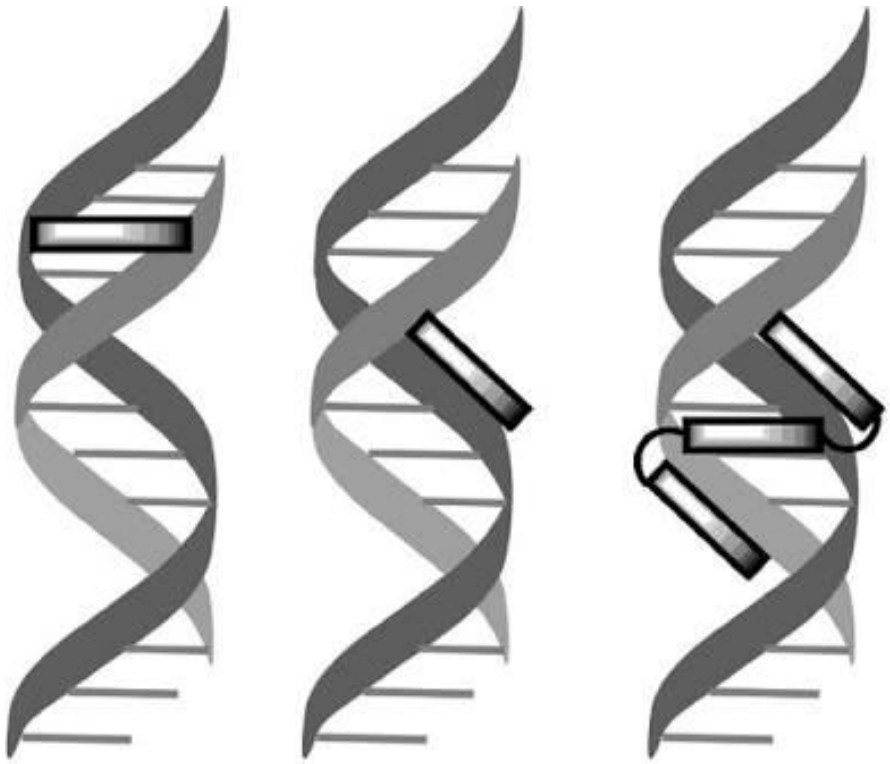


Figure 1.5: description of the selective uptake by the cancer cells.[1]

Ruthenium based-compounds have been developed and tested against cancer cell lines and were found to have fewer side effects compared to cisplatin.[21,33] In addition, their properties such as activation by reaction and the great coordination to cellular ligands make them to be well suited towards pharmaceutical applications.[38,39] The speculation of the possible binding mode of DNA to ruthenium is that the molecule gets inserted between the DNA base pairs.[40]

The application of ruthenium compounds as anti-cancer agents requires a precise understanding of the agents` mechanism of interaction with the molecule that is targeted, double helix DNA.[41] There are two possible ways that DNA binding agents can interact with the host molecule and this is through a groove-binding fashion, which is stabilized by a mixture of hydrophobic, electrostatic and hydrogen-bonding interaction as shown in figure 1.6.[41] Another mode of binding is through an intercalative association whereby a planar, hetero aromatic moiety slides between the DNA based pairs.[40] This type of binding is known as intercalation and applies to ruthenium compounds that contain planar fused aromatic ligands, an example of intercalation

association is illustrated in figure1.6(a).[40] The insertion results in the π-electron overlap of the aromatic ligands of the compounds with the base pair.



(a) (b) (c)

Figure 1.6: Illustration of modes of binding, intercalation (**a**), groove binding (**b**) and threading binding (**c**).

Studies show that Interaction of ruthenium with DNA can be monitored by changes in plasmid electrophoretic mobility[42], such that alteration of the mobility would imply disturbance of the DNA by a ruthenium compound.[42] Menendez *et al* successfully synthesized a series of mono-ruthenium complexes containing planar aromatic bridging ligands.[42] From the *in-vitro* experiment, it was found that mono-ruthenium compounds showed great solubility in aqueous media and interacted with plasmid DNA for the different enantiomers.[42]

Ruthenium containing complexes show promise in anti-cancer activity *in-vivo* and *in-vitro*.[42] So far, there are two ruthenium compounds which have entered clinical evaluation and that is, NAMI-A(imidazolium trans-(tetrachloro(dimethyl

sulfoxide)(imidazole) ruthenate (III)[43] and KP1019 (indazolium trans-(tetrachlorobis(1H-indazole)ruthenate (III)[44] (figure 1.7). These compounds contain ligands that can be hydrolysed and this leads to a chloride-water substitution reaction.[45]

Due to hydrolysis, the actual active molecules that reach cancer cells become different from the molecular structures shown in figure 1.7.[46] The investigated compounds, **4** and **5** appeared to be quite similar structurally, both having the III oxidation state with chloride, heterocyclic ligands and a heterocyclic counter ion, however, have shown great display of different types of anti-cancer activity.[46]

KP1019 was found to be active against the main tumour mass that forms first in a patient, known as primary cancer. It was reported that this compound is highly active against colon cancer.[19] **4** is active against the metastases that forms after cells from the primary tumour have moved to a different organ via the blood stream, and these are secondary tumour cells.[19] The two complexes are promising as anti-cancer agents as they have shown a high tolerance in clinical phase trials with low side effects more especially **5**.[43,44]

4 and **5** are both mono-ruthenium compounds with the Ru(III) oxidation state and there is still research going on for the mono-ruthenium complexes.[44] Following the Ru(III) compounds are the Ru(II) organometallic compounds with arene ligands which are still undergoing pre-clinical evaluation.[47] Ruthenium based compounds have shown highly promising anti-cancer activity cells both in animals and humans.[45]

Although some mono-ruthenium compounds exhibit anti-cancer properties, little knowledge is known about their exact mode of action,[48] therefore, this has urged chemists to synthesize and test a series of novel complexes in order to elucidate the modes of action. What is known about the mode of action of these compounds is that it targets the DNA.[47] In addition, their induced damage as well as their pharmacological and chemical behaviour was found to be different from those of platinum-based drugs.[47] This suggests that there could be additional cellular targets*in-vitro*.[47]

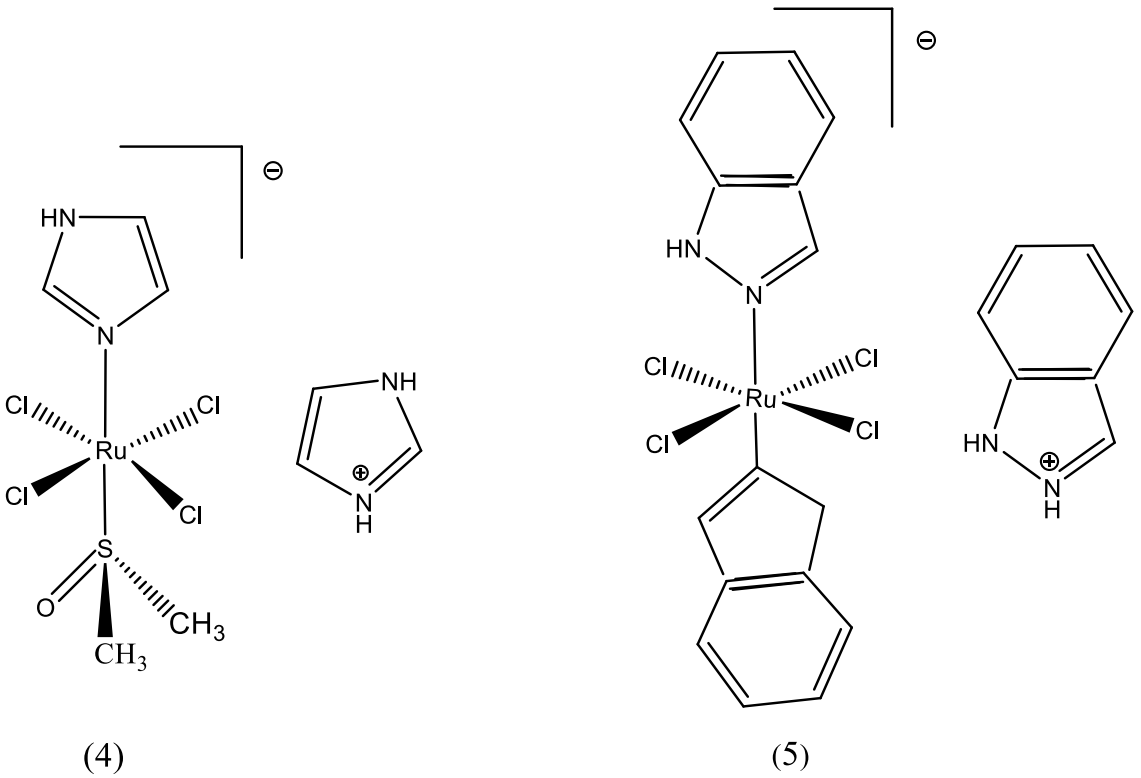
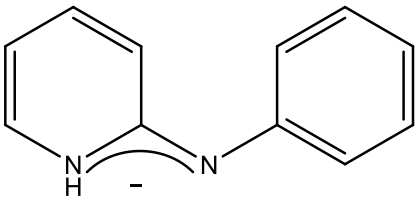


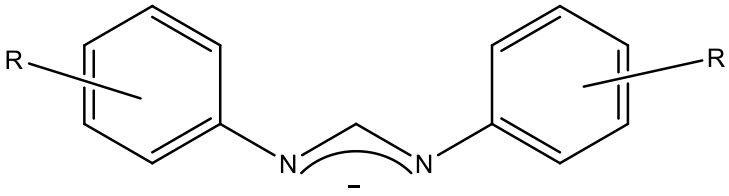
Figure 1.7: Chemical structures of NAMI-A (**4**) and KP1019 (**5**)

1.4 Dinuclear ruthenium complexes

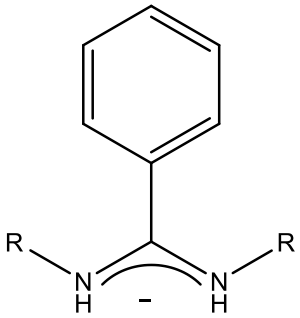
Metal-metal bonded complexes herein referred to as the dinuclear ruthenium complexes, have ignited growing interest since the discovery of the first dimetal complex, $Re_2Cl_8^{2-}$.[49] This complex was unusual in that it had multiple bonds between metals with no supporting equatorial bridging ligands. Following the discovery of $Re_2Cl_8^{2-}$, several other multiple bonded metal-metal complexes of ruthenium, rhenium, rhodium, molybdenum, platinum, iron, iridium, palladium and vanadium were reported in the literature.[13]The multiple metal-metal bonds are typically supported by O, O'(acetates), N, O' (hydroxypyridinates and oxopyridinates) or N, N' (pyridinates and formamidinates) equatorial bridging ligands. Examples of some of these ligands are illustrated in figure 1.8.



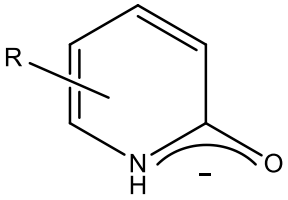
Anilinopyridinate (ap)



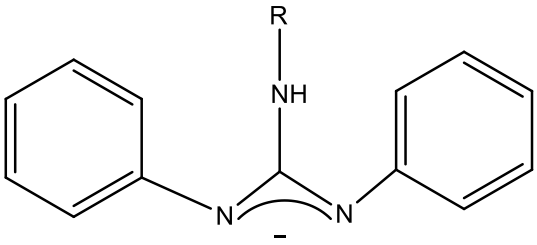
Diphenylformamidinate (dpf)



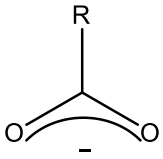
Benzamidinate



Hydroxypyridinate



Guaninidinate



Acetate anion

Where R = Alkyl or aryl subtituents

Figure 1.8: Examples of symmetrical or unsymmetrical ionic bridging ligands with varied donor groups.

In 1966, the structure of $Ru_2(OAc)_4Cl$, (OAc = an acetate bridging anion) was first reported by Stephenson and Wilkinson.[50] Subsequent work led to the characterization of the diruthenium tetracarboxylate having a paddle-wheel geometry as illustrated in figure 1.8.[50] Cotton and Co-workers provided evidence that the Ru-Ru bond is strong with a bond order of 2.5 and a short distance of 2.281(4) Å.[51]

A detailed computational analysis of the paddlewheel complexes with a Ru_2^{5+}dimetal unit led to a proposed electronic configuration of $(\delta)^2(\pi)^4(\delta)^2(\delta^*\pi^*)^3$.[40]

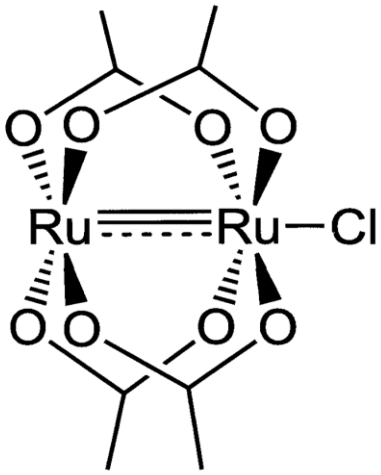


Figure 1.9: The structural representation of a diruthenium tetracarboxylate, $Ru_2(OAc)_4Cl$.[40]

Their unique physical and electronic properties are liable for the expansion of diruthenium complexes and analogous compounds.[52,53] Nowadays, the most investigated metal-metal complexes are mixed with nitrogen containing bridging ligands and are formulated in their neutral form as $Ru_2(L)_4Cl$ or $Ru_2(OAc)_{4-x}(L)_xCl$, where L is a symmetrical or unsymmetrical anionic bridging ligand (Chart 1.1). The deviation from diruthenium tetracarboxylates to mixed-ligand diruthenium complexes, is largely due to the fact that the order of the molecular orbitals of the metal centre varies with changes in the type of the equatorial ligands.[54]

The diruthenium complex has two oxidation states, one with the Ru(III) and the other with Ru(II) oxidation state. However, these atoms are chemically equivalent and are therefore represented as Ru_2^{5+}which is the overall oxidation state.[51] A diagram of the Ru_2^{5+} dimetal core with 11 electrons placed in a molecular orbital is shown below (figure 1.9). There are three unpaired electrons and a very small energy gap between the δ^* and π^* orbital thus favouring the high spin 3/2 configuration.

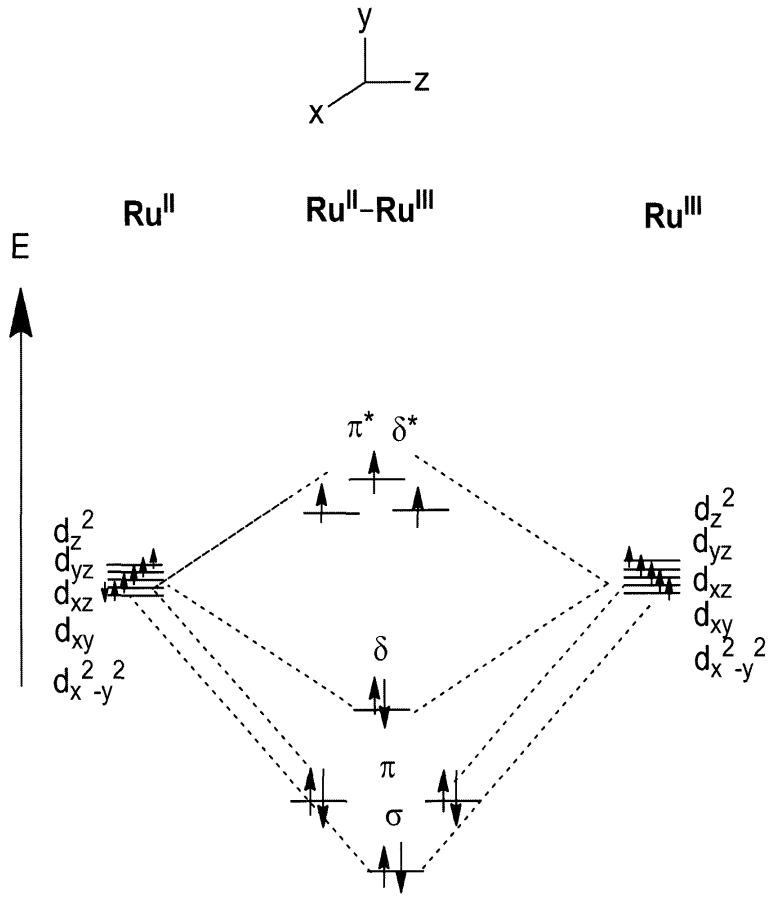


Figure 1.10: Diagram of the molecular orbitals of a Ru_2^{5+}dimetal core.[51]

Mixed-valent tetracarboxylate diruthenium complexes were found to be only moderately active against P388 lymphocytic leukaemia cell lines.[19] There was therefore a need to exploit this class of complexes by introducing ligands that greatly enhances their solubility. This was done by introducing nitrogen containing ligands towards the synthesis of a series of mixed-ligand diruthenium complexes.

The anionic bridging ligands introduced were found to have an impact on the dimetal core of the complex, in such a way that the metal centre varies with the changes in the type of the axial and equatorial ligands.[54] Varying the ligand types were found to also affect the redox potential, electronic configuration and the chemical reactivity of the diruthenium complexes in their different oxidations states.[54] The importance of pyridine ligands over acetate bridging ligands is that the dimetal unit of the compound can be tuned via ligand design.

1.5 Mixed-ligand diruthenium complexes.

Previously investigated diruthenium complexes such as $Ru_2(OAc)_4Cl$ were found to be moderately soluble in aqueous media.[45] In anti-cancer studies, the solubility of a compound is an important factor as it has an impact on the biological activity.[55] It was therefore important to modify mixed-ligand diruthenium complexes and make them suitable for application in medicinal field.

Diruthenium complexes having the general formula, $[Ru_2L_4]^{n+}$, where L is defined as an unsymmetrical bridging ligand and n = 0 or 1, have four possible isomer types, namely, (4,0), (3,1), (2,2)-*cis* and (2,2)-*trans* (chapter 2, chart 2.1).[56] However, most diruthenium complexes have been isolated as (4,0) or (3,1). The significance of pyridine and anilinopyridine based ligands is that they have been isolated as discrete molecules in the solid state.[57]This is a different behaviour to the complexes with N,O' and O,O' ligands that form polymeric structures.[58]

Kadish *et al* [59] synthesized a series of diruthenium complexes containing the ap-type bridging ligands according to eqn 1. The synthetic procedure involves the melt reaction of a substituted anilinopyridinate ligand with a tetracarboxylate diruthenium complex which could proceed for 4 - 15 hours depending on the type of the bridging ligand.

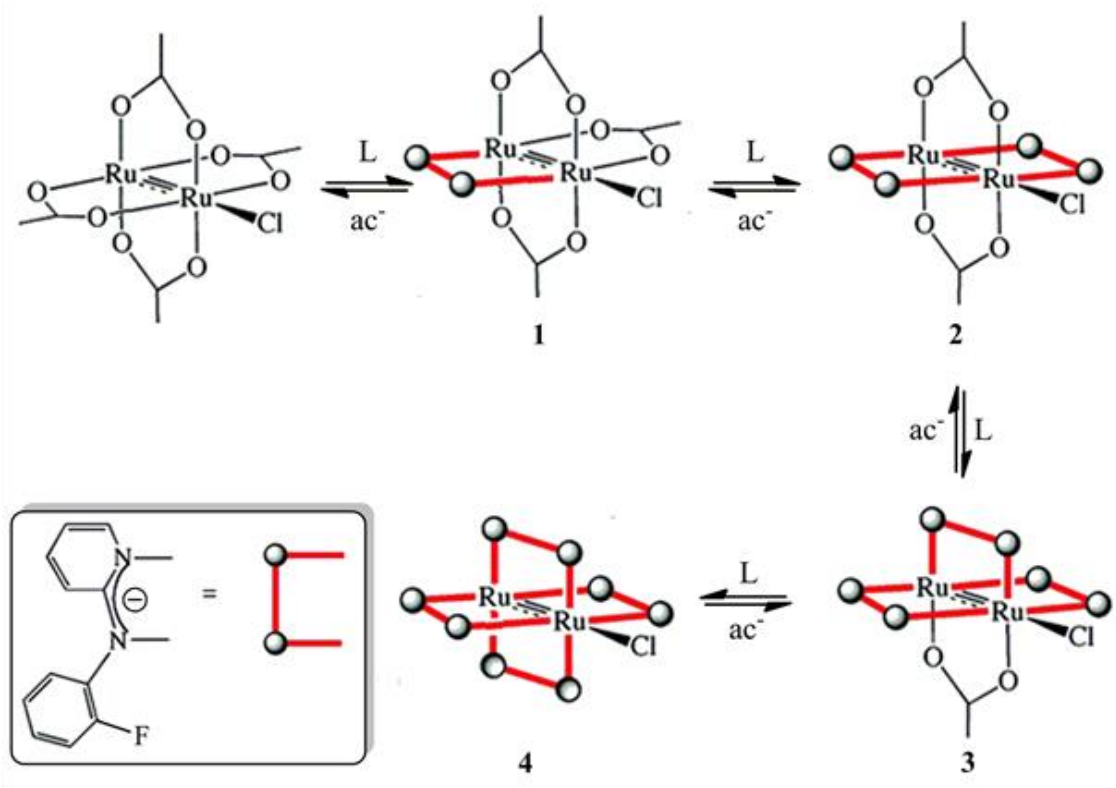
$$Ru_2(OAc)_4Cl + 4HL \longrightarrow Ru_2(L)_4Cl + 4(OAc) \qquad (1)$$

The reaction of the compound, $Ru_2(OAc)_4Cl$ with excess anilinopyridinate bridging ligand results in a stepwise metathesis displacement of the acetate ligand by the incoming ligand (scheme 1.1). The extent of the replacement of the acetate can be altered by varying the reaction conditions such as temperature, reaction time and choice of solvents.[60]For example, in the case of the fluorinated compound, in literature a series of diruthenium complexes with the general formula, $Ru_2(OAc)_x(Fap)_{4-x}Cl$ (x = 0-4) were isolated.[60]

The synthesis of $Ru_2(Fap)_4Cl$ and three lesser substituted mixed-ligand Ru_2^{5+} were synthesized from a single reaction of $Ru_2(OAc)_4Cl$ and H(2-Fap) in refluxing methanol. The yields for a 6 hour reaction under the conditions stated were 30.2, 20.1, 24.2 and 4.8 % obtained for the complexes $Ru_2(Fap)_4Cl$, $Ru_2(OAc)(Fap)_3Cl$, $Ru_2(OAc)_2(Fap)_2Cl$

and $Ru_2(OAc)_3(Fap)Cl$, respectively.[60] The complexes have the Ru_2^{5+} diruthenium core and are shown in scheme 1.1 (1-3).

Furthermore, an isolation of $Ru_2(OAc)(2,4,6\text{-}Me_3ap)_3Cl$ has been isolated from the reaction of $Ru_2(L)_4Cl$ with H(2,4,6-Me_3ap).[61] The findings proved that these types of metal-metal bonded ruthenium complexes lead to a stepwise metathesis displacement reactions. Whereby, it is possible not to only isolate a fully substituted diruthenium complex, $Ru_2(L)_4Cl$ but three more derivatives, $Ru_2(OAc)_2(L)_2Cl$, $Ru_2(OAc)(L)_3Cl$ and $Ru_2(OAc)_2(L)_2Cl$ can be isolated from a single reaction.



Scheme 1.1: Diagram indicating the structures of the complexes in the $Ru_2(OAc)_x(Fap)_{4-x}Cl$, (x = 0-3) series.[60]

Kadish and Bear have reported comprehensive studies on the asymmetric 2-anilinopyridinate, $Ru_2(ap)_4Cl$ and 2-fluoroanilinopyridinate, $Ru_2(Fap)_4Cl$ diruthenium complexes.[57] This series of complexes have been crystallized in either the (3,1) and (4,0) isomer types. The existence of (2,2)-*cis* and (2,2)-*trans* isomeric forms were postulated but compounds have not yet been isolated. The formation of the (4,0) and (3,1) isomer types were attributed to either electronic, steric effects or a combination of the factors.[57]

Diruthenium complexes [$Ru_2(L)_4Cl$] studied previously, with L being anilinopyridinate (ap), fluoroanilinopyridinate (2-Fap), and F_5ap were shown to have different isomeric distributions, this indicates that the steric and electronic effects of the anilinopyridinate ligands play a role in the preferred conformation of the complexes.[56]

Spectroscopic, electrochemical and structural characteristics of mixed ligand diruthenium complexes were analyzed.[59] From the findings, it was concluded that the complexes with 2-Meap and 5-F_2ap as bridging ligands only exist in a (4,0) isomeric form whereas both (3,1) and (4,0) was obtained for the Ru_2(2,4,6-F_3ap)$_4$Cl compound (table 1.1). Previous studies have reported on the effect bridging anilinopyridinate anions with electron donating/withdrawing group at the ortho, meta or para positions of the aniline ring have on the dimetal unit.[59] These compounds have been analyzed as to their spectroscopic, electrochemical and structural properties.[59]

According to the study by Kadish *et al* [59], the number or nature of the ligand affects the geometric isomer of a complex. Moreover, out of the compounds they have studied, the findings are that only those with two substituents at the ortho positions of the phenyl ring exist in more than one isomer.[59] Below is a table with isomeric distributions showing the impact an anilinopyridinate ligand coordinated to the dimetal core has on the isomer type of a complex.[62,63]

Table 1.1: UV/Visible spectral data of the (4,0) and (3,1) isomers of $Ru_2(L)_4Cl$, where L is 2-CH_3ap, ap, 2-Fap, 2,5-F_2ap, 2,4,6-F_3ap, 2,6-F_2ap, and F_5ap, in CH_2Cl_2 containing 0.2 M TBAP

		λ_{max} nm (ε x 10^{-3}, M^{-1} cm^{-1})			
Oxidation state	ligand	Band I	Band II	Band III	Band IV
			(4,0) Isomer		
Ru_2^{6+}	CH_3ap (1)	443(6.9)	530(6.5)		990(15.9)
	2,4,6-F_3ap(2)	432(2.9)	522(3.9)	842(sh)	1033(3.8)
	2,5-F_2ap (5)	413(5.5)	504(5.5)		975(11.2)
	F_5ap		520(6.4)	900(sh)	> 1050
Ru_2^{5+}	CH_3ap	424(4.3)	461(4.7)		764(7.3)
	ap	421(5.8)	452(5.7)		778(7.0)
	2,4,6-F_3ap	412(2.2)	476(2.6)	615(0.7)	895(2.7)
	2,5-F_2ap	422(4.8)	466(5.3)		774(5.8)
	F_5ap		482(5.8)	598(1.1)	910(5.0)
Ru_2^{4+}	CH_3ap		534(3.6)		
	2,4,6-F_3ap		507(1.4)		
	2,5-F_2ap		515(4.1)		
	F_5ap		518(3.2)		
			(3,1) Isomer		
Ru_2^{6+}	2-Fap	431(4.1)	494(3.9)		960(5.2)
	2,4,6-F_3ap	487(5.7)	670(4.4)		965(9.5)
Ru_2^{5+}	2-Fap	428(3.6)	463(3.6)		750(3.9)
	2,6-F_2ap	422(4.2)	475(4.0)		788(3.9)
	2,4,6-F_3ap	418(4.5)	476(4.7)		777(4.5)
Ru_2^{4+}	2-Fap		482(sh)		
	2,4,6-F_3ap		476(sh)		
	F_5ap		486(sh)		

It has been reported that the solubility of diruthenium complexes can be improved by abstracting the axial chloride ligand from the dimetal core, by reacting the compound with silver salts.[64] The reaction should leave the axial position of the dimetal unit available for coordination. To achieve a water soluble compound, halide abstraction experiments have been performed on diruthenium compounds such as $Ru_2(OAc)_4Cl$ with salts like $AgClO_4$ (silver perchloroate), AgTFA (silver trifluoroacetate), and $AgNO_3$ (silver nitrate).[64]

Moderate donor solvents such as acetone, methanol, ethanol and tetrahydrofuran involving the $[Ru_2(OAc)_4^+]$ core have been used. In this instance, a 50/50 methanol/water was found to be the most common mixture for axial de-chlorination.[65] Dunlap *et al* [65] synthesized a series of charged diruthenium complexes using different salts. The reaction of interest extracted from the literature was that of $Ru_2(OAc)_4Cl$ with $AgNO_3$, the starting materials were dissolved in de-ionized water which was then heated for 4 hours. The same methodology was used for axial de-chlorination using salts like $AgBF_4$, and AgTFA.

The main goal of these reactions was to afford de-chlorination and the precipitation of AgCl. From their study, it would seem that most of the investigated species can be produced from aqueous solutions.[65] Alcohol aqueous mixtures were of preference to produce the desired water soluble complexes and this was due to the fact that the reactions resulted in lower reaction times, lower temperature as well as higher yields.[65] It was however emphasized that ions that could bind to the $[Ru_2(OAc)_4]^+$core had restrictions. $AgNO_3$ is a good silver salt for de-chlorination because it was found to be one of the weakest donor anions.[65]

The driving force of their study was to invigorate further investigations into the aqueous chemistry of $[Ru_2(OAc)_4]^+$ as it is one of the significant compounds in the journey of understanding cytotoxic, kinetic and catalytic behaviour of the diruthenium complexes.[45] For anti-cancer studies, it was important that aqueous solvents are used as the cytotoxicity examination of the ruthenium compounds are done in aqueous media.[55]

1.6 Aims and objectives

The aim of this research was to synthesize and characterize mono-substituted mixed ligand diruthenium complexes. The design will be such that the complexes are more soluble in aqueous and most organic solvents. The target complexes will be such that the electric properties of the unsymmetrical bridging ligands affect the liability of the axial ligand. In this manner, the solubility properties of the complexes can be tuned. Substitution of the equatorial ligand with electron donating and withdrawing substituent allows for the accessibility of different oxidation states of the dimetal core. The desired complexes were exclusively isolated by optimizing reaction conditions such as reflux time, temperature and solvent type. We also attempted to abstract the chloride ion bound to the dimetal core to give a soluble diruthenium complex. The synthesized complexes were then evaluated as potential anti-cancer agents.

To achieve these aims, the project was divided as follows:

- The synthesis and characterization of unsymmetrical anilinopyridinate ligands i.e anilinopyridinate, (Hap), 2-methylanilinopyridine, H(2-Meap) and fluoroanilinopyridine, H(2-Fap).
- The synthesis and characterization of a series of mono-substituted mixed-ligand diruthenium complexes: $Ru_2(OAc)_3(ap)Cl$, $Ru_2(OAc)_3(2\text{-}Meap)Cl$ and $Ru_2(OAc)_3(2\text{-}Fap)Cl$.
- Electrochemical studies of the complexes
- Cytotoxicity studies of the synthesized diruthenium complexes.

1.7 References

(1) Allardyce, B. C. S.; Dyson, P. J. *Platinum Metals Reviews.* **2001**, *45* (2), 62–69.

(2) Cowley, A.; Woodward, B. *Platinum Metals Reviews.* **2011**, *55* (2), 98–107.

(3) Lippman, A. J.; Helson, C.; Helson, L.; Krakoff, I. H. *Cancer Chemotherapy Reports.***1973**, 57(2), 191.

(4) Clarke, M. J.; Zhu, F.; Frasca, F. R. *Chemistry Reviews.***1999**, *99*, 2511–2534.

(5) Guo, Z.; Sadler, P. J. *Medicinal Inorganic Chemistry.***1999**, *49*, 185–306.

(6) Rosenberg, B.; Vancamp, L.; Trosko, J. E.; Mansour, V. H. N. *Nature.***1969**, *222*, 385–386.

(7) Yu, J.; Xiao, J.; Yang, Y.; Cao, B. *Medicine.* **2015**, *94* (27), 1072.

(8) Rafique, S.; Idrees, M.; Nasim, A.; Akbar, H.; Athar, A. *Biology Reviews.* **2017**, *5(2)*, 38–45.

(9) *http://globocan.iarc.fr*.

(10) De Oliveira Silva, D. *Anti-cancer agents in Medicinal Chemistry.* **2010**, *10*, 312.

(11) Vorobiof, B. D. A.; Sitas, F.; Vorobiof, G. *Clinical Oncology*. **2001**, *19* (18), 125s–127s.

(12) Detty, M. R.; Gibson, S. L.; Wagner, S. J. *Medicinal Chemistry.* **2004**, *47*, 3897.

(13) Heffeter, P.; Jungwirth, U.; Jakupec, M.; Hartinger, C.; Galanski, M.; Elbling, L.; Micksche, M.; Keppler, B.; Berger, W. *Drug Resistance Updates.* **2008**, *11*, 1–16.

(14) Shen, Z. X.; Chen, G. Q.; Ni, J. H. *Blood.***1997**, *89*, 3354–3360.

(15) Zhe Liu, Sadler, P. J. *Reviews.***1998**, *339*, 1341–1348.

(16) Dilda, P. G.; Hogg, P. J. *Cancer Treatment Reviews.* **2007**, *33*, 542–463.

(17) Unnikrishnan, D.; Dutcher, J. P.; Varshneya, N.; Lucariello, R.; Api, M.; Garl, S.; Wiernik, P. H. Chiaramida, S.*Blood.* **2001**, *97* (5), 1514–1516.

(18) Kashif, M.; Andersson, C.; Hassan, S.; Karlsson, H.; Senkowski, W.; Fryknäs, M.; Nygren, P.; Larsson, R.; Gustafsson, M. G. *Scientific Reports.* **2015**, *5* (1), 14118.

(19) Hilderbrand, S. A.; Lim, M. H.; Lippard, S. J. *Journal of the American Chemical Society*. **2004**, 126(15):4972-8.

(20) Eastland, G. W., Jr.; Yang G.; Thompson, T. *Journal of Clinical*

*Pharmacology.***1983**, *5*, 435–438.

(21) Van Rensburg, C. E, J.; Kreft, E.; Swarts, J. C.; Dalrymple, S.R.; Macdonald, D.M.; Cooke, M. W.; Aquino, M. A. S. *Anticancer Research.* **2002**, *22*, 889–892.

(22) Chifotides, H.T.; Dunbar, K. R. *Accounts of Chemical Research.* **2005**, *38* (2),146–156.

(23) Ostrowski, A. D.; Ford, P. C. *Dalton Transactions.* **2009**, 48, 10660.

(24) Zhe Liu, P. J. S. *Accounts of Chemical Research.* **2014**, *47(4)*, 1174–1185.

(25) Wee, H. A.; Dyson, P. J. *Inorganic Chemistry.* **2006**, 20, 4003–4018.

(26) Wu, B.; Ong, M. S.; Groessl, M.; Adhireksan, Z.; Hartinger, C. G.; Dyson, P. J.; Davey, C. A. *European Journal.* **2011**, *17* (13), 3562–3566.

(27) Merker, J.; Lupton, D.; Topfer, M.; Knake, H. *Platinum Metals Reviews.* **2001**, *45* (2), 74–82.

(28) Rosenberg, B.; Vancamp, L.; Krigas, T. *Nature.***1965**, *205*, 698–699.

(29) Rosenberg, B.; Vancamp, L.; Trosko, J. E.; Mansour, V. *Nature.***1969**, *222*, 385–386.

(30) Zheng, J., Domsic, J.F., Cabelli, D., McKenna, R.; Silverman, D. N. *Biochemistry.* **2007**, *46*, 14830–7.

(31) Dasari, S.; Tchounwou, P. B. *European Journal of Pharmacology.* **2014**, *740*, 364–378.

(32) Dorcier, W. H.; Bolano, S.; Gonsalvi, L.; Juillerat-Jeannerat, L.; Laurenczy, G.; Peruzzini, M.; Phillips, A. D.; Zanobini, F.; Dyson, P. J. *Organometallic Chemistry.* **2006**, *25*, 4090.

(33) Detty, M. R.; Gibson, S. L.; Wagner, S. J. *Journal of Medicinal Chemistry.* **2004**, *47*, 3897.

(34) Sabine, H. *Inorganic Biochemistry.* **2009**, *14*, 1089–1097.

(35) Reedijk, J. *Platinum Metals Reviews.* **2008**, *52* (1), 2–11.

(36) Schluga, P.; Christian, G. H.; Egger, A.; Reisner, E.; Galanski, M.; Jakupec, M. A and Keppler, B. K. *Dalton Transactions.* **2006**, 1796.

(37) Motswainyana, W. M.; Ajibade, P. A. *Advances in Chemistry.* **2015**, *2015*, 1-21.

(38) Ribeiro, G.; Benadiba, M.; Colquhoun, A.; de Oliveira Silva, D. *Polyhedron.* **2008**, *27*, 1131–1137.

(39) Benadiba, M.; Santos, R. R. P.; de Oliveira Silva, D.; Colquhoun, A. *Journal of*

Inorganic Biochemistry. **2010**, *104*, 928–935.

(40) Lincoln, P.; Nordén. B.*Journal of Chemical Physics.***1998**, *102 (47)*, 9583–9594.

(41) Long, E. C.; Barton, J. K. *Accounts of Chemical Research.***1990**, *23* (9), 271–273.

(42) Menéndez-Pedregal, E.; Díez, J.; Manteca, Á.; Sánchez, J.; Bento, A. C.; García-Navas, R.; Mollinedo, F.; Gamasa, M. P.; Lastra, E. *Dalton Transactions.* **2013**, *42* (38), 13955.

(43) Rademaker-Lakhai, J. M.; Van den Bongard, D.; Pluim, D.; Beijnen, J. H.; Schellens, J. H. *Clinical Cancer Research.* **2004**, *10*, 3717–3727.

(44) Hartinger, C. G.; Zorbas-Seifried, S.; Jakupec, M. A.; Kynast, B.; Zorbas, H.; Keppler, B. K. *Inorganic Biochemistry.* **2006**, *100*, 891–904.

(45) Santos, R. L. S. R.; van Eldik, R.; de Oliveira Silva, D. *Dalton Transactions.* **2013**, *42* (48), 16796.

(46) Therrien, B.; Suss-Fink, G.; Govindaswamy, P.; Renfrew, A. K.; Dyson, P. *AngewandteChemie International Edition in English.* **2008**, *47*, 3773.

(47) Brabec, V.; Novakova, O. *Drug Resistance Updates.* **2006**, *9*, 111–122.

(48) Jungwirth, U.; Kowol, C. R.; Keppler, B. K.; Hartinger, C. G.; Berge, W.; Heffeter, P. *Molecular Pharmacology.* **2010**, *15*, 1085–1127.

(49) Cotton, F.A.; Curtis, N. F.; Harris, C. B.; Johnson, B. F. G.; Lippard, S. J.; Mague, J. T.; Robinson, W. R.; Wood, J. S. *Science.***1964**, *145 (3638)*, 1305.

(50) Stephenson, T. A.; Wilkinson, G. *Journal of Inorganic and Nuclear Chemistry.***1966**, *28*, 2285–2291.

(51) Bennett, M. J.; Caulton, K. G.; Cotton, F. A. *Inorganic Chemistry.***1969**, *8* (1), 1–6.

(52) Cotton, F. A.; Murillo, C. A.; Walton, R. A. *Multiple bonds between metal atoms, 3rd ed.; Springer science and business media, Inc: New York, USA*; **2005**.

(53) Aquino, M. A. S. *Coordination Chemistry Reviews.***1998**, *170*, 141–202.

(54) Manowong, M.; Han, B.; McAloon, T. R.; Shao, J.; Guzei, I. A.; Ngubane, S.; Van Caemelbecke, E.; Bear, J. L.; Kadish, K. M. *Inorganic Chemistry.***2014**, *53* (14), 7416–7428.

(55) Aliwaini, S.; Peres, J.; Kröger, W. L.; Blanckenberg, A.; de la Mare, J.; Edkins, A. L.; Mapolie, S.; Prince, S. *Cancer Letters*. **2015**, *357* (1), 206–218.

(56) Kadish, K. M.; Phan, T. D.; Giribabu, L.; Shao, J. G.; Wang, L. L.; Thuriere, A.; Van Caemelbecke, E.; Bear, J. L. *Inorganic Chemistry.* **2004**, *43* (3), 1012–1020.

(57) Kadish, K. M.; Phan, T. D.; Giribabu, L.; Caemelbecke, E. Van; Bear, J. L. *Dalton Transactions.* **2003**, *42* (26), 8663–8673.

(58) Ciardelli, F.; Tsuchida, E.; Wohrle, D. *Macromolecule-metal complexes*; **1996**.

(59) Kadish, K. M.; Nguyen, M.; Caemelbecke, E. Van; Bear, J. L. *Inorganic Chemistry.* **2006**, *45* (15), 10552–10553.

(60) Kadish, K. M.; Garcia, R.; Phan, T.; Wellhoff, J.; Van Caemelbecke, E.; Bear, J. L. *Inorganic Chemistry.* **2008**, *47 (23)*, 11423.

(61) Ngubane, S.; Kadish, K. M.; Bear, J. L.; Van Caemelbecke, E.; Thuriere, A.; Ramirez, K. P. *Dalton Transactions.* **2013**, *42*, 3571–3580.

(62) Majumdar, M.; Saha, S.; Dutta, I.; Sinha, A.; Bera, J. K. *Dalton Transactions.* **2017**, 46 (17), 5660–5669.

(63) Bear, J. L.; Li, Y.; Han, B.; Van Caemelbecke, E.; Kadish, K. M. *Inorganic Chemistry.***1997**, *36*, 5449.

(64) Santos, R. L. S. R.; Van Eldik, R.; De Oliveira Silva, D. *Inorganic Chemistry.* **2012**, *51* (12), 6615–6625.

(65) Dunlop, K.; Wang, R.; Stanley Cameron, T.; Aquino, M. A. S. *Journal of Molecular Structure.* **2014**, *1058* (1), 122–129.

Chapter 2

Synthesis and spectroscopic characterization of mono-substituted diruthenium complexes.

2.1 Introduction

Metal-metal bonded complexes containing chelating nitrogen ligands continue to be a highly researched area following the successful physical characterization of the Ru_2^{5+} diruthenium complex, $Ru_2(OAc)_4Cl$ for the first time in 1966.[1] Studies show that changing the donor atoms of the bridging ligands coordinated to the dimetal core does not only affect the structural characteristics of the complexes, but also modifies the electronic configuration.[2]

Cotton and co-workers showed that the near degeneracy of the π^* and δ^* orbitals (chapter 1, figure 1.10) can be lifted by changing the O, O' bridging carboxylate to N, O' or N, N' chelating ligands.[3,4] This is because the lowest unoccupied molecular orbitals (LUMOs) of pyridines have the right symmetry to interact with the Ru – Ru π^* highest occupied molecular orbital (HOMO).[5]

Owing to the increased basicity of H_2NOCCF_3 ligand compared to the acetate counterpart, the electrochemistry of the complex, $Ru_2(HNOCCF_3)_4Cl$ can be altered compared to the $Ru_2(OAc)_4Cl$ complex.[3,4] Nitrogen containing ligands are therefore of great importance mainly due to their ability to change the molecular orbital order of the dimetal centre. The choice of nitrogen containing bridging ligands is largely due to the fact that the anilinopyridinate anions have delocalized π systems which account for the stabilization of the Ru (II) – Ru (III) core.[5]

The substitution of the acetate ligand by the nitrogen containing ligands proceeds via a stepwise metathesis displacement with the mixed-ligand complexes $Ru_2(OAc)_xL_{4-x}Cl$ as intermediates. In this chapter, we report the synthesis and characterization of mono-substituted mixed-ligand diruthenium complexes having the general formula, $Ru_2(OAc)_3(L)Cl$, where L is an unsymmetrical bridging anilinopyridinate ligand. In literature, the Ru_2^{5+} complexes are reported to have four possible isomer types,

namely, (4,0), (3,1), (2,2)-*trans* and (2,2)-*cis* (figure 2.1) but most diruthenium complexes have been isolated as a mixture of (3,1) and (4,0) isomers.[6]

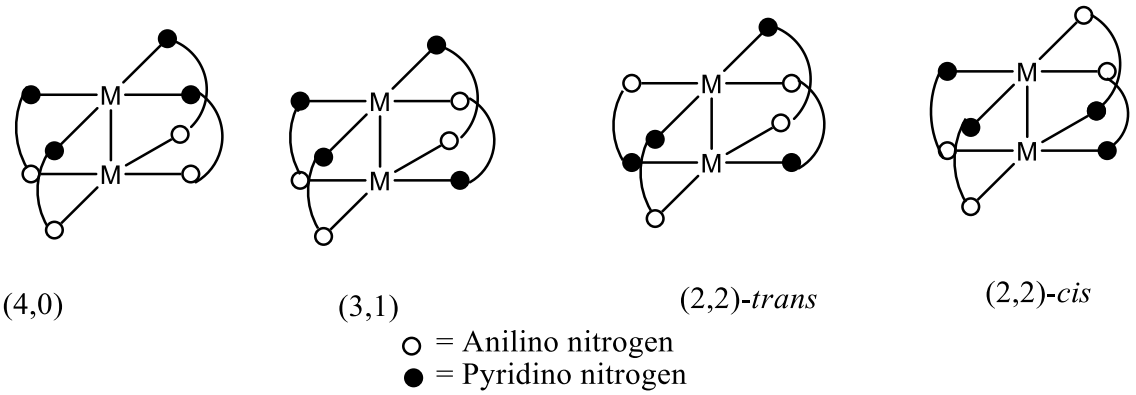


Figure 2.1: Possible geometric isomers of mixed-ligand diruthenium complexes

Unsymmetrical anilinopyridinate bridging ligands having different substituents are ligands of interest. This is because they have been shown to be able to stabilize different oxidation states of the dimetal centers.[5-8] The reactivity of these ligands has been studied on metals such as: Cr[9], Rh[10], Ru[5] and Mo[11], where tetracarboxylates were mostly used as starting materials for the synthesis of anilinopyridinate based metal complexes.[12]

Coordination with the dimetal centers occurs through the pyridino and anilino nitrogen atoms. The bidentate coordination results in a N-C=N three atom bridge. Studies show that the substituent bonded to the anilino ring of the investigated ligands affect the structural and spectroscopic characteristics of the complex.[13,14] Therefore, the effect these electron withdrawing or donating substituent have on the dimetal core were investigated and reported. The unsymmetrical substituted anilinopyridinate ligands investigated are labelled as: Hap **(L1)**, H(2-Meap) **(L2)** and H(2-Fap) **(L3)** (figure 2.2).

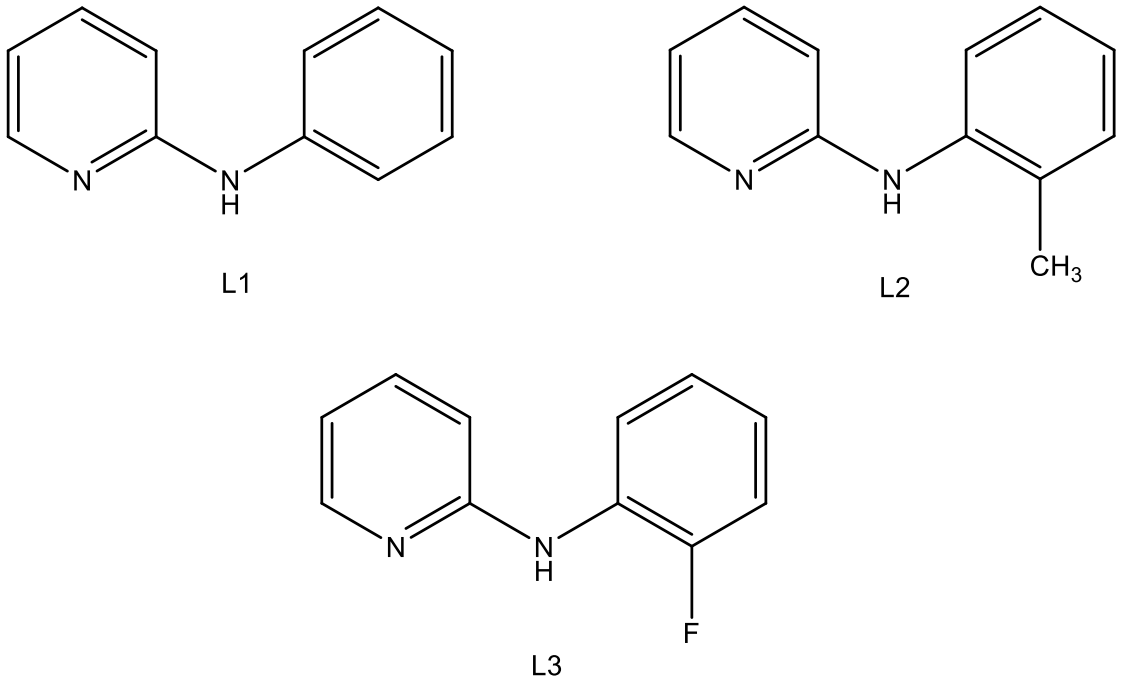


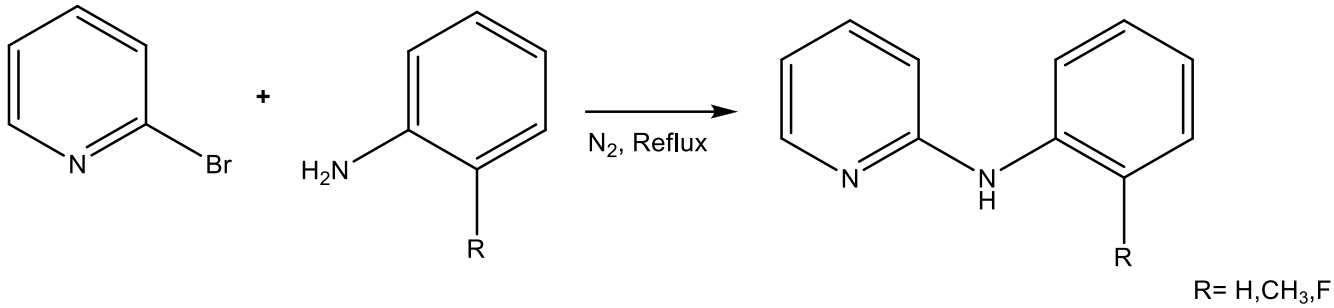
Figure 2.2: Anilinopyridinate ligand systems investigated in this study

2.2 Results and discussion

2.2.1 Synthesis and characterization of substituted anilinopyridinate ligands.

The ligands, anilinopyridine (Hap), 2-methylanilinopyridine (H(2-Meap)) and 2-fluoroanilinopyridine (H(2-Fap)) ligands were synthesized following a procedure reported in literature.[10] As shown in Scheme 2.1, 2-bromopyridine and substituted aniline were heated at 170 °C under a nitrogen atmosphere for 7 hours. All the ligands produced solid crude products.

The ligands were recrystallized three times in hot hexane to afford white crystals. All the ligands showed good solubility in polar solvents such as chloroform, dichloromethane, ethyl acetate, diethyl ether and methanol. The ligands were characterized by mass spectrometry, ^{1}H and ^{13}C NMR and FTIR spectroscopy as well as elemental analysis.



Scheme 2.1: General synthetic route of the anilinopyridinate ligands

2.2.1.1 Nuclear magnetic resonance of anilinopyridinate ligands.

All the ligands were characterized with proton and carbon NMR spectroscopy obtained in $CDCl_3$. In this section, a representative characterization of **L2** by NMR is discussed. The most characteristic signal, confirming the formation of the ligand from 2-bromopyridine and methylaniline is the N-H proton, the broad singlet observed at 6.30 ppm (figure 2.3). The ^1H NMR spectrum shows a singlet signal of the methyl group at 2.23 ppm. The peaks ranging from 6.5 – 8.10 ppm are assigned to the aromatic protons (H_a-H_h). The doublet signal (H_h) at 8.10 ppm is more de-shielded as compared to the other aromatic protons because it is only two bonds away from the electronegative nitrogen in the pyridino ring.

H_g is bonded to the pyridino ring whereas H_b to the anilino ring and they are both para to the N-H proton. Their signal is characterized by a doublet of doublet for H_g and a doublet of doublet H_b appearing as a multiplet at 6.60 ppm. H_g is slightly de-shielded because it is in the ring that contains Nitrogen. H_c and H_f, both at meta positions to the N-H group, both have doublet of doublets signals assigned to the multiplet peak at 7.41 ppm with H_f slightly de-shielded (7.43ppm) and H_f at 7.40 ppm.

H_d, in the pyridino ring ortho to N-H as well as H_e in the anilino ring which is also ortho to N-H are each characterized by a doublet signal and their signal appears at 7.15 ppm as a doublet of doublet. The doublet signal at 7.05 ppm is assigned to the H_a proton. Similar results with different multiplicities depending on the type of substituent were obtained for the other investigated ligands. The broad N-H peak tends to shift based on the nature of the substituent on the anilino ring. The N-H peak becomes de-shielded when there is an electron withdrawing substituent and shielded when the substituent is electron donating. For instance, **L2** has a N-H signal at 6.30 ppm

whereas **L3** has a N-H peak more de-shielded at 6.60 ppm. The discrepancy in the chemical shift of the broad peaks (N-H) is because **L3** contains an electron withdrawing substituent (F) on the anilino ring ortho to N-H. This substituent decreases the electron density around the N-H region resulting in an increased chemical shift. **L2** contains an electron donating substituent (CH_3) on the anilino ring; this group increases the electron density around the N-H region resulting in a more up-field broad peak at 6.30 ppm as compared to that of **L2**.

The **L1** ligand has a broad peak (N-H) appearing at 6.50 ppm, more de-shielded than the N-H peak of the **L2** ligand because CH_3 is a better electron donating group. **L1** contains aromatic protons, conforming the formation of the desired ligand.

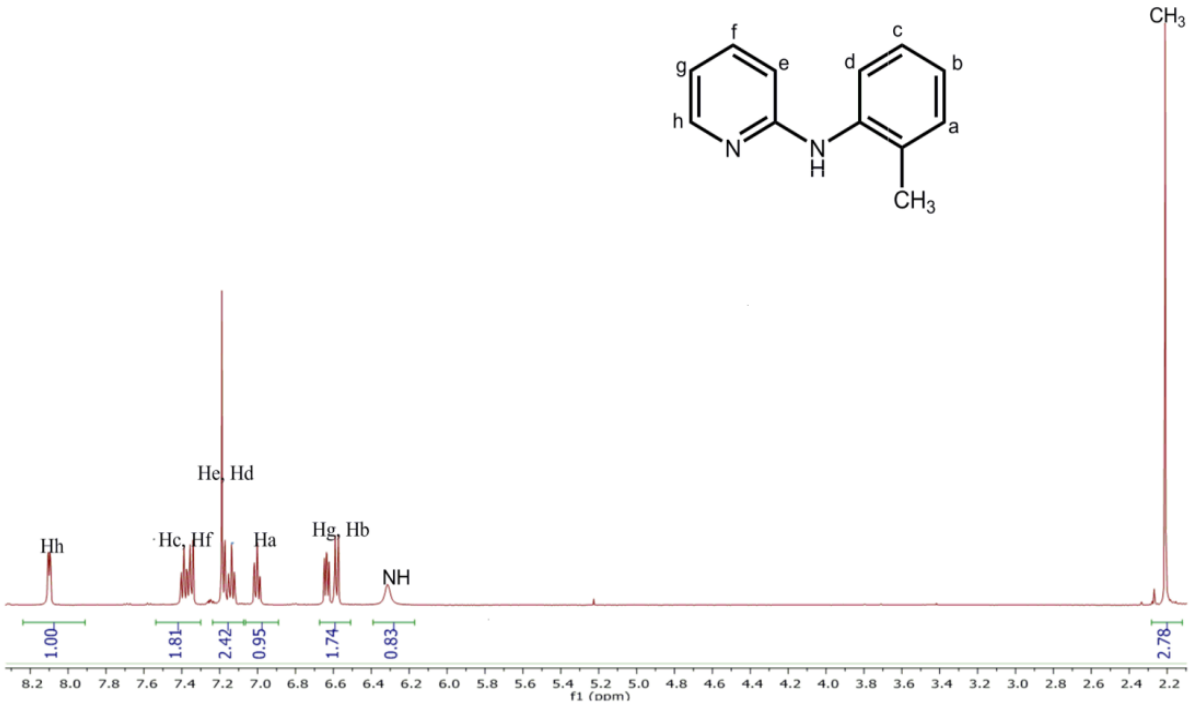


Figure 2.3: ^{1}H NMR spectrum of H(2-Meap) in $CDCl_3$

The corresponding ^{13}C NMR signal of **L2** occurring at 18.00 ppm is assigned to the single carbon bond (C-C) of the methyl group bonded to the anilino ring of the ligand. The chemical shift at 107.50 ppm is assigned to the single C-N bond connecting the two rings; this further confirmed the formation of the ligand. The chemical shift between the ranges of 114 – 150 ppm corresponds to the aromatic carbons of the ligand. The more de-shielded signal occurring at 155.50 ppm is assigned to the C=N functional

group of the pyridino ring. All the other investigated ligands, **L1** & **L3** exhibited similar ^{13}C NMR signals with slight shifts depending on the type of substituent.

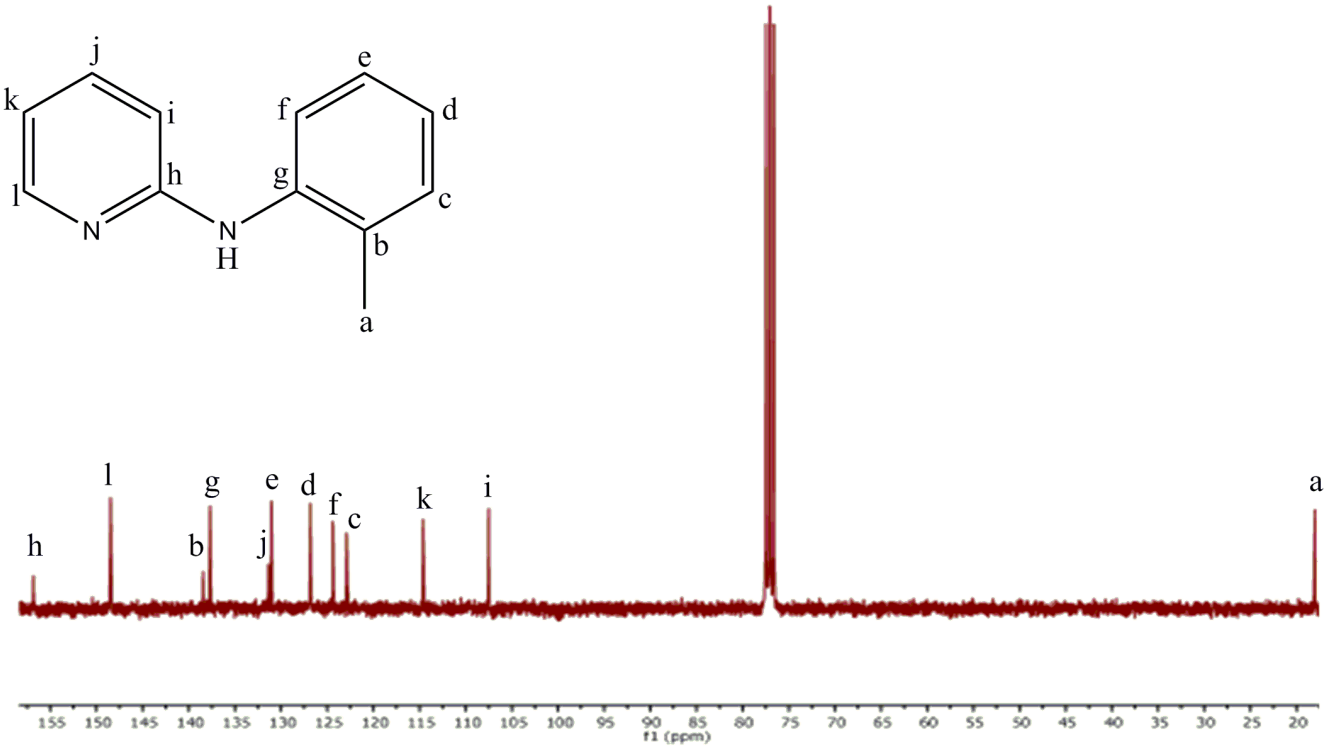


Figure 2.4: ^{13}C NMR spectrum of H(2-Meap) in $CDCl_3$

The investigated ligands exhibit a broad N-H signal which indicates the formation of the ligand of interest from 2-bromopyridine and substituted aniline. Moreover, aromatic protons of both the anilino and pyridino ring were observed on the spectrum. The change in chemical shift of the N-H signal upon moving from an electron donating to an electron withdrawing substituent indicates that the nature and positioning of the substituent influences the electron density of the N-H region.

2.2.1.2 Characterization of substituted anilinopyridinate ligands with FTIR.

A ν(N-H) vibration stretch was expected after the formation of **L2** from 2-bromo-pyridine and 2-methylaniline. This was indeed observed with a stretching frequency of 3155 cm^{-1} (figure 2.5). The vibrational stretch appearing at 2941 cm^{-1} was assigned to the ν(C-H) stretch. The positioning and intensity of the C-H stretch is related to the nature of the other substituents on the ring, in this case, the stretch is affected by the

methyl group at the ortho position of the ligand. The intense stretch at 1527 cm^{-1} is attributed to the ν(C=N) stretch and the 1425 cm^{-1} frequency assigned to ν(C-C).

All the investigated ligands have the same functional groups, C=N, C-H, C-C and N-H from the anilinopyridinate rings except that the stretches differ based on the type of substituent. For example, H(2-Fap) has a shorter ν(N-H) vibration stretch compared to Hap, this is due to the fact that H(2-Fap) contains an electron withdrawing substituent on the ortho position of the anilino ring. This substituent decreases the electron density of the N-H region resulting in a less intense stretch.

In the case of a methyl containing ligand, H(2-meap) has a longer ν(N-H) vibration stretch as compared to H(2-Fap). This this observation was attributed to the fact that the ligand contains an electron donating methyl group which increases the electron density of the N-H group resulting in a longer stretching frequency.

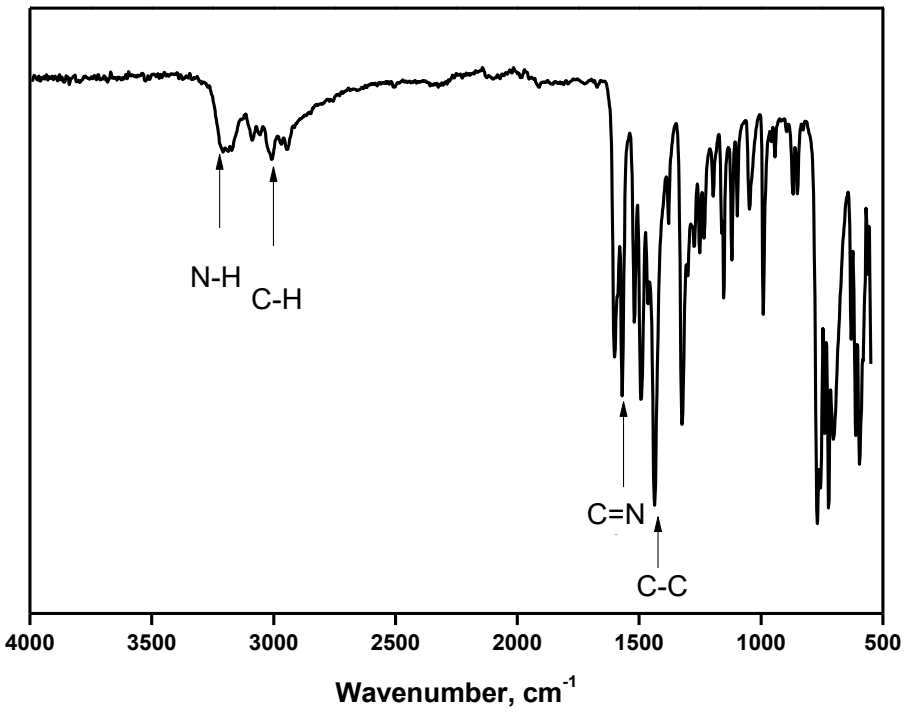


Figure 2.5: FTIR spectrum of H(2-Meap)

2.2.1.3 Mass spectrometry and elemental analysis of anilinopyridinate ligands.

A representative mass spectrum of ligand **L2** is shown in figure 2.6. The formation of the ligand was indicated by a sharp peak on the mass spectrum. The calculated molar mass (184.24 $g.mol^{-1}$) is consistent with that observed on the mass spectrum (185.4) and this further confirmed the successful synthesis of the ligand. The same consistency was observed from the mass spectra of the synthesized ligands, **L1** and **L3**. The obtained mass spectrometry results were the indication that the substituted anilinopyridinate ligands had been successfully synthesized given that they matched their theoretical values.

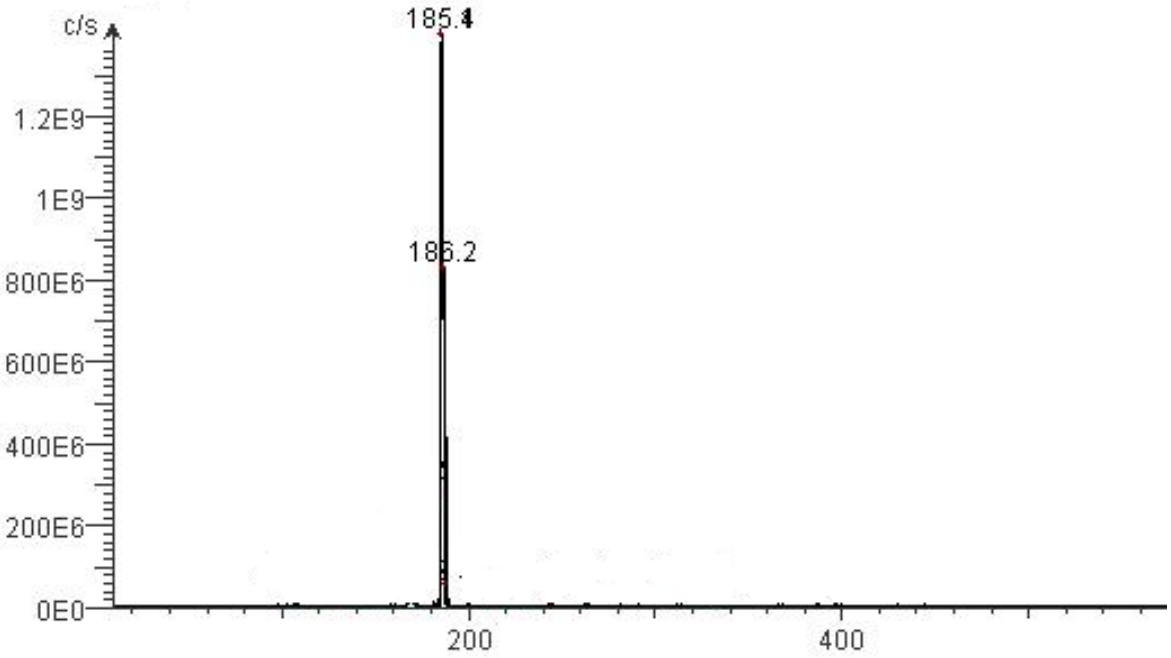


Figure 2.6: Mass spectrum of H(2-Meap)

The purity of the anilinopyridinate ligands were ascertained by elemental analysis. The calculated CHN composition of H(2-Meap) is C, 78.23; H, 6.57; N,15.21 and the deviation is less than 0.4 % from elemental analysis, C, 78.15; H, 6.25; N,15.23. The 0.4 % deviation of the calculated CHN values from the obtained CHN values means that the compound is pure and has all the expected atom composition.

The ≤ deviation of the calculated CHN values from elemental analysis results was obtained from the other investigated. This correlation was a confirmation that all three

ligands, Hap, H(2-Meap) and H(2-Fap), were successfully synthesized and characterized.

2.2.2 Synthesis and characterization of mixed-ligand diruthenium complexes.

There are various types of the mixed-ligand diruthenium complexes synthesized from a mixture of diruthenium tetracarboxylate with substituted bridging anilinopyridinate ligands.[12] One example being the formation of four mixed ligand complexes, $Ru_2(OAc)_x(L)_{4-x}Cl$ (x = 0-3) having different ratios of the acetate and anilinopyridinate ligand which is an unsymmetrical N,N' donor bridging ligand.[16]

Kadish and co-workers reported in studies that refluxing $Ru_2(OAc)_4Cl$ with excess 2-fluoroanilinopyridinate bridging ligand in methanol, under nitrogen for 3 hours results in the isolation of three mixed-ligand complexes; $Ru_2(OAc)_3(Fap)Cl$, $Ru_2(OAc)_2(Fap)_2Cl$, $Ru_2(OAc)(Fap)_3Cl$ and the fully substituted complex, $Ru_2(Fap)_4Cl$.[15] This can be attributed to the stepwise metathesis displacement mechanism shown in equations 1 - 4.[15]

$$Ru_2(OAc)_4Cl + HL \longrightarrow Ru_2(OAc)_3LCl + HOAc \quad (1)$$

$$Ru_2(OAc)_3LCl + HL \longrightarrow Ru_2(OAc)_2L_2 + HOAc \quad (2)$$

$$Ru_2(OAc)_2L_2Cl + HL \longrightarrow Ru_2(OAc)L_3Cl + HOAc \quad (3)$$

$$Ru_2(OAc)L_3Cl + HL \longrightarrow Ru_2(L)_4Cl \quad (4)$$

Scheme 2.2: Stepwise metathesis displacement.

The progress of the reaction was monitored on a thin layer chromatography and the derivatives separated on a silica column using 1:1-(v:v hexane/acetone) as eluent. Four fractions, two green, one blue and one purple were collected. The fractions had the following R_f values, 0.875, 0.825, 0.525 and 0.125 from the TLC and were identified as $Ru_2(Fap)_4Cl$ (**4**), $Ru_2(OAc)(Fap)_3Cl$ (**3**), $Ru_2(OAc)_2(Fap)_2Cl$(**2**) and $Ru_2(OAc)_3(Fap)Cl$ (**2**), respectively. The yields obtained for each of the compounds were reported to be, 30.20 (**4**), 20.10 (**3**), 24.20 (**2**) and 4.80 (**1**) %.[15]

The UV/Visible spectrum of $Ru_2(OAc)_x(Fap)_{4-x}Cl$ (x = 0-3) in CH_2Cl_2 reported is shown in figure 2.7. Each Ru_2^{5+} species exhibits a low-energy absorption in the 581-750 nm region which was attributed to an allowed charge-transition π (ligand, metal) to π*(Ru_2)

or δ*(Ru_2) and a less intense band around 415 - 513 nm. Moreover, the $Ru_2(OAc)_3(Fap)Cl$ (x = 3) compound has a band at 990 nm which was assigned to a δ ⟶ δ* transition.[16] The 580 - 800 nm transition was shown to be responsive to the type of bridging ligand coordinated to the dimetal core.[17]

This is apparent as indicated by the wavelength shift of the major bands in the visible region of the absorption spectrum of the compound upon going from $Ru_2(OAc)_3(Fap)Cl$ to $Ru_2(Fap)_4Cl$. It was also clear that the mixed ligand diruthenium derivatives with two or three Fap groups on the molecule exhibited spectroscopic behavior similar to the compound with four Fap ligands. However, the complex with only one Fap bridging ligand exhibited vastly different characteristics.

This difference was attributed to the existence of chemical equilibria in solution which involved the associated and non-associated anionic axial ligand on the complex splitting at 580 – 650 nm for x = 3.[16] Because of the different characteristics of mono-substituted complexes in solution compared to the other derivatives, the mono-substituted mixed ligand diruthenium complex became the complex of interest.

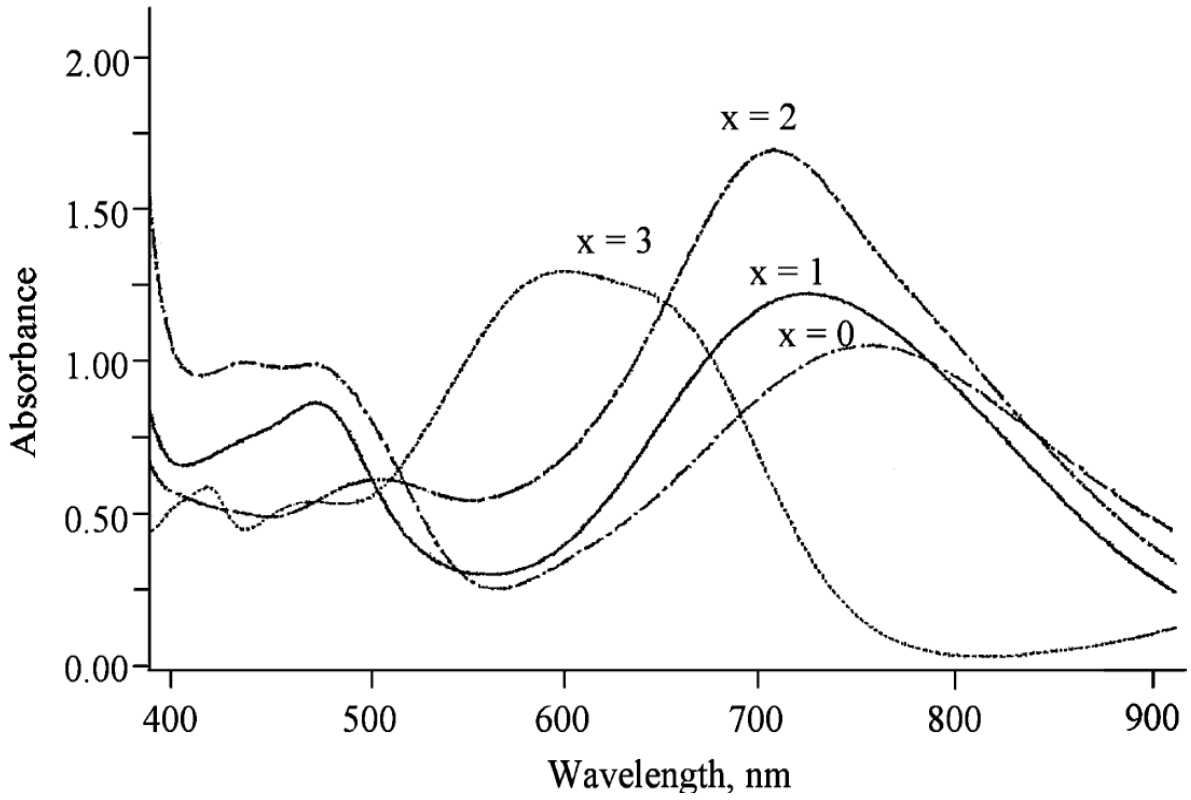


Figure 2.7: UV/Visible spectrum of $Ru_2(OAc)_x(Fap)_{4-x}Cl$ in CH_2Cl_2.[15]

In this work, various mono-substituted diruthenium complexes have been synthesized, whereby, an acetate bridging ligand was replaced by an incoming anilinopyridinate ligand as shown in scheme 2.2, eqn 1 - 4. The extent of the replacement of the acetate was controlled by varying the reaction conditions such as temperature, reaction time and choice of solvents.[15]

By reacting $Ru_2(OAc)_4Cl$ with a substituted anilinopyridinate ligand, it is possible to obtain a mono-substituted diruthenium complex only having one substituted anilinopyridinate ligand and three acetate ligands (scheme 2.2, eqn 1). To exclusively isolate a mono-substituted complex, reaction conditions such as temperature, reaction time and solvent type were optimized. The focus was on monitoring the reactions to avoid further substitution. In this case, UV/Visible spectroscopy was used to monitor the product formed.

Prior to synthesizing the investigated mono-substituted complexes under reflux conditions, the compound, $Ru_2(OAc)_4Cl$ with excess 2-fluoroanilinopyridinate bridging ligand reaction was first carried out at room temperature in cold methanol. This methodology was employed to prevent the formation of the subsequent reaction products, $Ru_2(OAc)_2(L)_2Cl$, $Ru_2(OAc)(L)_3Cl$ and $Ru_2(L)_4Cl$. Stirring the reaction for 30 minutes did not result in any spectroscopic changes, the reaction was left to stir for a further 120 minutes which then started showing the formation of a product as shown in figure 2.8.

From the UV/Visible spectral changes, it could be concluded that with time, more product was formed hence the mixture was left to react for 350 minutes in methanol at room temperature. Although a mono-substituted complex formed from the room temperature reaction, the yields were very low due to poor solubility of the starting materials in cold methanol. Furthermore, the room temperature method required a longer reaction time.

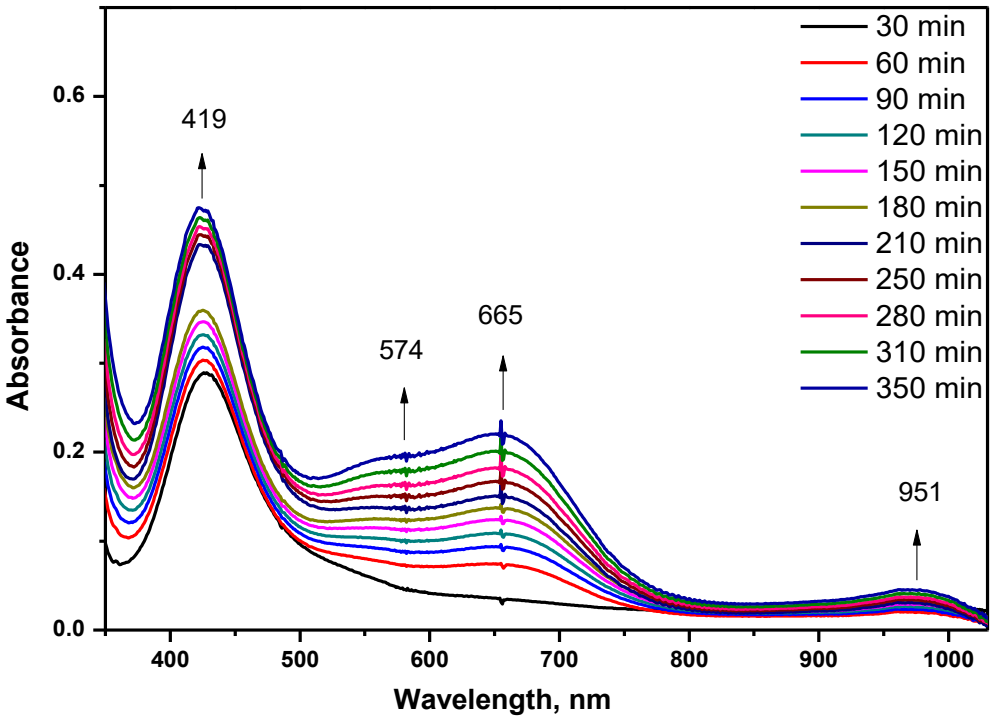


Figure 2.8: Monitoring of $Ru_2(OAc)_3$(2-Fap)Cl by UV/Visible spectroscopy at room temperature.

Although the room temperature synthesis resulted in low yields due to poor solubility, the findings led to the suggestion that solubility could be improved by synthesizing these complexes at higher temperatures. In this study, we have synthesized and isolated complexes of the type $Ru_2(OAc)_3$(L)Cl, (L = ap, 2-Meap and 2-Fap). By optimizing the reaction time, temperature and solvent type, we managed to exclusively isolate only the mono-substituted mixed-ligand diruthenium complexes.

The synthesis and characterization of mixed-ligand diruthenium complexes, $Ru_2(OAc)_3$(ap)Cl, $Ru_2(OAc)_3$(2-Meap)Cl and $Ru_2(OAc)_3$(2-Fap)Cl are discussed in this section. A diruthenium tetracarboxylate compound, $Ru_2(OAc)_4$Cl, was used as a starting material for the synthesis of the investigated mixed-ligand diruthenium complexes and this precursor was synthesized following a procedure reported in literature.[1,18]

The complexes, $Ru_2(OAc)_3(ap)Cl$, $Ru_2(OAc)_3(2\text{-}Meap)Cl$ and $Ru_2(OAc)_3(2\text{-}Fap)Cl$ were prepared using the same procedure,[15] by refluxing a mixture of $Ru_2(OAc)_4Cl$ and substituted aniline in methanol for 90 minutes. The progresses of the reactions were monitored on a thin layer chromatography plate using ethyl acetate as an eluent. During the reactions, the brown homogeneous solution changed into a blue-green solution. After completion of the reactions, the solutions were concentrated using a rotary evaporator. This was followed by adding 100 ml of CH_2Cl_2 to remove unreacted diruthenium tetracarboxylate. The solution was concentrated, and the residue purified by column chromatography using ethyl acetate as an eluent. Three bands, green, brown and blue were observed and collected.

After analysis of the fractions on a TLC plate and by mass spectrometry, it was concluded that the blue fraction is the compound of interest. The solvent was then removed using a rotary evaporator and was dried on a high vacuum pump to isolate blue products. The compounds were obtained in yields of 62 % for $Ru_2(OAc)_3(ap)Cl$, 59 % for $Ru_2(OAc)_3(2\text{-}Meap)Cl$ and 48 % for $Ru_2(OAc)_3(2\text{-}Fap)Cl$. The mono-substituted diruthenium complexes are air stable and show good solubility in dichloromethane, methanol, ethyl acetate and acetonitrile.

The investigated complexes are all insoluble in hexane. $Ru_2(OAc)_3(2\text{-}Meap)Cl$ is soluble in DMSO and H_2O whereas $Ru_2(OAc)_3(ap)Cl$ is partially soluble in these solvents (DMSO and H_2O). $Ru_2(OAc)_3(2\text{-}Fap)Cl$ is insoluble in DMSO and H_2O. These complexes are paramagnetic because they have three unpaired electrons at the π^* and δ^* orbitals, therefore, they could not be characterized using NMR spectroscopy. Mass spectrometry, UV/Visible and FTIR spectroscopy were all used to analyze the compounds. Elemental analysis was used to ascertain purity of the complexes. The investigated complexes have the Ru_2^{5+} diruthenium core and are shown in figure 2.9.

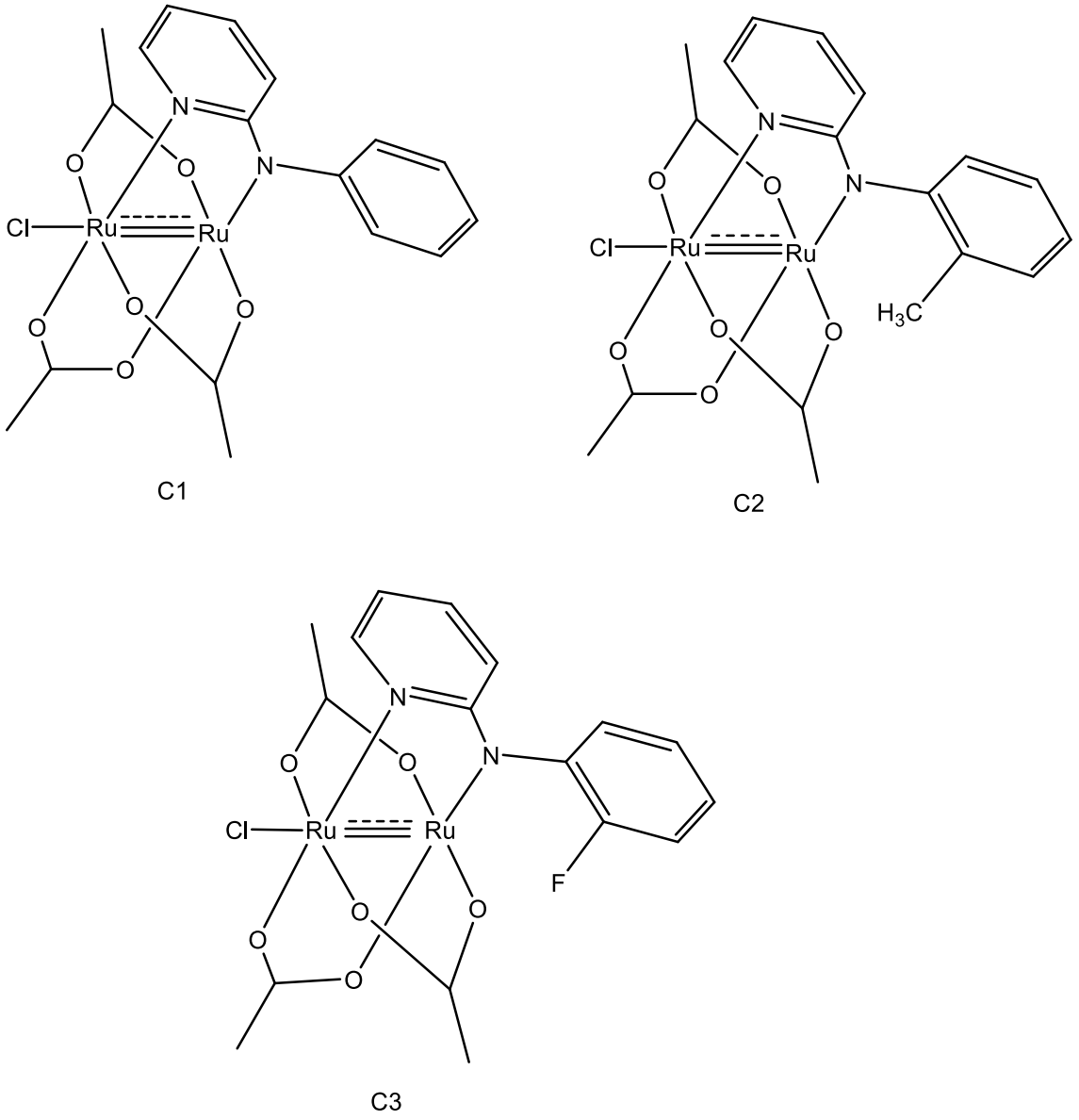


Figure 2.9: Structures of the synthesized complexes, $Ru_2(OAc)_3$(ap)Cl (**C1**), $Ru_2(OAc)_3$(2-Meap)Cl (**C2**) and $Ru_2(OAc)_3$(2-Fap)Cl (**C3**).

2.2.2.1 Characterization of mixed-ligand diruthenium complexes with FTIR.

FTIR analyses were conducted to investigate if complexation had occurred through the pyridino nitrogen, anilino nitrogen and the dimetal core. This was done under the premise that upon complexation, the anilinopyridinate ν(N-H) stretch would disappear. Indeed, this was observed on the FTIR spectrum of the $Ru_2(OAc)_3$(2-Meap)Cl complex (figure 2.10), where it was observed that the complex did not have a ν(N-H) vibration stretch at 3247 cm^{-1} which is present on the FTIR spectrum of the Hap ligand.

A stretch appearing at 3070 cm^{-1} was characterized to the ν(C-H) frequency stretch of the anilinopyridinate ligand, Hap. The FTIR spectrum also shows a band at 1589 cm^{-1} for the ν(C=N) stretching frequency of the pyridino ring as well as ν(C-C) stretching frequency at 1463 cm^{-1} present in both the ligand and complex FTIR spectrum. The strong stretching frequency at 400 cm^{-1} which does not occur in the ligand spectrum was also an indication that the acetate ligands were still coordinated, and that the desired compound was formed. The trend that the N-H stretch collapses upon complexation was observed for all the synthesized complexes. This indicates the successful coordination of the dimetal core to the anilino and pyridino nitrogen of the anilinopyridinate ligand.

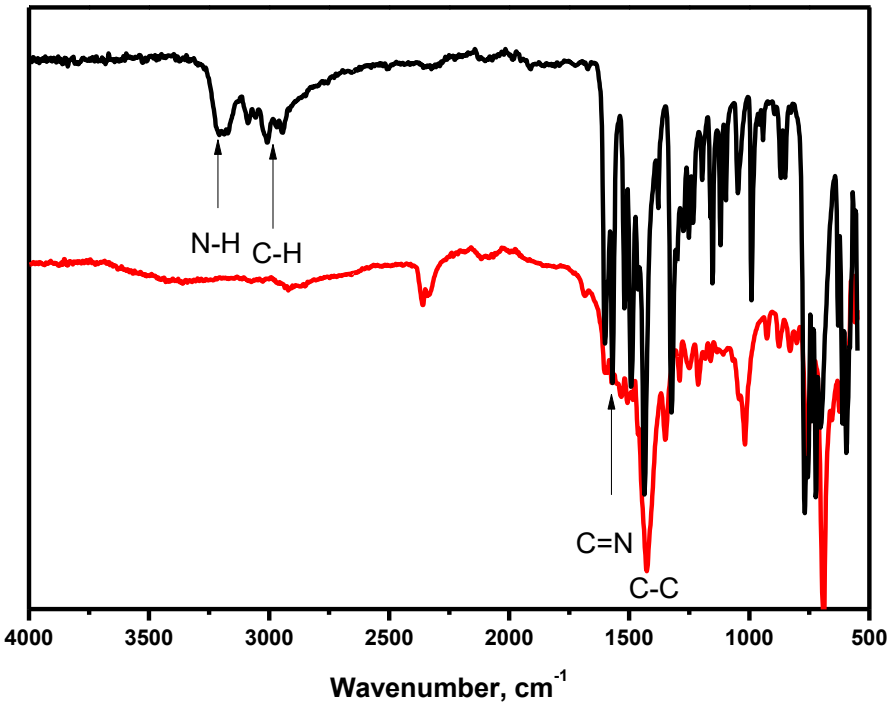


Figure 2.10: FTIR spectrum of free ligand, H(2-Meap) and mixed-ligand diruthenium complex, $Ru_2(OAc)_3$(2-Meap)Cl.

2.2.2.2 Mass spectrometry + CHN analysis of diruthenium complexes.

Mass spectrometry was conducted to investigate that the compounds had been successfully synthesized. The mass spectra shown in figure 2.11 shows that one fraction is predominant with $[M+H]^+$ (fragment)] of 594.8 which matched the calculated

molar mass of the complex $Ru_2(OAc)_3$(2-Meap)Cl, 593.2 g.mol^{-1}. The spectrum shows a minor peak with the value of 560 g.mol^{-1}, this value amounts to the molar mass of the compound without the chloride anion. The observation further confirmed the hypothesis that there is two forms of the compound in solution, the non-associated, $[Ru_2(OAc)_3(2\text{-Meap})]^+$ and associated, $Ru_2(OAc)_3$(2-Meap)Cl compound.

MS analyses were also performed on $Ru_2(OAc)_3$(ap)Cl and the major peak $[M + H]^+$ (fragment)] was found to be 584.2.The molar mass of the target complex $[(Ru_2(OAc)_3(ap)Cl)]^+$ was calculated to be 583.2 g.mol^{-1} which matched the empirical value obtained from mass spectrometry. For the $Ru_2(OAc)_3$(2-Fap)Cl complex, It was observed that the $[M + H]^+$ (fragment)] (601.2 g.mol^{-1}) was consistent with the calculated value of the target compound (600.2 g.mol^{-1}).

A good correlation between elemental analysis and the calculated CHN values of the investigated complexes was obtained. This implies that purifying the mixed-ligand complexes on a column chromatography were a success and that the expected composition of the complexes was obtained.

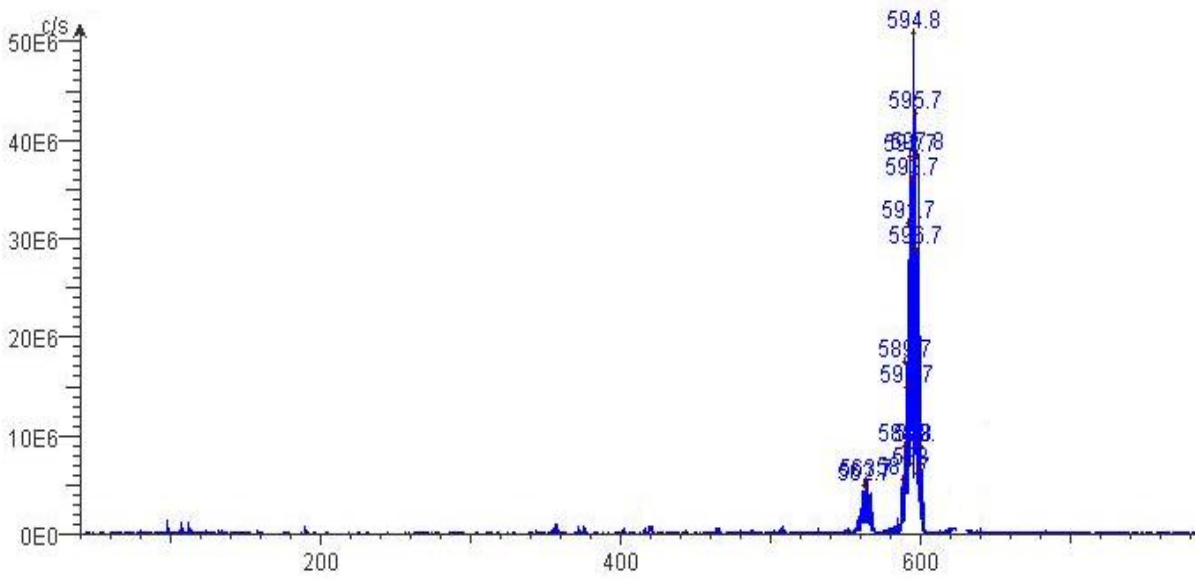


Figure 2.11: Mass spectrum of $Ru_2(OAc)_3$(2-Meap)Cl.

2.2.2.3 UV/Visible spectroscopy of diruthenium complexes.

In our study, three mixed-ligand diruthenium complexes, $Ru_2(OAc)_3(ap)Cl$, $Ru_2(OAc)_3$(2-Meap)Cl and $Ru_2(OAc)_3$(2-Fap)Cl have been investigated as to their spectroscopic behavior. The major peaks of the synthesized complexes occurred at similar wavelengths and have similar extension coefficients as those that were reported in literature (figure 2.7).[15] Therefore, the accompanying transitions could be assigned: the split band with the range at 581 and 680 nm can be attributed to an allowed charge-transfer transition π (ligand, metal) $\longrightarrow$ $\pi^*(Ru_2)$ or δ^* (Ru_2), and the band approximately 950 nm band of all three complexes assigned to an allowed δ to δ^* transition.

The complexes were all studied in solution and the resulting spectra are shown in figure 2.12. In the case of the mixed-ligand complex with an unsubstituted anilinopyridinate compound, $Ru_2(OAc)_3(ap)Cl$, we see an increased intensity for the band at 666 nm and a shoulder at 590 nm (figure 2.12(C1)). This is the opposite of what was observed from the Fap containing complex. The difference was expected because the $Ru_2(OAc)_3(ap)Cl$ complex is without an electronegative substituent at the ortho position. Therefore, the increased electron density around the dimetal core due to the electronegative anilino nitrogen results in the axial chloride ligand loosely bound to the dimetal core, favouring the positively charged species, $[Ru_2(OAc)_3(ap)]^+$ in solution. This observation means that there is more of the species, $[Ru_2(OAc)_3(ap)]^+$ than $Ru_2(OAc)_3(ap)Cl$ in solution. Therefore, the proposed equilibrium of this complex in solution is:

$$[Ru_2(OAc)_3(ap)]^+ \rightleftharpoons Ru_2(OAc)_3(ap)Cl \qquad (I)$$

It is observed from the UV/Visible spectrum of the complex, $Ru_2(OAc)_3$(2-Meap)Cl, in figure 2.12 (C2) that it was no clear indication as to which form is dominant in solution. The broad band between 602 and 656 nm could mean that there is an equal amount of the two forms, $[Ru_2(OAc)_3$(2-Meap)$]^+$ and $Ru_2(OAc)_3$(2-Meap)Cl in solution. The chemical equilibrium of the compound in solution is then suggested to be:

$$[Ru_2(OAc)_3(2\text{-}Meap)]^+ \rightleftharpoons Ru_2(OAc)_3(2\text{-}Meap)Cl \qquad (II)$$

The UV/Visible spectroscopic behaviour of $Ru_2(OAc)_3$(2-Fap)Cl is shown in figure 2.12 (C3). Herewith, a split band between 588 and 678 nm as well as a weak band at 955 nm were observed. These bands do not appear on the UV/Visible spectra of further substituted products i.e. they appear for only mono-substituted products (see figure 2.7). Based on each spectrum (figure 2.12), the complexes have different characteristics around the split band (580 – 680 nm) region. This indicates that the type of substituent on the anilino ring of the ligand plays a role in determining the type of form the compound exists in when in solution.

For instance, in the case of $Ru_2(OAc)_3$(2-Fap)Cl compound, the band at 588 nm is more intense than the band at 678 nm. The split band indicates an overlapping of two bands, meaning that there are two forms of this compound in solution and one is in greater amounts as compared to the other. The $Ru_2(OAc)_3$(2-Fap)Cl compound contains an electronegative substituent, fluorine. This electron withdrawing substituent decreases the electron density around the anilino nitrogen bridged with the ruthenium metal, which in turn strengthens the coordination of the axial chloride anion bound to the dimetal unit. The fluorine withdrawing substituent has an effect on the dimetal core such that the species, [$Ru_2(OAc)_3$(2-Fap)Cl] is favoured in solution. This explains the increased absorbance of the band at 588 nm and a shoulder at 678 nm. Therefore, the proposed equilibrium of the complex, $Ru_2(OAc)_3$(2-Fap)Cl in solution is:

$$[Ru_2(OAc)_3(Fap)]^{+} \rightleftharpoons Ru_2(OAc)_3(Fap)Cl \qquad (III)$$

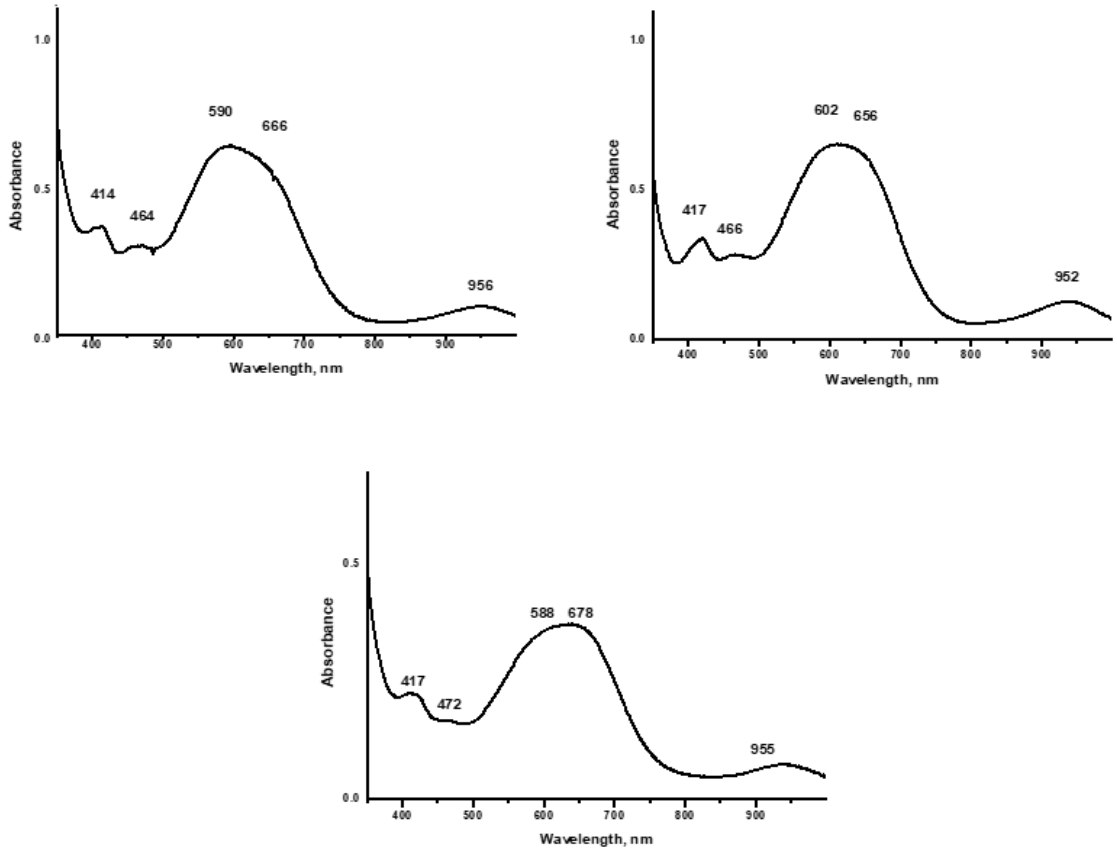


Figure 2.12: UV/Visible spectra of $Ru_2(OAc)_3(ap)Cl$(**C1**), $Ru_2(OAc)_3$(2-Meap)Cl(**C2**), $Ru_2(OAc)_3$(2-Fap)Cl(**C3**).

Table 2.1: UV/Visible peaks of the synthesized complexes.

Compound	λ_{max}, nm, (ε x 10^{-3} mol.cm^{-1})				
	Band 1	Band 2	Band 3	Band 4	Band 5
C1	414(3.27)	464(3.18)	590(3.50)	666(3.46)	956(2.69)
C2	417(3.23)	466(3.15)	602(3.52)	656(3.47)	952(2.80)
C3	417(3.05)	472(2.92)	588(3.25)	678(3.26)	955(2.57)

2.3 $Ru_2(OAc)_3(L)Cl$ with excess halides

It has been reported on one of the fully substituted diruthenium complexes, $Ru_2(F_3ap)_4Cl$ (F_3ap = 2,4,6-trifluoroanilinopyridinate anion) that the compound can axially bind another Cl^- to give, $[Ru_2(F_3ap)_4Cl_2]^-$ in solution.[15] Based on the findings, it was gathered that ion binding could occur for the presently investigated complexes in

the presence of tetrabutylammonium chloride (TBACl) and tetraethylammonium bromide (TEABr), subsequently.

From the UV/Visible spectral results of the synthesized mono-substituted complexes, it could be concluded that the compounds exist in two forms, $[Ru_2(OAc)_3(L)Cl]$ and $[Ru_2(OAc)_3(L)]^+$ in solution. Furthermore, it was shown that that the band at 580-599 nm was as a result of the coordinated species whereas that at 648-690 nm was from the non-coordinated species. In order to prove this hypothesis, excess of halide ions, i.e. Cl^- and Br^- from TBACl and TEABr, respectively, were each added to a series of solutions containing the five complexes investigated and UV/Visible measurements were taken.

In order to study the behaviour of the investigated diruthenium complexes in solution, quaternary ammonium salts such as (TBACl) and (TEABr) were added separately.[19]This procedure was done by preparing 4 x 10^{-4} M concentration of the complexes, $Ru_2(OAc)_3(L)Cl$, as well as 0.01 M of TBACl and TEABr in separate flasks. From the prepared samples, about 3.60 ml of the compound was placed in a quartz cuvette and the UV/Visible spectroscopy was measured. This was followed by an addition of 0.5 ml TBACl to the same cuvette and the spectroscopic measurement was taken for all the investigated complexes. The same process was employed using TEABr instead of TBACl.

UV/Visible spectroscopy measurements of the complexes before and after the addition of TBACl and TEABr were conducted and the results are presented in figure 2.13. The addition of TBACl to **C1** resulted in the band at 666 nm collapsing and that at 590 nm increasing in intensity (figure 2.13). A similar response was observed when TBACl was added to **C2** (figure 2.13). Herewith, it was observed that the equilibrium shifted to the 602 nm region. The difference between **C1** and **C2** UV/Visible spectra can be attributed to the fact that **C2** contains an electron donating group, CH_3 at the ortho position of the nitrogen anilino ring whereas **C1** is without an electron donating group at that position.

The same behaviour was observed when TBACl was added to **C3**, it resulted in a collapse of the band at 678 nm and an increase in intensity of the band at 588 nm (figure 2.13). The addition of TEABr to the same compound (C3) yielded similar results as seen in figure 2.13.

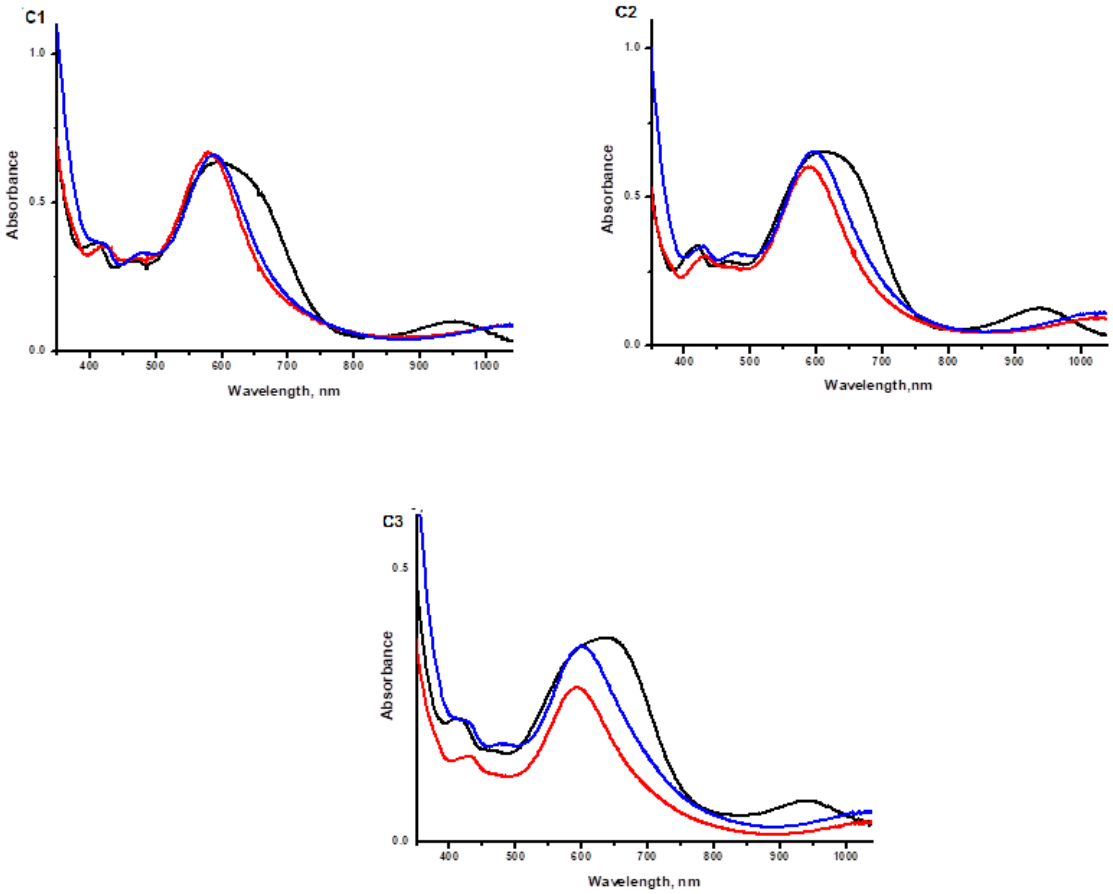


Figure 2.13: UV/Visible spectra of $Ru_2(OAc)_3(ap)Cl$ (**C1**), $Ru_2(OAc)_3(2\text{-}Meap)Cl$ (**C2**) and $Ru_2(OAc)_3(2\text{-}Fap)Cl$ (**C3**) in neat CH_2Cl_2 with TBACl (red) and in neat CH_2Cl_2 with TEABr (blue).

The change in the spectrum after the addition of the halide ions indicated that some of the ions bind to the complex. This observation was supported by Le Chatelier`s principle as the association of chloride is promoted to decrease the concentration of free ions in solution. To further confirm that these compounds behaved in a similar manner when exposed to other anions in solution, TEABr was introduced and the results were similar to those of TBACl (a collapse of 580 – 599 nm and an increase in intensity of 648 – 690 nm). In addition, the addition of halide anions resulted in the disappearance of the weak band at 940-980 nm.

It is interesting to note that whilst the bands may have increased in intensity or collapse after a substitution of the axial ligand, the peak position of the band did not shift. This means that the substitution of the axial ligand does not change the peak position but changing the equatorial ligand results in a peak shift. The change in the spectral behaviour upon the addition of the quaternary ammonium halide salts (TBACl & TEABr) indicated the presence of two species in solution and confirmed the hypothesis that mono-substituted mixed-ligand diruthenium complexes have different spectroscopic properties compared to the other three derivatives, $Ru_2(L)_4Cl$, $Ru_2(OAc)_2(L)_2Cl$ and $Ru_2(OAc)(L)_3Cl$.

The conclusion is that the complexes under investigation exist in two forms, $Ru_2(OAc)_3(L)Cl$ and $[Ru_2(OAc)_3(L)]^+$ in solution before the addition of halide anionic ligands. After the addition of the salts, the spectra changes as the band at 593 nm becomes more pronounced while the shoulder at 661 nm collapses.

The information obtained from UV/Visible spectroscopy indicates that there was a formation of new species involving the coordination of the newly introduced halide. The identity of the species may be $Ru_2(OAc)_3(L)X$ or $[Ru_2(OAc)_3(L)X_2]^-$ as suggested by Kadish *et al*.[15] Below is the equilibrium in solution showing different characteristics before and after the addition of halide anions:

$$[Ru_2(OAc)_3(L)]^+ \rightleftharpoons Ru_2(OAc)_3(L)Cl$$

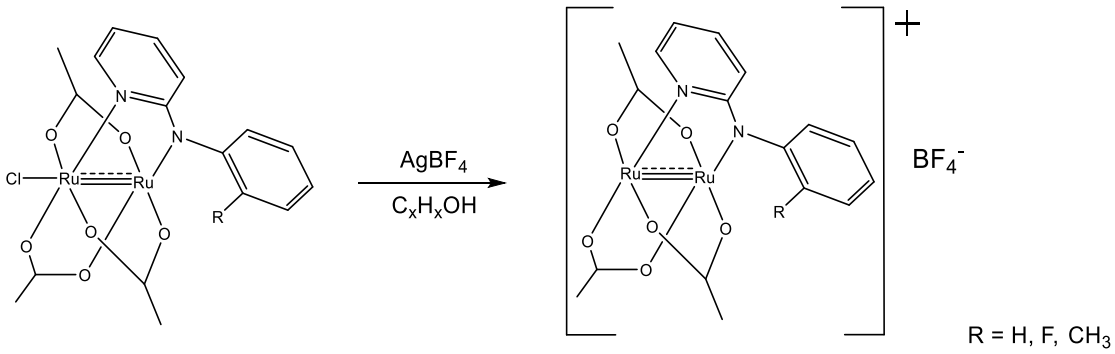
$$[Ru_2(OAc)_3(L)]^+ + X^- \rightleftharpoons Ru_2(OAc)_3(L)X$$

$$[Ru_2(OAc)_3(L)]^+ + 2X^- \rightleftharpoons [Ru_2(OAc)_3(L)X_2]^-$$

2.4 Halide abstraction experiments

Following the successful isolation and characterization of mixed-ligand diruthenium complexes, $Ru_2(OAc)_3(ap)Cl$, $Ru_2(OAc)_3(2\text{-}Meap)Cl$ and $Ru_2(OAc)_3(2\text{-}Fap)Cl$. The next step was to create anionic systems out of the synthesized complexes. Studies show that reacting a mixed-ligand diruthenium complex with a silver containing reagent should precipitate out in the form of AgCl resulting in an outer-sphere positively charged compound.[20]

The goal of the study was to develop diruthenium compounds that are soluble in aqueous solvents such as DMSO and H_2O. To understand the influence of structural changes on the biological activity of these compounds as metallodrugs, the dimetal core was modified by abstracting the axial ligand (Cl^-). A structure of the complex with the axial ligand undergoing structural modification is shown in scheme 2.3.



Scheme 2.3: Modification of a substituted diruthenium complex.

Three complexes, $Ru_2(OAc)_3(ap)Cl$, $Ru_2(OAc)_3(2\text{-}Meap)Cl$ and $Ru_2(OAc)_3(2\text{-}Fap)Cl$ were used as representatives to study the effect silver tetrafluoroborate ($AgBF_4$) has on the dimetal unit and to test a suitable alcohol solvent for every type of a mono-substituted mixed-ligand diruthenium complex. The modified complexes, $[Ru_2(OAc)_3(L)]^+BF_4^-$, were compared to the neutral diruthenium complexes, $Ru_2(OAc)_3(L)Cl$ by UV/Visible spectroscopy to study the effect chloride abstraction has on the dimetal core (figure. 2.14).

2.4.1 UV/Visible spectroscopy of cationic diruthenium complexes.

UV/Visible spectroscopy measurements of the complexes, $Ru_2(OAc)_3(ap)Cl$, $Ru_2(OAc)_3(2\text{-}Fap)Cl$ and $Ru_2(OAc)_3(2\text{-}Meap)Cl$ in different solvents, EtOH, MeOH and *i*-PrOH are shown below. The $Ru_2(OAc)_3(2\text{-}Fap)Cl$ complex is insoluble in iso-propanol hence ethanol was used. A 1:1 molar reaction of this compound with $AgBF_4$ shows a shift in equilibrium whereby the original spectrum shows one form, $Ru_2(OAc)_3(2\text{-}Fap)Cl$ dominant in solution. After the chloride anion abstraction, the intensity of the band at 660 nm increased whereas that at 590 nm decreased.

The reaction of $Ru_2(OAc)_3(ap)Cl$ with $AgBF_4$ in iso-propanol proved to favour the dissociated species, $[Ru_2(OAc)_3(ap)]^+$ in solution. From TBACl and TEABr tritrations, we could conclude that the addition of a halide anion favours the coordinated species in solution. The opposite was observed upon the addition of $AgBF_4$ whereby, a decrease in intensity of the peak at 588 nm and an increase in intensity of 678 nm band were observed. This implies that reactions of these complexes with $AgBF_4$ has an impact on the dimetal core as evidenced by UV/Visible spectroscopy (figure 2.14).

For the $Ru_2(OAc)_3(2\text{-Meap})Cl$ complex, reaction with $AgBF_4$ in iso-propanol also proved to favour the positively charged species, $[Ru_2(OAc)_3(2\text{-Meap})]^+$ in solution. However, the peak at 602 nm was still present but it was not well defined, this was a positive sign because it confirmed that with time and a different solvent type, the chloride anion can be removed altogether leaving only the charged species in solution.

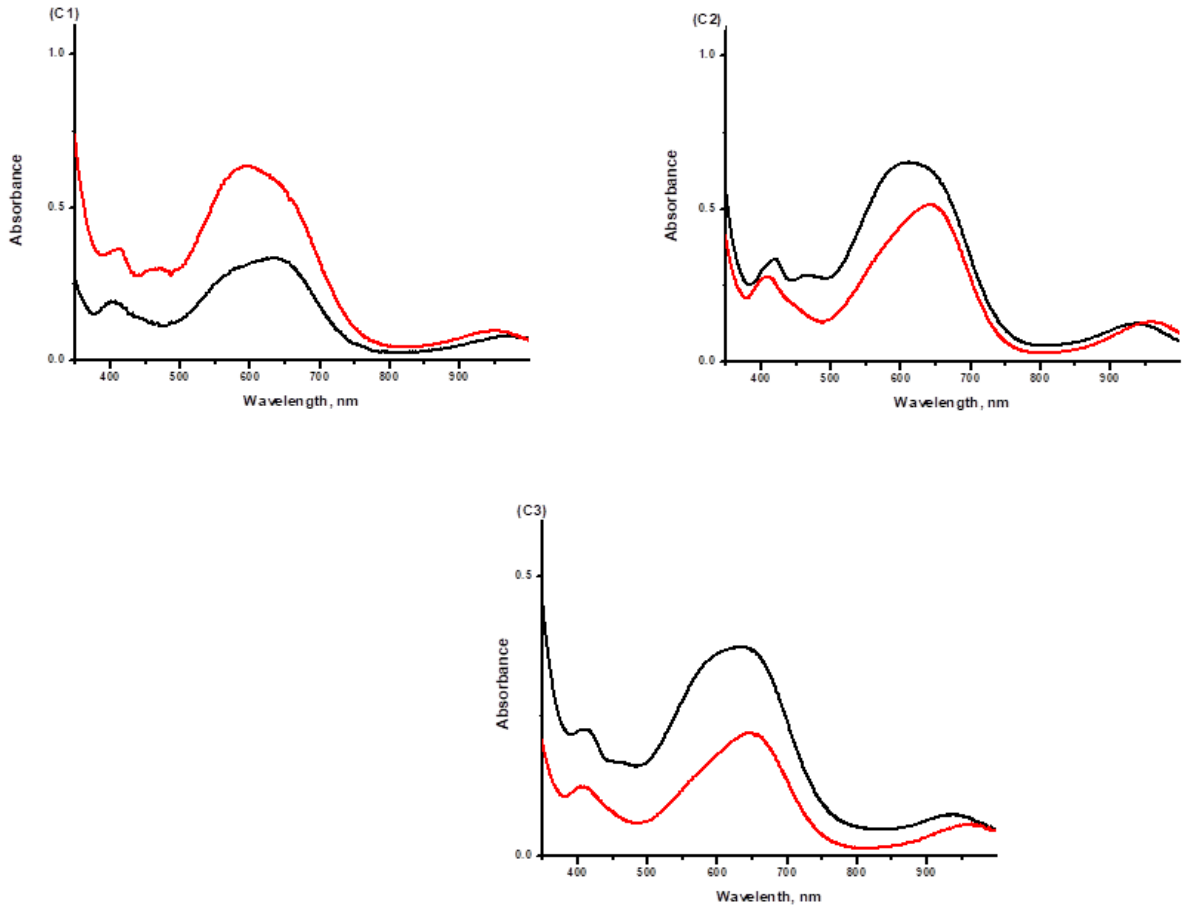


Figure 2.14: UV/Visible spectra of $Ru_2(OAc)_3(ap)Cl$ in *i*-prOH , $Ru_2(OAc)_3(2\text{-Meap})Cl$ in i-prOH and $Ru_2(OAc)_3(2\text{-Fap})Cl$ in etOH after reacting with $AgBF_4$.

The UV/Visible spectral changes discussed above confirmed that reaction of mixed-ligand diruthenium complexes with $AgBF_4$ results in changes in the behaviour of the species in solution. According to the results obtained from UV/Visible spectra, it is evident that the $AgBF_4$ is a good reagent for chloride axial abstraction, and that optimizing reaction time and solvent type can completely remove the halide anion (Cl^-) from the diruthenium unit.

2.5 Conductivity studies

To further study the nature of the investigated complexes, molar conductivities were measured in different solvents, MeOH, EtOH and *i*-PrOH. Conductivity measurements have normally been used in complexes coordinated to various ligands to test their solubility in different solvents. The degree of ionization of the complex can be provided by measuring its conductivity.[21] This was done under the premise that soluble complexes will have a higher molar conductivity as compared to partially or non-soluble complexes. A higher molar conductivity implies that the complex liberates molecular ions in solution.[22]

The molar conductivities of the three compounds were found to be in the electrolytic range 4-12 µs. It is clear from the conductivity data that the complex containing an electronegative substituent, F, is more soluble in MeOH and this is because the compound is more polar, therefore, expected to dissolve in polar solvents because ‘’like dissolves like’’.

2.6 Conclusions

Mixed-ligand diruthenium complexes were successfully synthesized and characterized as to their spectroscopic properties. These compounds were prepared in a stepwise metathesis displacement reaction by reacting tetracarboxylate compound with HL in refluxing methanol. Mono-substituted diruthenium complexes were found to exhibit different spectroscopic behavior in solution as compared to the further substituted diruthenium complexes, $Ru_2(OAc)_2(L)_2Cl$, $Ru_2(OAc)(L)_2Cl$ and $Ru_2(L)_4Cl$.

The difference is seen on the UV/Visible spectra where there is an overlapping of two peaks, resulting in a shoulder at the 640 nm region, this behavior was attributed to the existence of chemical equilibrium involving the association and dissociation of the anionic axial ligand of the neutral complex.

The change in the UV/Visible spectra after the addition of the quaternary halide salt, TBACl and TEABr indicates the presence of two species in solution which is a characteristic of mono-substituted mixed-ligand diruthenium complexes. Electron withdrawing containing diruthenium complexes show good solubility in polar solvents such as MeOH whereas methyl containing diruthenium complexes are soluble in slightly polar solvents; the observations agree with conductivity measurements.

2.7 Experimental

2.7.1 Materials and instrumentation

The reagents, 2-bromopyridine and all the substituted anilines (aniline, 2-fluoroaniline and 2-methylaniline) were purchased from Sigma-Aldrich and were used as received. All solvents, acetonitrile, acetone, chloroform, dichloromethane, ethanol, ethyl acetate, hexane, iso-propanol and methanol were purchased from Sigma-Aldrich and were distilled before use. Silica gel (Merck 230-400 mesh 60 Å) was purchased from sorbent technologies and used as received. Tetra-n-butylammonium chloride (TBACl), tetraethylammonium bromine (TEABr) and tetra-n-butylammonium perchlorate (TBAP) were purchased from Sigma-Aldrich and were used without further purification. Silver trifluoroborate ($AgBF_4$) was purchased from Sigma-Aldrich.

The NMR spectra were recorded on a Bruker Avance 300 MHz and 500 MHz. The infrared spectra were recorded on a Bruker FTIR spectrometer. Mass spectrometry was performed using Advison Expression L compact. CHNS elemental microanalysis was performed on a Flash 2000 CHNS-O Analyzer fitted with an Auto sampler. UV/Visible spectroscopy experiments were carried out with a BASi instrument.

2.7.2 Ligand synthesis

2.7.2.1 Synthesis of Hap

2-Bromopyridine (13.00 ml; 0.136mol) and aniline (25.00ml; 0.273 mol) were placed in a 250 ml round-bottom flask equipped with a condenser and magnetic stirring bar. The mixture was heated at 170 °C for 9 hours. During the reaction, the mixture changed colour from transparent yellow to purple. Upon completion of the reaction, 10% NaOH (100 ml) was added to the flask, and the mixture was stirred for a further 15 minutes at room temperature. The contents of the flask were then steam distilled.

The residue remaining in the flask was extracted with CH_2Cl_2 (3 x 50 ml). The organic phase was then collected and dried with $MgSO_4$. The CH_2Cl_2 distilled with a rotary evaporator and the deposit was recrystallized with boiling hexane to afford white crystals. Yield:20.16 g, 87 %. [*m/z* (fragment)]: 171.0 $[Hap]^+$.^{1}H NMR in $CDCl_3$: 8.24(d, H^a), 7.53(dd, H^c), 7.35(d, H^e;H^f), 7.05(m, H^g), 6.90(d, H^d), 6.50(dd, H^b), 6.50(s, NH) ppm.^{13}C NMR: 108.3, 115.0, 120.40, 122.8, 129.3, 137.50, 140.4, 148.35, 156.03 ppm. FTIR (cm^{-1}): ν(N-H) 3247, ν(C-H) 307, ν(C=N) 1589, ν(C-C) 1463. Anal. Calc for $C_{11}H_{10}N_2$: C, 77.62; H, 5.92, N, 16.46. Found: C, 77.55, H, 5.24, N, 16.74.

2.7.2.2 Synthesis of H(2-Meap)

2-Methylaniline (30.00 ml; 0.282 mol) and 2-bromopyridine (15.00 ml; 0.157 mol) in a 250 ml round bottom flask at 170 °C for 14 hours. During the reaction, the contents of the round bottom flask were observed to have changed colour form transparent yellow to brown-orange. At the end of the reaction, 10% NaOH (100 ml) was added to the reaction mixture. The product was then steam distilled and the crude product that remained in the flask was extracted with CH_2Cl_2 (3 x 50 ml). The organic phase was collected and dried with $MgSO_4$.

This was followed by the removal of the solvent using a rotary evaporator and the resulting residue was recrystallized with boiling hexane and white crystals were isolated and dried under high vacuum. Yield:27.48 g, 95 %. [*m/z* (fragment)]: 185.40 $[H(2\text{-Meap})]^+$. ^{1}H NMR in $CDCl_3$: 8.10(d, H^h), 7.43(td, H^c; H^f), 7.18(m,H^e;H^d), 7.05(d, H^a), 6.62 (m, H^g;H^b), 6.30(s, NH), 2.23(s, CH_3) ppm. ^{13}C NMR: 18.00, 107.5, 114.00, 122.40, 124.3, 127.40, 132.21, 133.58, 135.66, 137.32, 148.54, 155.5 ppm. FTIR (cm^-

[1]): ν(N-H) 3155, ν(C-H) 2941, ν(C=N) 1527, ν(C-C) 1425. Anal. Calc for $C_{12}H_{12}N_2$: C, 78.23; H, 6.57, N, 15.21. Found: C, 78.15, H, 6.25, N, 15.23.

2.7.2.3 Synthesis of H(2-Fap)

2-Fluoroaniline (25.00 ml; 0.258 mol) and 2-bromopyridine (13.00 ml; 0.136 mol) were placed in a 250 ml round-bottom flask equipped with a condenser and a magnetic stirrer bar. The homogeneous mixture was heated at 170 °C overnight. A colour changed from yellow to purple was observed. 10% NaOH (100 ml) was added to the mixture, which was stirred for a further 15 minutes at room temperature. The mixture was steam distilled and the crude product was extracted withCH_2Cl_2 (3 x 50 ml) and the organic phase was collected and dried with $MgSO_4$.

The solvent was removed with a rotary evaporator and the residue was recrystallized with hot hexane to afford white crystals. Yield: 21.70 g, 85%. [*m/z* (fragment)]: 189.1[H(2-Fap)]$^+$.^{1}H NMR in $CDCl_3$: 8.26(d, H^a), 8.04(dd,H^c), 7.54(m, H^b), 7.15(m, H^h;H^e), 7.00(m, H^f), 6.80 (dd, H^d;H^g), 6.65(s, NH) ppm. ^{13}C NMR 109.90, 115.25, 115.41, 115.51, 121.05, 122.55, 122.60, 124.38, 124.42, 128.83, 128.85, 137.81, 147.88, 154.51, 155.30, 155.60 ppm. FTIR (cm^{-1}): ν(N-H) 3257, ν(C-H) 2991, ν(C=N) 1682, ν(C-C) 480. Anal. Calc for $C_{11}H_9N_2F$: C, 70.20; H, 4.82; N, 14.88. Found: C, 70.18; H, 4.66; N, 15.18.

2.7.3 Complex synthesis

2.7.3.1 Synthesis of $Ru_2(OAc)_4Cl$

The precursor, $Ru_2(OAc)_4Cl$ was successfully synthesized by stirring and refluxing $RuCl_3 \cdot 3H_2O$ (2.5 g, 0.012 mol) with LiCl (2.67 g, 0.062 mol) in a 42 ml solution of 17 % acetic anhydride in glacial acetic acid. The dark brown reaction mixture was heated to 160 °C in a slow stream of oxygen for 16 hours. The reaction was left to cool in the refrigerator overnight and the solution changed colour from brown to military green. The precipitate was filtered and washed with glacial acid (2 x 40 ml).

Red-brown micro crystals were isolated and dried. Yield: 4.59 g, 80 %. [*m/z* (fragment)]: 474.593 [$(Ru_2(OAc)_4Cl)$]$^+$. FTIR data (cm^{-1}): ν(COO)1403, ν(COO)1445. UV/Visible spectrum data in MeOH, ($\lambda_{max,}$ nm): 445.

2.7.3.2 Synthesis of $Ru_2(OAc)_3(ap)Cl$

The $Ru_2(OAc)_3(ap)Cl$ complex was synthesized by heating $Ru_2(OAc)_4Cl$ (520 mg; 1.09 mmol) and Hap (939 mg; 1.09 mmol) in methanol (100 ml) at 63 °C for 90 minutes. During the reaction, the solution changed colour from brown to blue-green. After the reaction had been completed, the resulting solution was concentrated, and the residue was washed with dichloromethane (3 x 40 ml).

The resulting sample was isolated on a silica chromatography using ethyl acetate as an eluent. The fraction of interest was dried, and a blue powder was isolated. Yield: 0.39 g, 62 %. [*m/z* (fragment)]: 584.80 $[Ru_2(OAc)_3(ap)Cl]^+$, 549.34 $[Ru_2(OAc)_3(ap)]^+$. Anal. Calc for $Ru_2C_{17}O_6H_{21}N_2Cl$: C, 34.79; H, 3.61; N, 4.77. Found: C, 35.67; H, 3.54; N, 4.36.

2.7.3.3 Synthesis of $Ru_2(OAc)_3(2\text{-}Meap)Cl$

A mixture of $Ru_2(OAc)_4Cl$ (512 mg; 1.08 mmol) and H(2-Meap*)* (200 mg; 1.08 mmol) in methanol (100 ml) was heated at 63 °C for 2 hours. During this period, the solution changed colour from brown to blue-green. The resulting solution was washed with dichloromethane (3 x 40 ml) to remove the unreacted diruthenium tetracarboxylate, ($Ru_2(OAc)_4Cl$). The filtrate was dried using a rotary evaporator.

This was followed by purification on a column chromatography using silica gel as a stationery phase and ethyl acetate as an eluent. A blue solid was isolated. Yield: 0.37 g, 59 %. [*m/z* (fragment)]: 594.20 $[Ru_2(OAc)_3(2\text{-}Meap)Cl]^+$,558.74 $[Ru_2(OAc)_3(2\text{-}Meap)]^+$. Anal. Calc for $Ru_2C_{18}O_6H_{23}N_2Cl$: C, 35.97; H, 3.86; N, 4.66. Found: C, 35.99; H, 3.87; N, 4.53.

2.7.3.4 Synthesis of $Ru_2(OAc)_3(2\text{-}Fap)Cl$

$Ru_2(OAc)_4Cl$ (500 mg; 1.05 mmol) and H(2-Fap) (198 mg; 1.05 mmol) in methanol (100 ml) was heated at 63 °C for 90 minutes. The progress of the synthesis was monitored by thin-layer chromatography and ethyl acetate was used as an eluent. During this period, the solution changed colour from brown to blue-green and resulting suspension was washed with dichloromethane (3 x 40 ml) to remove unreacted starting material, $[Ru_2(OAc)_4Cl]$.

The filtrate was dried using a rotary evaporator and this was followed by purification of the compound on a silica chromatography. The solvent was removed on a rotary evaporator and the residue was dried on a high vacuum pump to isolate a blue solid. Yield: 0.30 g, 48 %. [*m/z* (fragment)]: 601.20 $[Ru_2(OAc)_3(2\text{-Fap})Cl]^+$, 565.74 $[Ru_2(OAc)_3(2\text{-Fap})]^+$. Anal. Calc for $Ru_2C_{17}O_6H_{20}N_2ClF$: C, 33.15; H, 3.33; N, 4.63. Found: C, 33.51; H, 3.87; N, 3.60.

2.8 References

(1) Stephenson, T. A.; Wilkinson, G. *Journal of Inorganic and Nuclear Chemistry.***1966**, *28*, 2285–2291.

(2) Manowong, M.; Han, B.; McAloon, T. R.; Shao, J.; Guzei, I. A.; Ngubane, S.; Van Caemelbecke, E.; Bear, J. L.; Kadish, K. M. *Inorganic Chemistry.* **2014**, *53* (14), 7416–7428.

(3) Bennett, M. J.; Caulton, K. G.; Cotton, F. A. *Inorganic Chemistry.***1969**, *8* (1), 1–6.

(4) Majumdar, M.; Saha, S.; Dutta, I.; Sinha, A.; Bera, J. K. *Dalton Transactions.***2017**, *46 (17)*, 5660–5669.

(5) Kadish, K. M.; Phan, T. D.; Giribabu, L.; Shao, J. G.; Wang, L. L.; Thuriere, A.; Van Caemelbecke, E.; Bear, J. L. *Inorganic Chemistry.* **2004**, *43* (3), 1012–1020.

(6) Chisholsm, M. H.; Christou, G.; Folting, K.; Huffman, J. C.; James, C. A.; Samuels, J. A.; Wesemann, J. L.; Woodruff, W. H. *Inorganic Chemistry.***1996**, *35*, 3643–3658.

(7) Barral, M. C.; Herrero, S.; Jiménez-Aparicio, R.; Torres, M. R.;Urbanos, SpavF. A. *Angewandte Chemie International Edition in English*. **2005**, *44*, 305–307.

(8) Barral, M. C.; Gallo, T.; Herrero, S.; Jiménez-Aparicio, R.;Torres, M. R.; Urbanos, F. A. *Inorganic Chemistry.* **2006**, *45*, 3639−3647.

(9) Bararuddin, E.; Aiyub, Z.; Abdullah, Z. *Malaysian journal of analytical science.* **2008**, *12(2)*, 285–290.

(10) Bear, J.L.; Han, B.; Wu, Z.; Van Caemelbecke, E.; Kadish, K. M. *Inorganic Chemistry.* **2001**, *40*, 2275–2281.

(11) Schmedate, T. A.; Haaf, M.; Paradise, B. J.; Millervolte, A. J.; Powell, D. R.; West, R. *organometallic Chemistry.* **2001**, *636(1)* (636(1)), 17–25.

(12) Cotton, F. A.; Murillo, C. A.; Walton, R. A. *Multiple bonds between metal atoms, 3rd ed.; Springer science and business media, Inc: New York, USA*; **2005**.

(13) Klei, B.; Teuben, J. H. J. *Chemical Communications.***1978**, 1978.

(14) Bruce, M. T. *Angewandte Chemie International Edition in English.***1977**, *16*, 73.

(15) Kadish, K. M.; Garcia, R.; Phan, T.; Wellhoff, J.; Van Caemelbecke, E.; Bear,

J. L. *Inorganic Chemistry.* **2008**, *47 (23)*, 11423.

(16) Miskowski, V. M.; Wange, L,-L.; Thuriere, A.; Van Caemelbecke, E.; Bear, J. L. *Inorganic Chemistry.* **2003**, *42*, 834.

(17) Kadish, K. M.; Phan, T. D.; Giribabu, L.; Caemelbecke, E. Van; Bear, J. L. *Dalton Transactions.* **2003**, *42* (26), 8663–8673.

(18) Bino, A.; Cotton, F. A.; Felthouse, T. R. *Inorganic Chemistry.***1979**, *18*, 2599.

(19) Hinz, A.; Schulz, A.; Villinger, A. *Chemical Communications.* **2013**, *0* (37), 1–3.

(20) Dunlop, K.; Wang, R.; Stanley Cameron, T.; Aquino, M. A. S. *Journal of Molecular Structure.* **2014**, *1058* (1), 122–129.

(21) Refat. M.S. *Molecular structure.* **2007**, *842*, 24.

(22) Refat, M.S.; El-Deen, I. M.; Zein, M. A.; Adam, A. M. A.; Kobeasy, M. I.*International Journal Electro Science.* **2013**, *8*, 9894–9917.

Chapter 3

Electrochemistry of mixed-ligand diruthenium complexes

3.1 Introduction

Electrochemical characterization of Ru_2^{5+} diruthenium complexes can undergo two-metal centered oxidations and a one metal centered reduction to give Ru_2^{6+}, Ru_2^{7+} and Ru_2^{4+} oxidation states of the compound, respectively.[1] This was observed under nitrogen atmosphere. Under CO atmospheric conditions, five oxidation states Ru_2^{6+}, Ru_2^{5+}, Ru_2^{4+}, Ru_2^{3+}, Ru_2^{2+} of the same compounds are accessible and it was found to be due to the substitution of CO with the axial ligand.[1,2] CO coordination results in the stabilization of lower oxidation states due to molecular orbitals interactions of CO and d orbitals of the metal core.[3]

It has been reported that systematic changes in the bridging ligands affects the redox potential of the dimetal core.[2] The discovery led to the interest in investigating the effect different substituents have on the Ru_2^{5+} unit, and to monitor how half-potentials ($E_{1/2}$) vary moving from an electron donating to an electron withdrawing substituent.

Previous studies have shown that there are four redox reactions for mixed-ligand diruthenium complexes with the general formula, $Ru_2(OAc)_x(L)_{4-x}Cl$ (x = 1- 4).[4] These compounds are mostly analyzed in non-aqueous solvents such as anhydrous acetonitrile, dichloromethane or benzonitrile and are always reversible, this corresponds to the reduction or oxidation processes of the dimetal unit.[4]

The redox properties of the mixed-ligand diruthenium complexes can be altered by the electronic properties of the bridging ligands with different subtituents.[5] These anionic bridging ligands have electron withdrawing or donating substituents at the ortho, meta and para position on the anilino ring of the ligand. The electronic factor of the ligand affects the axial ligand coordinated to the dimetal core. [4,5]

Mixed-ligand diruthenium Ru_2^{5+} complexes with two or fewer acetate (OAc) groups were shown to exhibit one-electron reductions and oxidations in CH_2Cl_2 containing 0.1 MTBAP under N_2.[6] A different electrochemical behaviour under the same conditions were observed for the mono-substituted diruthenium complex, $Ru_2(OAc)_3(L)Cl$, and this was attributed to the multiple equilibria that involves different forms of the axially coordinated ligand.[6]

The goal of the study was to examine mono-substituted mixed-ligand diruthenium complexes with different substituents of the anilinopyridinate ligands. The complexes discussed in this section were synthesized from substituted anilinopyridinate ligand and $Ru_2(OAc)_4Cl$ in boiling methanol. Redox chemistry of the mixed-ligand diruthenium complexes presented as $Ru_2(OAc)_3(L)Cl$, where L is one of the anionic bridging ligands (chapter 2, chart 2.2) are discussed.

3.2 Results and discussion

3.2.1 Redox activity of $Fe(C_5H_5)_2$ at electrode surface

Cyclic voltammetry is the most widely used voltammetric techniques for studying the redox behaviour of species in solution and for studying the reaction intermediates.[7] This technique is based on the measuring diffusion controlled current observed in an electrolysis cell. Upon the application of potential in an electrolysis cell which contains electroactive species, redox reactions occur at the electrode surface and current is generated.[7]

The observed current at a particular potential is directly proportional to the concentration of the active species in the absence of interferences.[8] A plot of current versus potential which is called a voltammogram is obtained and it gives analytical useful information on the analyte.[8] In order to confirm diffusion control of the redox process, a small amount of ferrocene, roughly about 5×10^{-5} M was dissolved in CH_2Cl_2 containing 0.10 M TBAP as a supporting electrolyte. A cyclic voltammogram was carried out at different scan rates as shown in figure 3.1.

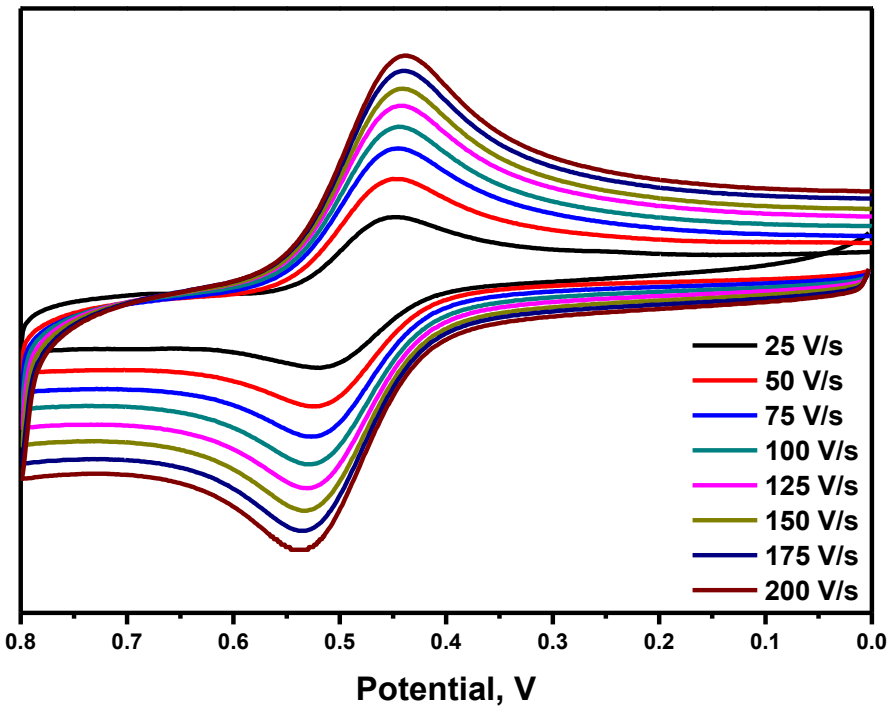


Figure 3.1: Cyclic voltammogram of ferrocene

The Randles-sevcik equation $i_p = 0.4463nFAC(nF\nu D/RT)^{1/2}$ where i_p = current maximum, n= number of electrons transferred in the redox process, A= electrode area in cm^2, F = Faraday constant in C mol^{-1}, D = diffusion coefficient in cm^2/s, ν = Scan rate in mV/s, T = temperature and R = gas constant in K, predicts a linear relationship between ip and $(\nu)^{1/2}$ (figure 3.2).[7,9] The regression was calculated to be $R^2 = 0.984$ which measures the linear relationship between current and scan rate, a value of $R^2 = 0.984$ implies linearity. This confirmed the accuracy of the machine and that it was diffusion controlled, therefore, the investigated compounds could be analyzed using cyclic voltammetry.

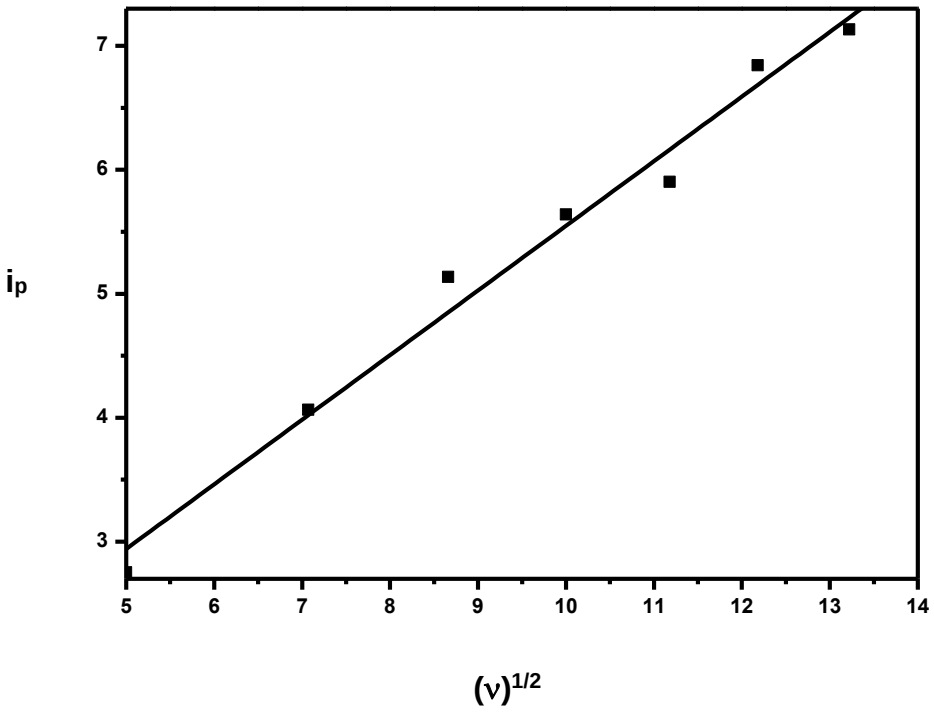


Figure 3.2: An anodic current vs scan rate straight-line graph of ferrocene.

3.2.2 Electrochemistry analysis of Ru_2^{5+} diruthenium complexes.

Previous studies have reported on how the redox potential is affected by changing bridging ligands.[10] Kadish reported on how the redox potential changes from moving from Ru_2(ap-4-Meap)Cl to Ru_2(2-Meap)$_4$Cl as well as $Ru_2(L)_4Cl$ compounds where L= 2-Meap, 2-Fap, ap, 2,3-F_2ap, 2,4-F_2ap, 2,5-F_2ap or 3,4-F_2ap.[10] The findings were that the position of the methyl substituent on the pyridyl group did not affect the structural framework; it however, greatly induced the lability of the axial Cl^- ligand.[10] The induction of the axial chloride results in changes in the electrochemical behaviour and redox activity of the compound.[11]

The compound, Ru_2(3,4-F_2ap)$_4$Cl in CH_2Cl_2 containing 0.1 M TBAP was analyzed under both N_2 and CO atmosphere and compared with other compounds. The cyclic voltammogram of this compound had similar shapes to that of the other compounds and it was observed that their half potentials ($E_{1/2}$) for each electrode reaction, were dependent on the specific number and position of the substituent of the anilinopyridinate ligand.[12] The other $Ru_2(L)_4Cl$ under the same reaction conditions were found to undergo a single one-electron reduction under N_2 but three one-electron reductions were observed under CO atmosphere.[12]

The reduction process of $Ru_2(dpf)_4CO$ was accompanied by axial coordination and this resulted in the formation of two species in solution, $Ru_2(dpf)_4CO$/ $[Ru_2(dpf)_4CO_2]^-$ and it was observed that the $E_{1/2}$ values shifted by 100 mV from the ones obtained under N_2 atmosphere.[13] The existence of two species in solution after the reduction process $Ru_2^{5+/4+}$ of $Ru_2(dpf)_4Cl$ under CO to give $Ru_2(dpf)_4CO$, and the irreversibility of the $Ru_2(3,4\text{-}F_2ap)4Cl$ suggests a similar mechanism for all the $Ru_2(L)_4Cl$ derivatives.[13] It could also be concluded that, $E_{1/2}$ depends on the electronic effect of the anilinopyridinate (ap) substituent.[11,4]

Similar studies were conducted on mixed ligand diruthenium complexes, $Ru_2(OAc)_x(Fap)_{x-4}Cl$ (x = 1-4) where four derivatives were synthesized from a single reaction.[6] These complexes show a reversible one-electron reduction and oxidation processes in CH_2Cl_2 containing 0.10 M TBAP, for multiple substituted compounds with two or less acetate groups, ($Ru_2(OAc)_2(Fap)_2Cl$, $Ru_2(OAc)(Fap)_3Cl$ and $Ru_2(Fap)_4Cl$). A more complex behaviour was observed for a mixed-ligand diruthenium complex substituted by only one anilinopyridinate ligand (H(2-Fap)). This was due to the multiple equillibria ($Ru_2(OAc)_3(L)Cl \rightleftharpoons [Ru_2(OAc)_3(L)]^+$) involving different forms of the axially coordinated chloride.[6]

It was anticipated on the basis of our UV/Visible spectra (chapter 2, figure 2.12) that the axial Cl^- ligand of the investigated complexes might dissociate and associate in solution from each $Ru_2(OAc)_3(L)Cl$ to yield forms, $Ru_2(OAc)_3(L)Cl$ and $[Ru_2(OAc)_3(L)]^+$.In order to further qualify that hypothesis, cyclic voltammetry analyses of the complexes were performed. A representative characterization of the compound, $Ru_2(OAc)_3(2\text{-}Fap)Cl$ by cyclic voltammetry is discussed. Results with a similar consistency were obtained for the other complexes, $Ru_2(OAc)_3(ap)Cl$ and $Ru_2(OAc)_3(2\text{-}Meap)Cl$ and their half potential values are summarized in table 3.1.

3.2.3 Characterization of $Ru_2(OAc)_3(2\text{-}Fap)Cl$ by cyclic voltammogram

$Ru_2(OAc)_3(2\text{-}Fap)Cl$ was dissolved in CH_2Cl_2 containing 0.10 M TBAP under N_2 atmosphere to make up a $4x10^{-4}$ M solution and the cyclic voltammograms are shown in figure 3.3. The cyclic voltammogram of $Ru_2(OAc)_3(2\text{-}Fap)Cl$ was recorded from 0 to 1.60 V (figure 3.3). Herewith, two anodic potentials at 1.14 V and 1.29 V were observed. These potentials indicate that there is two forms, $Ru_2(OAc)_3(2\text{-}Fap)Cl$ & $[Ru_2(OAc)_3(2\text{-}Fap)]^+$ of the compound in solution. The $Ru_2(OAc)_3(2\text{-}Fap)Cl$ species is

easier to oxidize whereas $[Ru_2(OAc)_3(2\text{-Fap})]^+$ harder to oxidize as it is already in its oxidized form. The first oxidation $Ru_2^{5+/6+}$ process under N_2 atmosphere is reversible and the anodic potential is coupled with the re-reduction peak whose Epc value is 0.90 V. Once the chloride is in solution, the positively charged species, $[Ru_2(OAc)_3(Fap)]^+$ coordinates the axial Cl^- ligand and the anodic potential is 1.28 V. After re-oxidation, the chloride dissociated into solution hence there is one reversible peak (figure 3.3).

These findings supported the assumption that there are two forms of the complex in CH_2Cl_2 containing 0.10 M TBAP. The two species could be the neutral and charged species, $Ru_2(OAc)_3(2\text{-Fap})Cl$ and $[Ru_2(OAc)_3(2\text{-Fap})]^+$. When the potential was increased to higher positive potentials, 0 to 1.60 V, the complex became more positively charged, which favoured the coordination of the chloride (figure. 3.3). This explained why multiple peaks were observed on figure 3.3and upon switching potentials, one peak disappeared (figure 3.3). A switch in potential resulted in the uncoordinated chloride coordinating; hence there is one reversible peak. The results imply that at higher positive potentials, there was a higher concentration of the coordinated complex in solution.

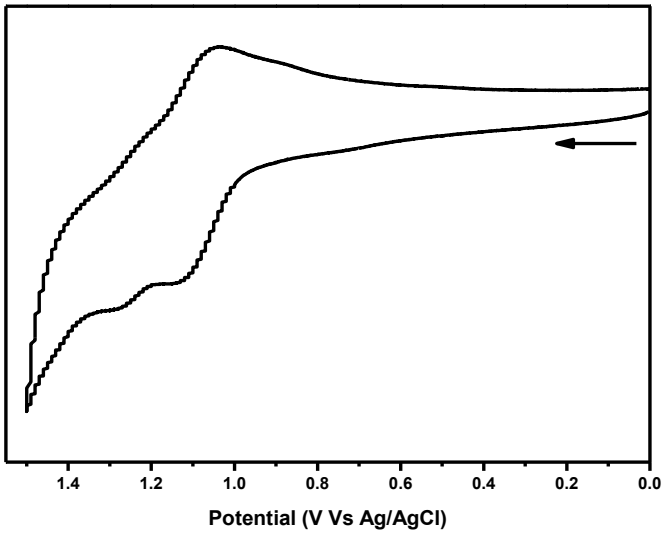


Figure 3.3: Oxidation cyclic voltammograms of $Ru_2(OAc)_3(2\text{-Fap})Cl$ in CH_2Cl_2 containing 0.10 M TBAP at 0.10 V/s scan rate.

coordinated chloride resulting in a positively charged compound, $[Ru_2(OAc)_3(2\text{-Fap})]^+$ in solution. This species was reduced at a cathodic potential of -0.74 V and it is reversible. From the readings, it could be concluded that negative potentials favoured the dissociated species $Ru_2(OAc)_3(2\text{-Fap})]^+$.

After reduction, when the compound got re-oxidised, the coordinated chloride ion dissociated from the ruthenium metal and the dissociated species became favoured. There was no electron transfer in the dissociated species but a chemical reaction, this is because it was in its oxidised form already; hence there was no reversibility of the species (figure 3.4). Similarly, $Ru_2(OAc)_3(2\text{-Fap})Cl$ is harder to reduce than $Ru_2(OAc)_3(2\text{-Fap})]^+$.

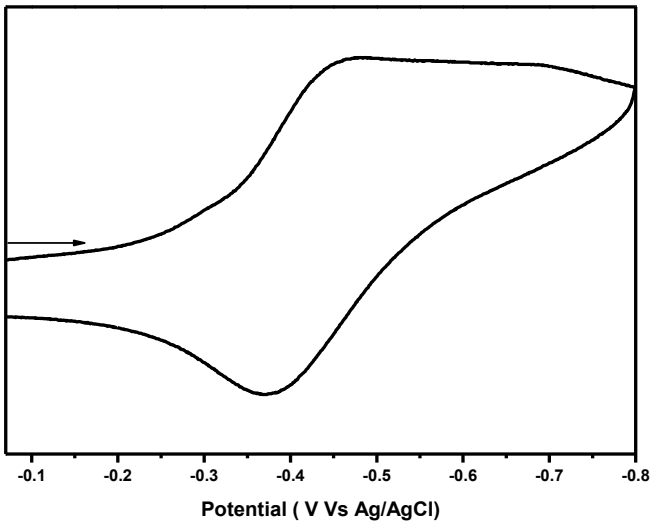
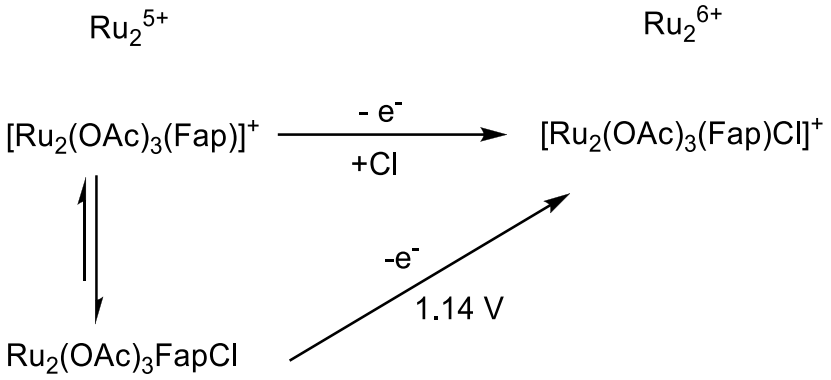


Figure 3.4: Reduction cyclic voltammogram of $Ru_2(OAc)_3(2\text{-Fap})Cl$ in CH_2Cl_2 containing 0.10 M TBAP at 0.10 V/s scan rate.

The results are in agreement with the findings that mono-substituted mixed-ligand diruthenium complexes have a more complex behaviour in solution as 2 anodic potentials, Epa were observed and assigned to the two forms, $Ru_2(OAc)_3(2\text{-Fap})Cl$ and $[Ru_2(OAc)_3(2\text{-Fap})]^+$ of the complex in solution.The proposed redox behaviour mechanism of the complex, $Ru_2(OAc)_3(2\text{-Fap})Cl$ in CH_2Cl_2 containing 0.10 M TBAP at 0.10 V/s scan rate is shown below (scheme.3.1). The compound undergoes one

reversible oxidation state $Ru_2^{5+/6+}$ and a reversible reduction process assigned to $Ru_2^{5+/4+}$.



Scheme 3.1: Reaction mechanism of $Ru_2(OAc)_3$(2-Fap)Cl

The other investigated mixed-ligand diruthenium complexes show similar shaped voltammograms under N_2 atmosphere with values of $E_{1/2}$ for each electrode reaction, depending upon the number and position of substituent of the anilinopyridinate ligands (table 3.1). The complexes undergo a single reversible one-electron reduction in CH_2Cl_2 containing 0.1 M TBAP under N_2.

Table 3.1: Half-wave potentials for $Ru_2^{5+/4+}$ and $Ru_2^{5+/6+}$processes of $Ru_2(OAc)_3$(L)Cl in CH_2Cl_2 containing 0.1 M TBAP.

Ru_2^{5+} compounds	$Ru_2^{5+/4+}$		$Ru_2^{5+/6+}$	
	$E_{1/2}$	ΔE_p[a]	$E_{1/2}$	ΔE_p[a]
$Ru_2(OAc)_3$(ap)Cl	-530	-167	800	149
$Ru_2(OAc)_3$(2-Meap)Cl	-490	180	1060	190
$Ru_2(OAc)_3$(2-Fap)Cl	-570	-260	1020	240

[a]The difference between anodic and cathodic peaks in potential (mV)

3.3 Conclusions

Complexes of the type $Ru_2(OAc)_3(L)Cl$ were examined as to their electrochemistry under N_2. Each compound was converted to Ru_2^{6+} after their first oxidation and to Ru_2^{4+} after their first reduction. Results obtained from cyclic voltammetry were in agreement, showing that mono-substituted mixed-ligand diruthenium complexes exist in two forms in solution. Two anodic peak potentials were observed on the cyclic voltammograms confirming multiple equilibria involving different forms of the axially coordinated chloride.

The compounds were analyzed under the same reaction conditions for comparison purposes. The oxidation properties vary from 0.85 V to 1.20 V in the case of compounds containing electron donating substituents, $Ru_2(OAc)_3$(2-Meap)Cl. As well as $Ru_2(OAc)_3$(ap)Cl, which is without an electron donating substituent. In the case of compounds containing electron withdrawing substituents, $Ru_2(OAc)_3$(2-Fap)Cl, the values were observed from 1.10 V to 1.60 V. This suggests that the type of bridging ligand is an important factor in controlling the redox properties of these compounds.

The substitution of Fap by ap led to a slight positive potential shift for all redox processes. The $Ru_2(OAc)_3$(ap)Cl compound was easily oxidized as compared to the $Ru_2(OAc)_3$(2-Fap)Cl compound and this led to the conclusion that electron withdrawing substituents require higher positive potentials for oxidation. The substituent of the anilinopyridinate ligand has an impact on the half-potential of the Ru_2^{5+} complexes. Varying the substituent type on the anilino ring of the ligand causes a shift of electron density from the dimetal core, anilino and pyridino ring and this results in the change in redox potential.

3.4 Experimental

3.4.1 Material and instrumentation

Cyclic voltammetry was carried out at room temperature under N_2 using a three-electrode system on a BASI Epsilon potentiostat instrument. All the experiments were carried out in dichloromethane. Tetra-n-butlyammonium perchlorate (TBAP) was used as supporting electrolyte. The three-electrode system consisted of a glassy carbon working electrode, Ag/AgCl (sat`dNaCl) reference electrode and platinum auxiliary

electrode. Ferrocene was purchased from Sigma-Aldrich and was used as received. Tetra-n-butlyammonium perchlorate (TBAP) was purchased from Sigma- Aldrich and was stored in the desiccator prior use. Dichloromethane was purchased from Sigma-Aldrich and was distilled over calcium hydride. All the freshly prepared solutions were degassed under nitrogen gas flow before experiments.

3.5 References

(1) Kadish, K. M.; Phan, T. D.; Giribabu, L.; Shao, J. G.; Wang, L. L.; Thuriere, A.; Van Caemelbecke, E.; Bear, J. L. *Inorganic Chemistry.* **2004**, *43* (3), 1012–1020.

(2) Ngubane, S.; Kadish, K. M.; Bear, J. L.; Van Caemelbecke, E.; Thuriere, A.; Ramirez, K. P. *Dalton Transactions.* **2013**, *42*, 3571–3580.

(3) Hoffmann, R.; Alvarez, S.; Meallis, C.; Falceto, A.; Thomas, J. C.; Zeng, T. and M. G. *Chemistry Reviews.* **2016**, *116 (14)*, 8173–8192.

(4) Manowong, M.; Han, B.; McAloon, T. R.; Shao, J.; Guzei, I. A.; Ngubane, S.; Van Caemelbecke, E.; Bear, J. L.; Kadish, K. M. *Inorganic Chemistry.* **2014**, *53* (14), 7416–7428.

(5) Majumdar, M.; Saha, S.; Dutta, I.; Sinha, A.; Bera, J. K. *Dalton Transactions.* **2017**, 46(17),5660-5669.

(6) Kadish, K. M.; Garcia, R.; Phan, T.; Wellhoff, J.; Van Caemelbecke, E.; Bear, J. L. *Inorganic Chemistry.* **2008**, *47 (23)*, 11423.

(7) Zanello, P. *Inorganic Electrochemistry.* **2003**, 661–665.

(8) Grieshaber, D.; MacKenzie, R.Voros.; R.; Reimhult, E.*Biochemistry.* **2008**, *8(3)*, 1400–1458.

(9) Neghmouche, N. S.; Lanez, T. *International Journal of Chemical Studies.* **2013**, *1* (1), 2321–4902.

(10) Kadish, K. M.; Wang, L. L.; Thuriere, A.; Van Caemelbecke, E.; Bear, J. L. *Inorganic Chemistry.* **2003**, *42* (3), 834–843.

(11) Kadish, K. M.; Phan, T. D.; Giribabu, L.; Caemelbecke, E. Van; Bear, J. L. *Dalton Transactions.* **2003**, *42* (26), 8663–8673.

(12) Kadish, K. M.; Nguyen, M.; Caemelbecke, E. Van; Bear, J. L. *Inorganic Chemistry.* **2006**, *45* (15), 10552–10553.

(13) Bear, J.L.; Han, B.; Wu, Z.; Van Caemelbecke, E.; Kadish, K. M. *Inorganic Chemistry.* **2001**, *40*, 2275–2281.

Chapter 4

Cell proliferation studies: Preliminary screening against cancer

4.1 Introduction

Studies of transition metal complexes as anti-cancer agents have been an interesting area since the remarkable efficacy of cisplatin.[1] This study focuses on the development of ruthenium containing compounds as anti-cancer agents. Monoruthemic compounds such as ImH[*trans*-ImDMSORuCl$_4$], (NAMI-A) is one of the compounds undergoing clinical trials.[2,3] This compound has successfully completed phase I clinical trials and functions by inhibiting a membrane protein kinase C, this action triggers a sequence of events that eventually causes the death of cancer cells.[4] The compound, NAMI-A was found to be one of the few agents that have shown favourable results for the treatment of lung tumors.[3]

Other monoruthemic complexes that attracted a lot of interest as chemotherapeutic agents are ruthenium (II) complexes containing arene ligands.[5] Studies of [(Ru(ɲ^6-C$_6$H$_6$)(DMSO)Cl$_2$] show the ability of the compound to inhibit topoisomerase II activity.[5] This compound has three derivatives which can be prepared by substituting the DMSO ligand with 3-aminopyridine, p-aminobenzoic acid and aminoguanidine. [5]

The three analogues of the ruthenium complex show great efficacy against breast and colon carcinoma cells as compared to the parent ruthenium compound.[6] The discovery suggested that substituting ligands coordinated to the metal core can enhance the efficacy against human breast cancer.[7]

The diruthenium complex also examined for potential ant-cancer properties is diruthenium tetracarboxylates, Ru$_2$(OAc)$_4$Cl. This compound was found to be moderately active against P388 lymphocytic leukemia cell lines.[8] The study provided information that the solubility of the tetracarboxylate diruthenium complex can be improved by changing the type of bridging ligand.[9]

4.2 Cytotoxicity studies of mono-substituted diruthenium complexes

In this work, three mono-substituted diruthenium complexes, $Ru_2(OAc)_3$(2-Fap)Cl, $Ru_2(OAc)_3$(ap)Cl and $Ru_2(OAc)_3$(2-Meap)Cl have been studied as potential anti-cancer agents. This was done under the premise that diruthenium complexes containing anilinopyridinate ligands will exhibit different properties from those of the acetate ligands. The three compounds were analyzed using the same procedure as follows:

Ruthenium compounds were tested for their cytotoxicity on adenocarcinoma MCF-7 breast cancer cells using the thiazolyl blue tetrazolium bromide colorimetric assay (MTT assay).[7] This assay was based on the reduction of yellow tetrazolium salt to purple formazan crystals by metabolically active cells. Cells were treated with varying concentrations of the compounds for 48 hours after which the viable cells were quantitated through their ability to convert yellow MTT to purple formazan. The formazan crystals were solubilized in detergent and the resultant absorbance was quantitated spectrophotometrically at 595nm. The absorbance data was fitted to a dose response curve from which an IC_{50} inhibitory concentration for the compound was determined.

Analysis was done based on the fact that cells that were alive were capable of converting the MTT to formazan which is purple in colour. The purple colour on the well plate implied that the cells were alive. The purple colour was obtained and it was sampled as the baseline at 595nm.The introduction of ruthenium complexes under investigation resulted in a decrease in absorbance which was measured in reference to the DMSO. The decrease in absorbance was evidence that the compounds have the potential to inhibit cell replication.

The cytotoxic effect of $Ru_2(OAc)_3(L)Cl$, (L= Fap, ap or Meap) on the adenocarcinoma MCF-7 breast cancer cell lines were examined using MTT assay. A concentration of 5 μM of $Ru_2(OAc)_3(L)Cl$ was used to evaluate the survival rate of the cells for 24 and 48 hours. The same procedure was repeated but with a concentration of 10μM of $Ru_2(OAc)_3(L)Cl$ for 24 and 48 hours.

After 24 hours of 5 μM $Ru_2(OAc)_3$(2-Meap)Cl treatment, a strong dose of cell proliferation was observed. This cell inhibition was indicated by a great decrease of cells from 100 to 30% survival rate shown in figure 4.1. The same effect was observed when 5 μM $Ru_2(OAc)_3$(2-Fap)Cl was used, the metallodrug killed about 60 % of the cells in the well place after 24 hours. The use of $Ru_2(OAc)_3$(ap)Cl resulted in the killing of 50 % of the cells, less effective than the other 2 metallodrugs, $Ru_2(OAc)_3$(2-Fap)Cl and $Ru_2(OAc)_3$(2-Meap)Cl but the decrease in cell survival rate was evident that the drug also exhibit anti-cancer properties.

The three compounds were examined for 48 hours and the increase in cell survival rate could be due to the replication of cells in the plate with time. For comparison and determination of factors that affect apoptosis, the concentration of the metallodrugs were increased to 10 μM. The results of the evaluation are shown in figure 4.2. Examination of $Ru_2(OAc)_3$(ap)Cl shows a decrease of 50 % cell survival rate for both 24 and 48 hours. A strong cell proliferation was observed for the $Ru_2(OAc)_3$(2-Meap)Cl treatment, killing about 70 % of the cells for 24 hours.

For the same compound, increasing incubation to 48 hours resulted in cell multiplication as an increase was from 30 % survival rate for 24 hours to 40 % survival rate for 48 hours. The opposite was observed with the $Ru_2(OAc)_3$(2-Fap)Cl compound, the graph shows a great cell proliferation rate, killing about 73 % of the cells, this implies increasing examination time for the fluoro containing compound inhibits cell multiplication. At 24 hours, the compound only killed 50 % of the cells in the plate. From the survival percentages, we see that the $Ru_2(OAc)_3$(2-Meap)Cl is more effective against breast cancer stem cells as demonstrated by the decrease in the number of cells.

Examination of the methyl containing complex shows a strong cell proliferation at lower and higher concentrations as well as at both times, 24 and 48 hours. The findings were expected because the $Ru_2(OAc)_3$(2-Meap)Cl compound is more soluble in aqueous media, DMSO and H_2O whereas $Ru_2(OAc)_3$(ap)Cl is partially soluble in these solvents. $Ru_2(OAc)_3$(2-Fap)Cl is insoluble in DMSO and H_2O, this is due to the electron withdrawing subtituent on the anilino ring of the ligand.

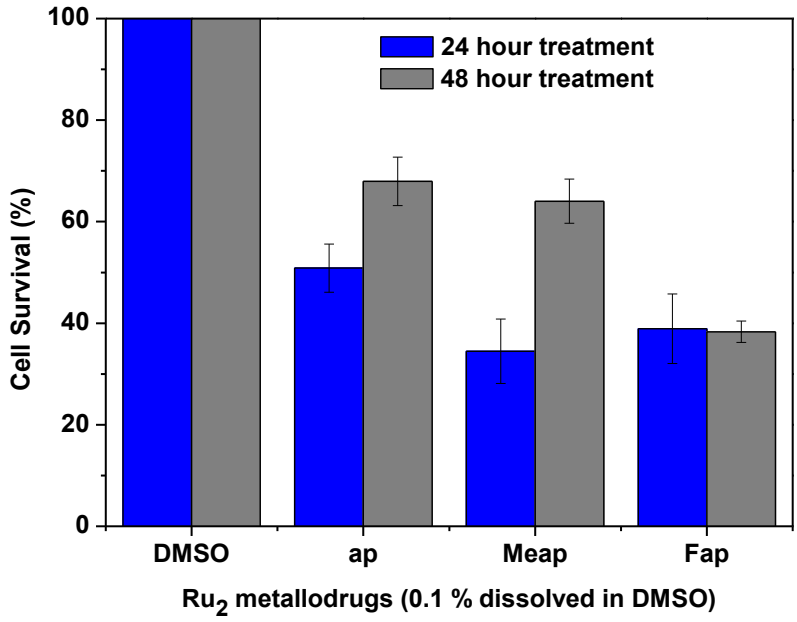


Figure 4.1: Survival rate of MCF-7 cell lines treated with Ru_2 metallodrugs (5 μM) for 24 & 48 hours.

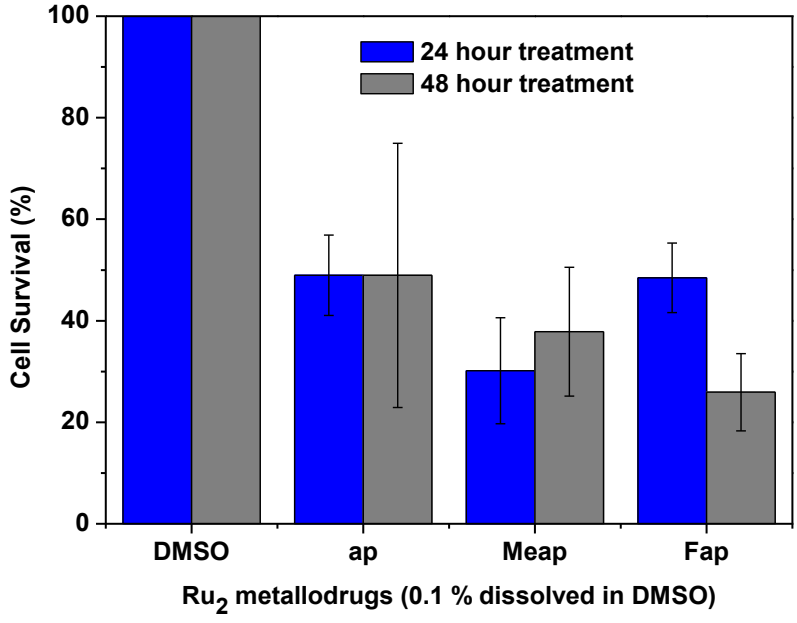


Figure 4.2: Survival rate of MCF-7 cell lines treated with Ru_2 metallodrugs (10 μM) for 24 & 48 hours.

Ruthenium compounds were successfully evaluated for their antiproliferative activity against MCF7 breast cancer cell line at single-dose concentrations of 5 µM and 10µM. Cisplatin and its analogues are some of the most commonly used anti-cancer drugs.[11] However, the side effects as well as multi-drug associated with this line of therapy could not be ignored.

The desired compounds promise improved properties with better solubility as they dissolved in DMSO. Other metallodrugs that have attracted a lot of attention as chemotherapeutic agents are palladium complexes.[11] These complexes were shown to exert anti-tumour activity in cells that resist platinum coordination complexes.[11] The solubility of the synthesized complexes has shown that the compounds are effective as anti-cancer and can be tuned such that cancer cells are not resistant towards them,

4.3 Conclusions

These results show that mono-substituted mixed-ligand diruthenium complexes, $Ru_2(OAc)_3(L)Cl$ exhibit anti-proliferation against breast cancer cells. Moreover, the type of substituent on the ortho position of the anilino ring has an impact on the solubility of the compound in DMSO. Ligand design is paramount in the development of anti-cancer drugs because the methyl containing compound was found to be soluble in aqueous media such as DMSO and H_2O whereas $Ru_2(OAc)_3(ap)Cl$ was partially soluble in these solvents.

Furthermore, the findings indicate that the metallodrugs exert great anti-cancer growth against breast cancer cells even at low concentrations. Taken together, the study indicated that the mixed-ligand diruthenium complexes display cytotoxic effect against breast cancer cells and that the type of substituent on the anilino ring of the ligand has a great impact on the effectiveness of the complex as a drug. The study also suggests that the mono-substituted diruthenium compounds may be useful in the treatment of many different cancers.

4.4 Experimental

4.4.1 Material and instrumentation

Human breast adenocarcinoma MCF-7 (oestrogen receptor positive) cells were maintained in RPMI 1640 medium (Highveld Biological, Lyndhurst, UK).[7] All media were supplemented with 10% fetal bovine serum (FBS), 100U/ml penicillin and 100µg/ml streptomycin. Cells were maintained at 37°C in CO_2 (5%) – air (95%) humidified incubator.

4.4.2 Cytotoxicity assays

Ruthenium compounds were dissolved in DMSO (0.50 ml) to give stock solution concentrations of 5 µM and 10 µM for each compound. The stock solutions were then separately added to the medium to give a master mix concentration such that the concentration of DMSO is kept consistent (0.1% in RPMI medium). Complexes were prepared to their appropriate concentration on the day of treatment and incubated for 24 and 48 hours.

4.4.2.1 24-hour treatment

MCF7 breast cancer cell lines (4.5×10^3) were seeded in 96-well plates. After reaching 60-80 % confluence, cell lines were treated with ruthenium compounds (10µM dissolved in 0.1%DMSO). DMSO was used as the vehicle control. The plate was incubated for 24 hours. After incubation period, MTT solution (10µl) was added to the 96-wells and incubated for 4 hours. 4 hours later, the solubilizing agent (100µl) was added to the 96-wells and the plate was incubated overnight. Cytotoxicity of compounds was assessed by MTT assay (Roche, USA).[10]

Absorbance (595nm) was determined and the mean cell viability was calculated as a percentage of the mean vehicle control. The experiment was conducted in triplicates for each period of treatment and was performed in quadruples for each test compound. The same procedure was followed for the 48 hours incubation.

4.4.2.2 Statistical analysis

Data presented are mean ± SEM (standard error of the means) of two independent experiments and a value of $P < 0.05$ was accepted as statistically significant. The TTEST was used to compare the two experimental time frames

4.5 References

(1) Rosenberg, B.; Vancamp, L.; Trosko, J. E.; Mansour, V. *Nature.***1969**, *222*, 385–386.

(2) Garza-Ortiz, A.; Maheswari, P. U.; Siegler, M.; Spek, A. L.; Reedijk, J. *Inorganic Chemistry.* **2008**, *47* (15), 6964–6973.

(3) Kostova, I. *Current Medicinal Chemistry.* **2006**, *13(9)*, 1085.

(4) Aguirre, J. D.; Angeles-Boza, A. M.; Chouai, A.; Turro, C.; Pellois, J.; Dunbar, K. R. *Dalton Transactions.* **2009**, No. 48, 10806–10812.

(5) Zhang, C. X.; Lippard, S. J. *Current Opinion in Chemical Biology*. **2003**, *7* (4), 481–489.

(6) Gopal, Y. N. V.; Konuru, N.; Kondapi, A. K. *Archivesof Biochemistry and Biophysics*. **2002**, *401*, 53–62.

(7) Aliwaini, S.; Peres, J.; Kröger, W. L.; Blanckenberg, A.; de la Mare, J.; Edkins, A. L.; Mapolie, S.; Prince, S. *Cancer Letters*. **2015**, *357* (1), 206–218.

(8) Chifotides, H.T.; Dunbar, K. R. *Accounts of Chemical Research.* **2005**, *38* (2), 146–156.

(9) Van Rensburg, C. E, J.; Kreft, E.; Swarts, J. C.; Dalrymple, S.R.; Macdonald, D.M.; Cooke, M. W.; Aquino, M. A. S. *Anticancer Research.* **2002**, *22*, 889–892.

(10) Carmichael, J.; Degraff, W.G.; Garzdor, A.F.; Minna, J.D.; Mitchell, J. B. *Cancer Research.* **2010**, *47*, 997–1013.

(11) Westbrook, K.; Stearns, V. *Pharmacology & Therapeutics*. **2013**, 139,1–11.

Chapter 5

Summary and Future work

5.1 Summary and Future work

A series of metal-metal bonded diruthenium complexes, having four equatorial bridging ligands and one axial chloride group have been successfully synthesized and characterized using UV/Visible and FTIR spectroscopy, cyclic voltammetry, elemental analysis as well as mass spectrometry. Stoichiometric amounts of the unsymmetrical aninilinopyridinate derivatives were reacted with $Ru_2(OAc)_4Cl$ in methanol to yield mono-substituted mixed-ligand diruthenium compounds with the general formula, $Ru_2(OAc)_3(L)Cl$.

Each complex exhibited a band between the 581 and 668 nm region as well as a weak band at the 950 nm region which is a characteristic of mono-substituted diruthenium complexes. Complexation of the examined complexes was confirmed by FTIR spectroscopy as the ν(N-H) stretching frequency was expected to disappear upon complexation and this was indeed achieved for all the complexes.

The electrochemical behavior of the compounds in solution under N_2 was studied using cyclic voltammetry. Each compound was converted to Ru_2^{6+} in a one-electron transfer oxidation process and to Ru_2^{4+} in a one-electron transfer reduction process. Two anodic potential peaks, confirming the presence of two forms in solution were observed. Cyclic voltammogram is dependent on the type of substituent of the anilinopyridinate ligand as the chemical equilibrium shifted depending on how electron withdrawing/donating the substituent is.

The change in the spectra after the addition of TBACl and TEABr was an indication that there is a presence of two species of the compound in solution. The addition of a halide anion (Cl^-, Br^-) resulted in a shoulder at 643 nm collapsing and that at 581 nm becoming more pronounced. This indicated the formation of a species involving the co-ordination of the newly formed halide. The identity of the species may be $Ru_2(OAc)_3(L)X$ or $[Ru_2(OAc)_3(X_2)]^-$ as suggested by Kadish and co-workers.

Our cytotoxicity studies results show that the complexes of the formula, $Ru_2(OAc)_3(L)Cl$ have a cytotoxic effect against breast cancer stem cells. The methyl containing complex displayed a low survival rate of the cells, meaning that it killed majority of the cells.The $Ru_2(OAc)_3$(2-Meap)Cl complex is soluble in aqueous media (DMSO and H_2O)and has shown anti-neoplastic activity against tumor cells.

Although the axial chloride ligand was not completely dissociated, there was a clear indication from UV/Visible spectra that reaction with $AgBF_4$ results in a spectral change as the band at 666 nm became more pronounced and that at 581 nm less intense. In future, a bulkier silver salt and a non-coordinating solvent should be used to avoid coordination to the dimetal core as this has an impact on the spectroscopic behavior in solution.

The investigated complexes promise to be effective anti-cancer agents, in future, a series of these complexes will be synthesized and characterized. It is also important to study the effect the position of the subtituent has on the dimetal core of the compound. Moreover, our study focused on examining the complexes on breast cancer cells, it is recommended that their effectiveness is studied on a spectrum of cancers.

6.1 Appendix

Characterization of anilinopyridinate ligands

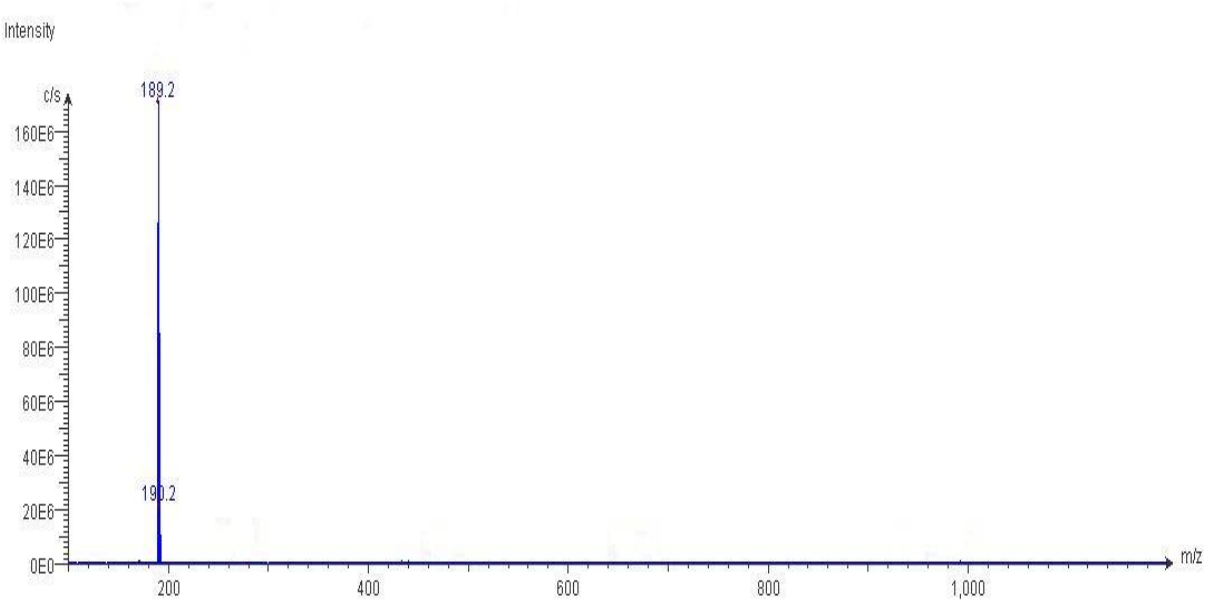


Figure 1x: Mass spectrum of H(2-Fap).

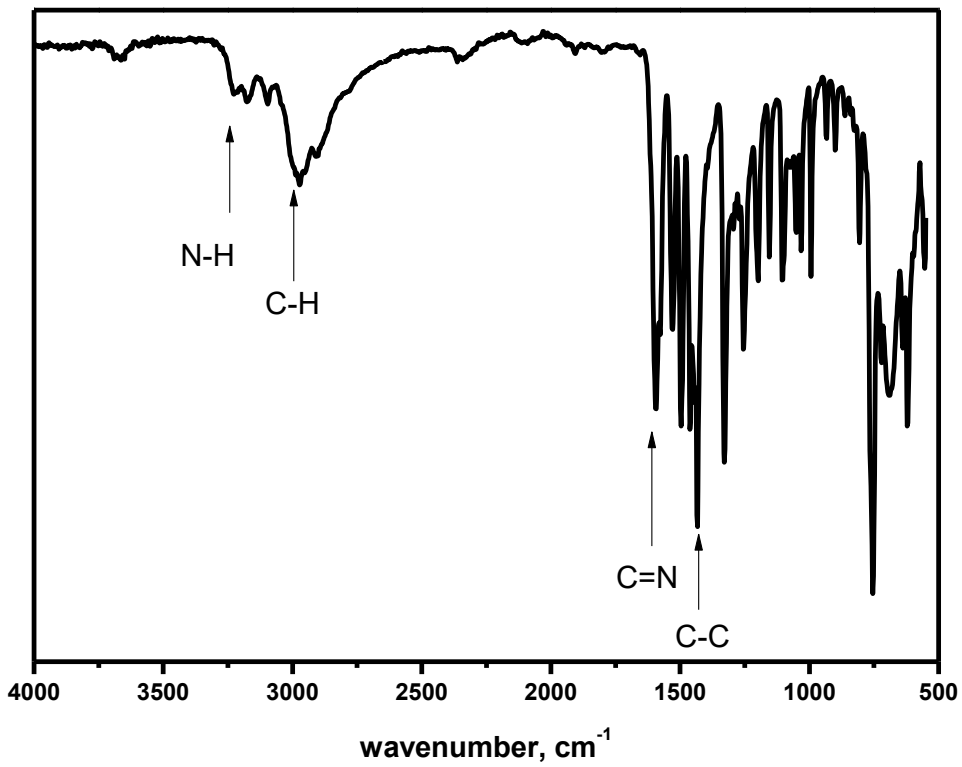


Figure 2x: FTIR spectrum of H(2-Fap).

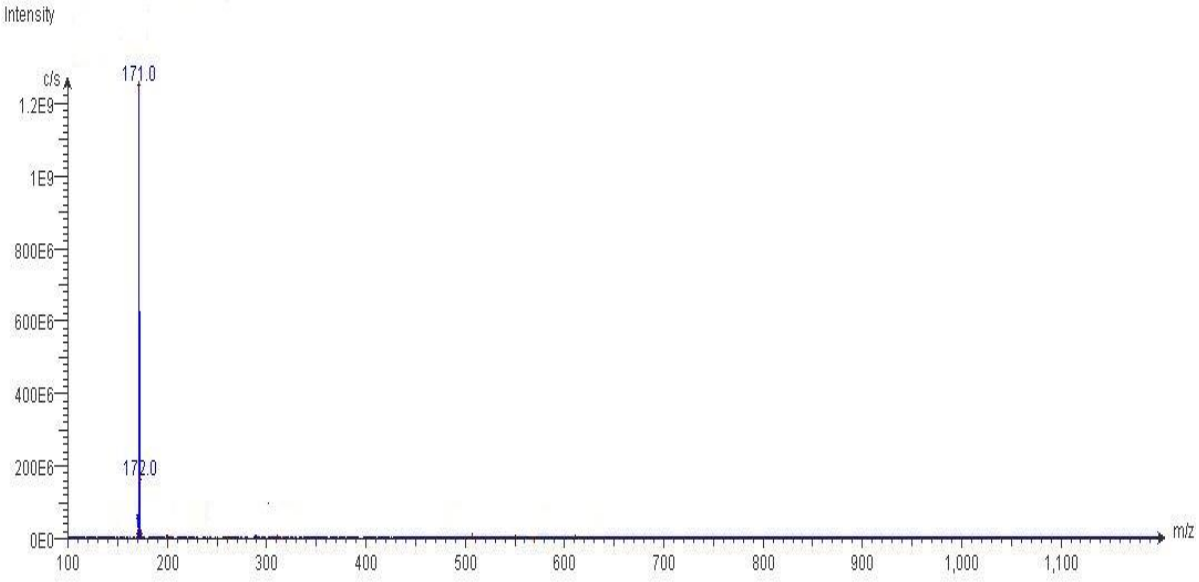


Figure 3x: Mass spectrum of Hap

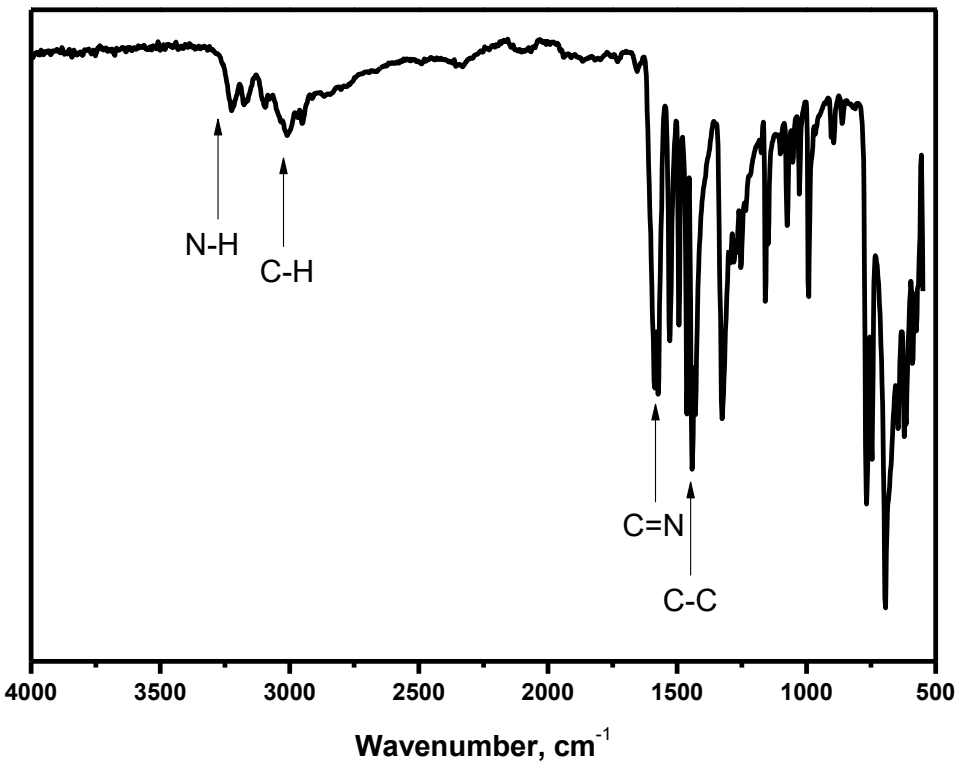


Figure 4x: FTIR spectrum of Hap.

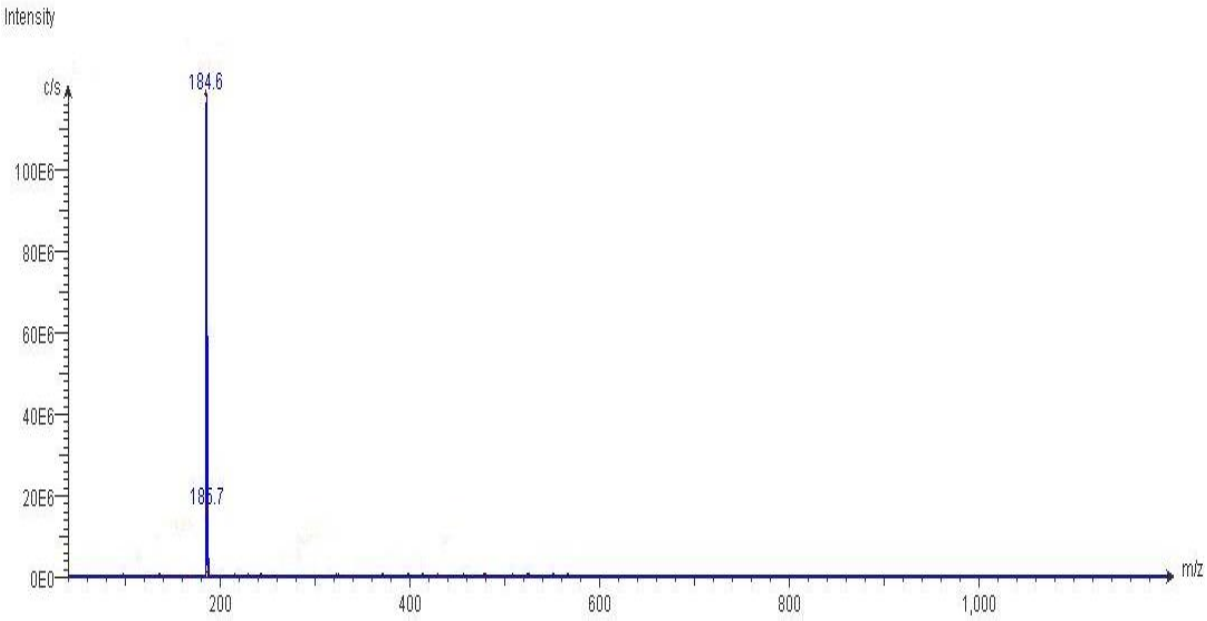


Figure 5x: ^{1}H NMR spectrum of H(2-Meap)

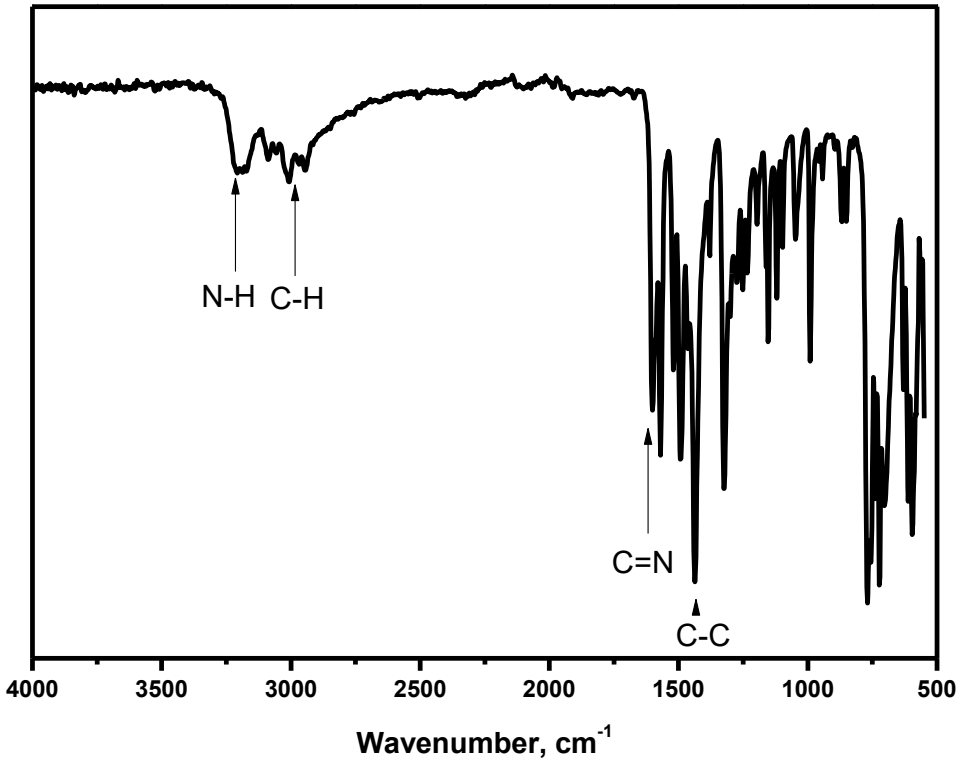


Figure 6x: FTIR spectrum of H(2-Meap).

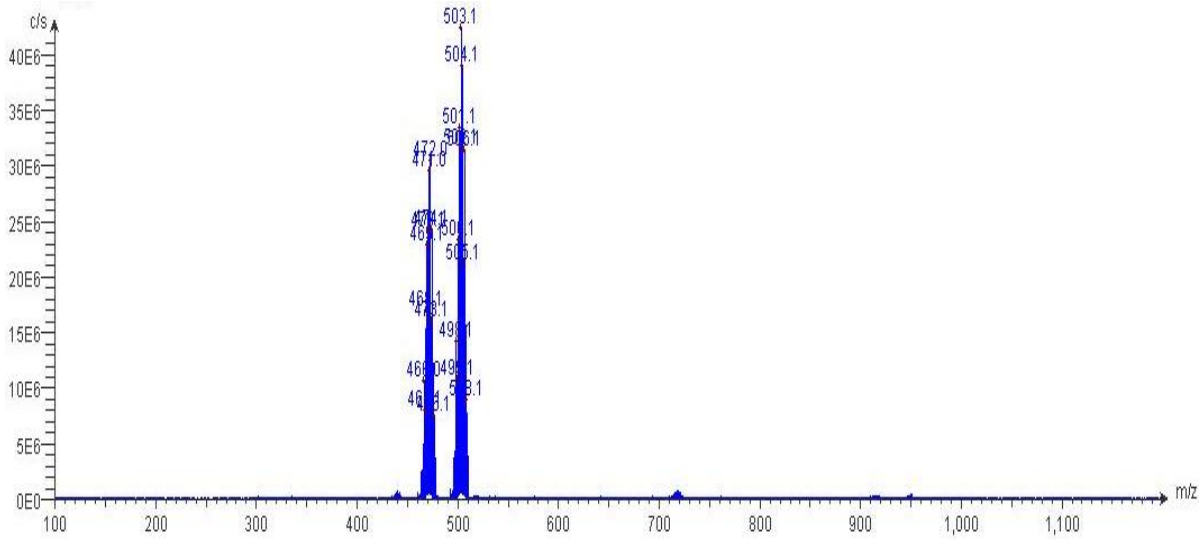


Figure 7x: Mass spectrum of $Ru_2(OAc)_4Cl$

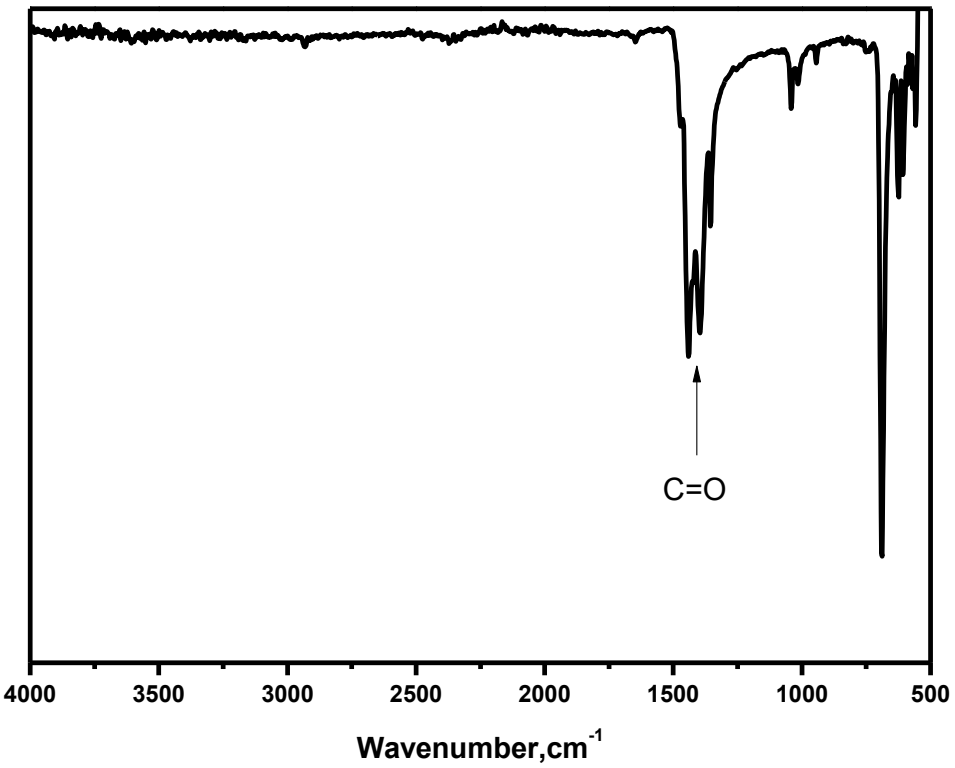


Figure 8x: FTIR spectrum of $Ru_2(OAc)_4Cl$

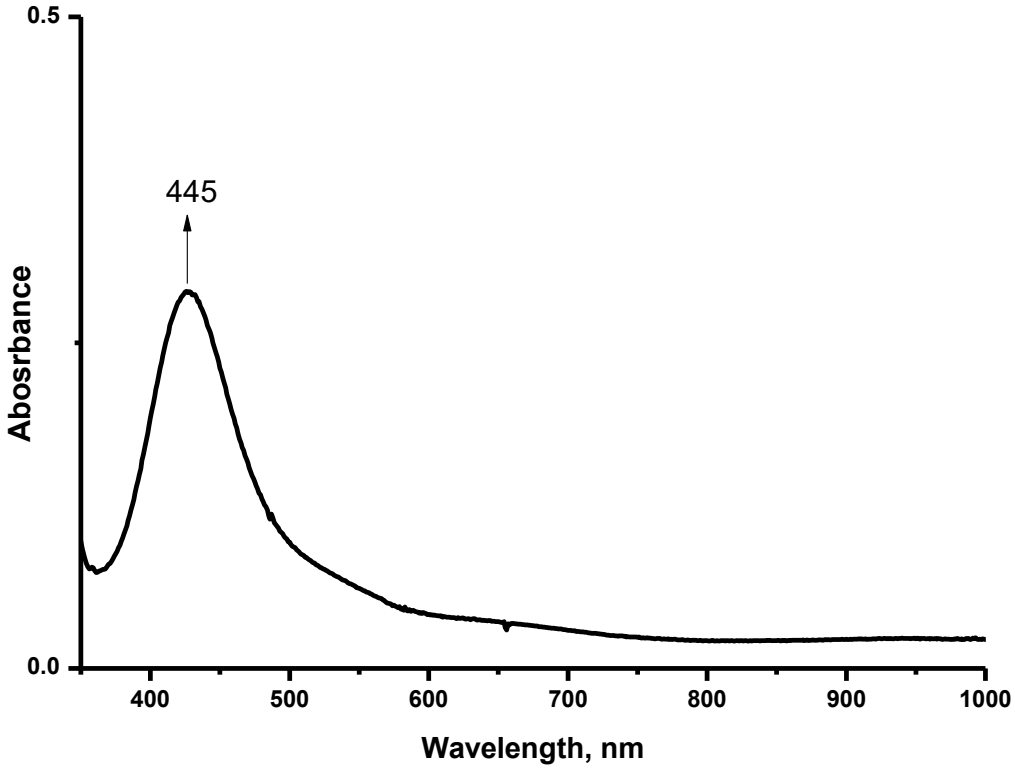


Figure 9x: UV/Visible spectrum of $Ru_2(OAc)_4Cl$ in MeOH

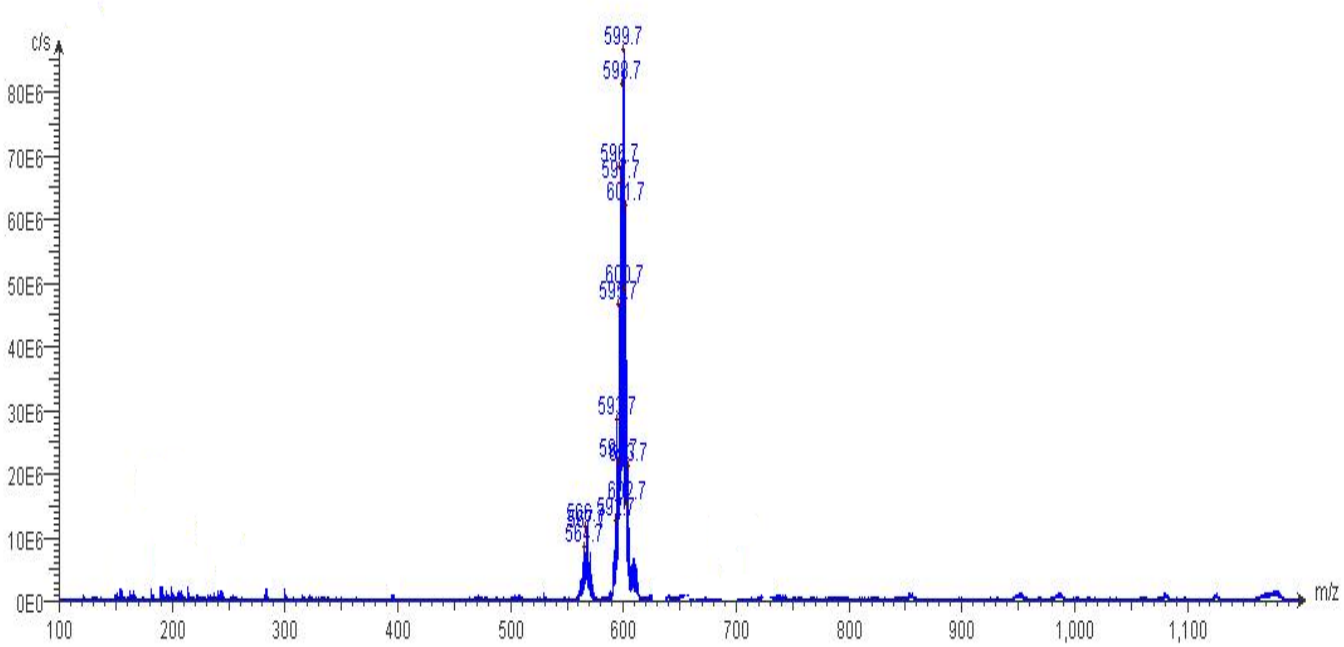


Figure 10x: Mass spectrum of $Ru_2(OAc)_3(2\text{-Fap})Cl$

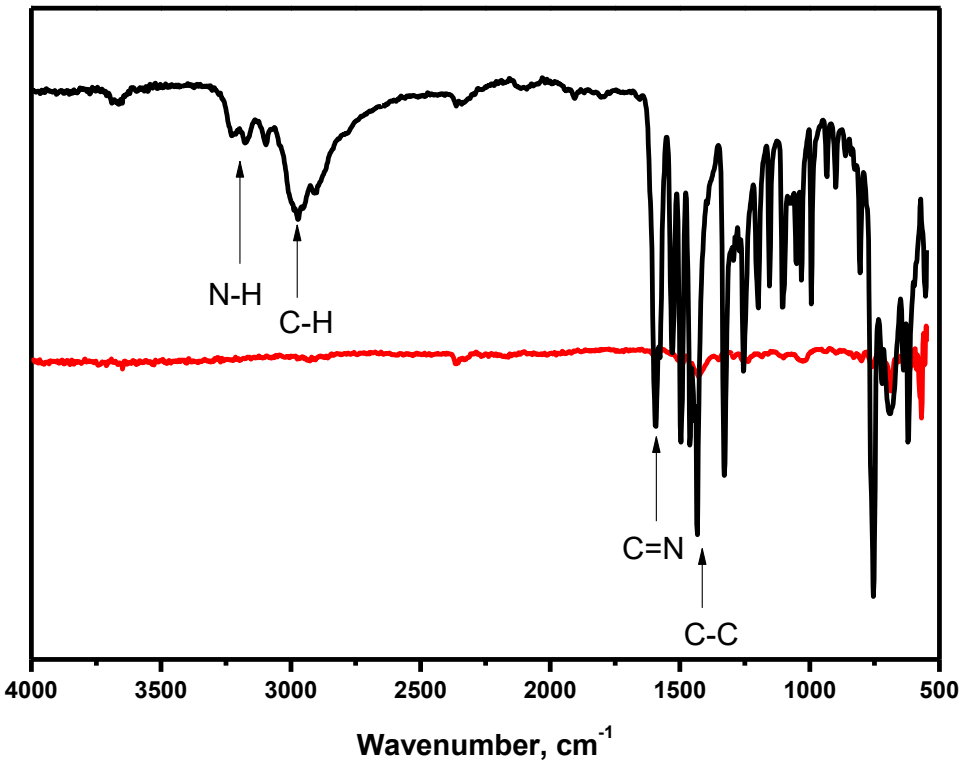


Figure 11x: FTIR spectrum of free ligand, H(2-Fap) and mixed-ligand diruthenium complex, $Ru_2(OAc)_3$(2-Fap)Cl.

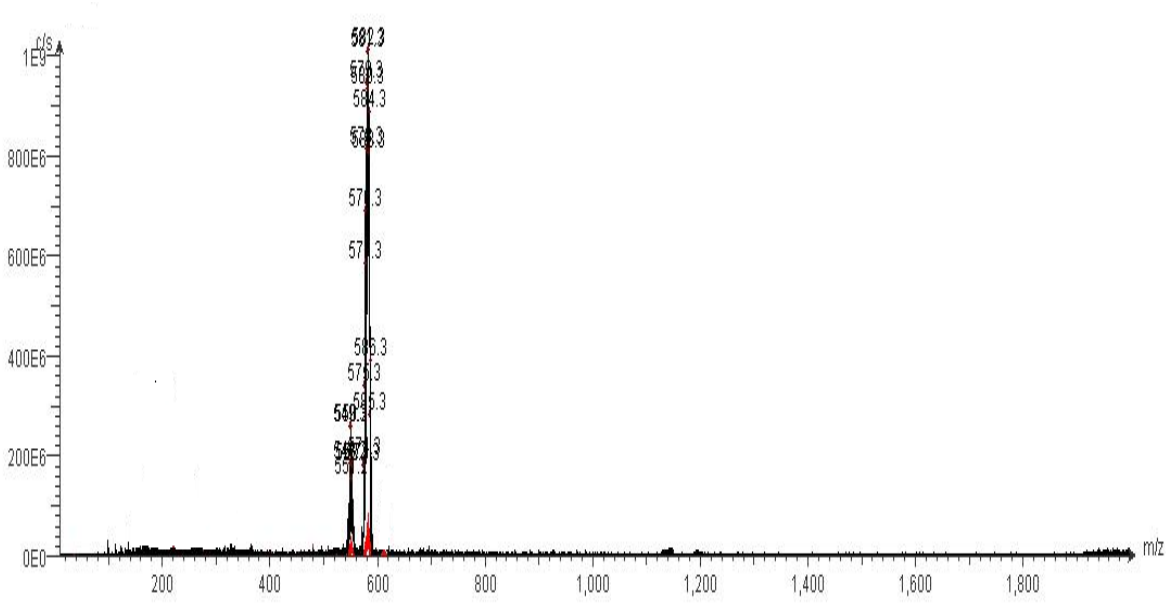


Figure 12x: Mass spectrometry of $Ru_2(OAc)_3$(ap)Cl

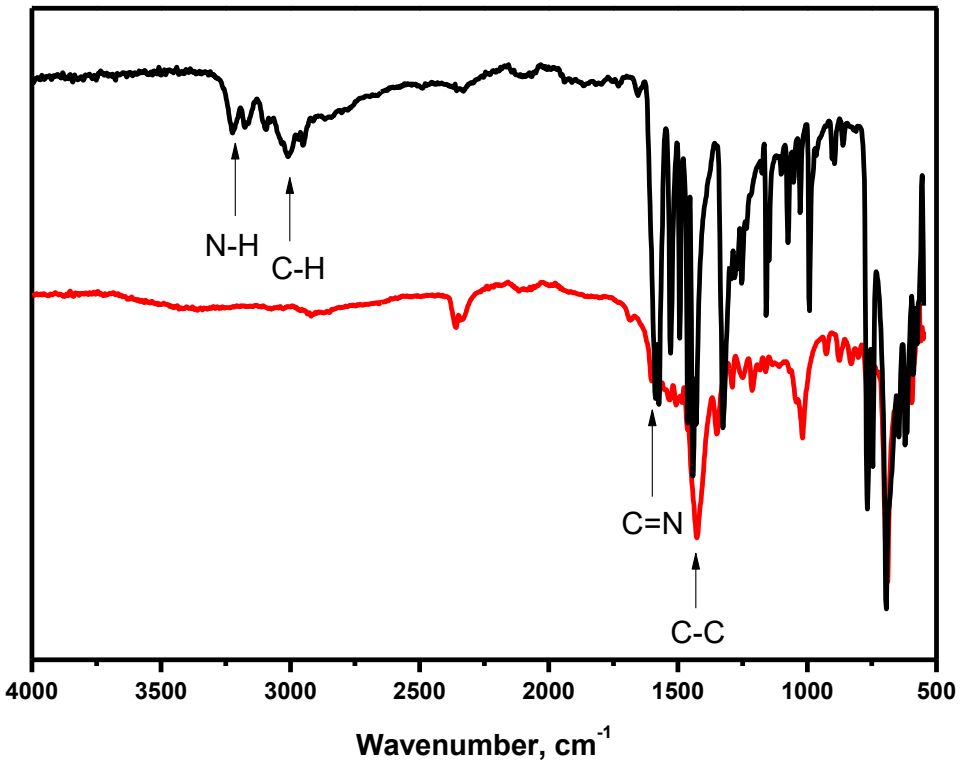


Figure 13x: FTIR spectra of free ligand, Hap and mixed-ligand diruthenium complex, $Ru_2(OAc)_3(ap)Cl$.

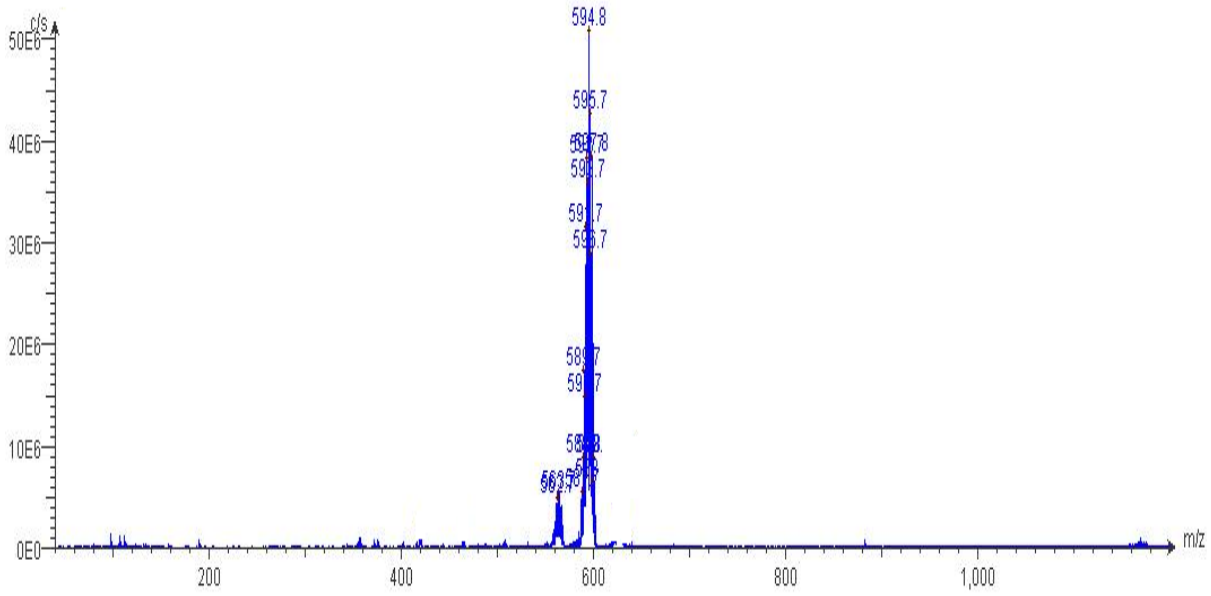


Figure 14x: Mass spectrum of $Ru_2(OAc)_3(2\text{-}Meap)Cl$.

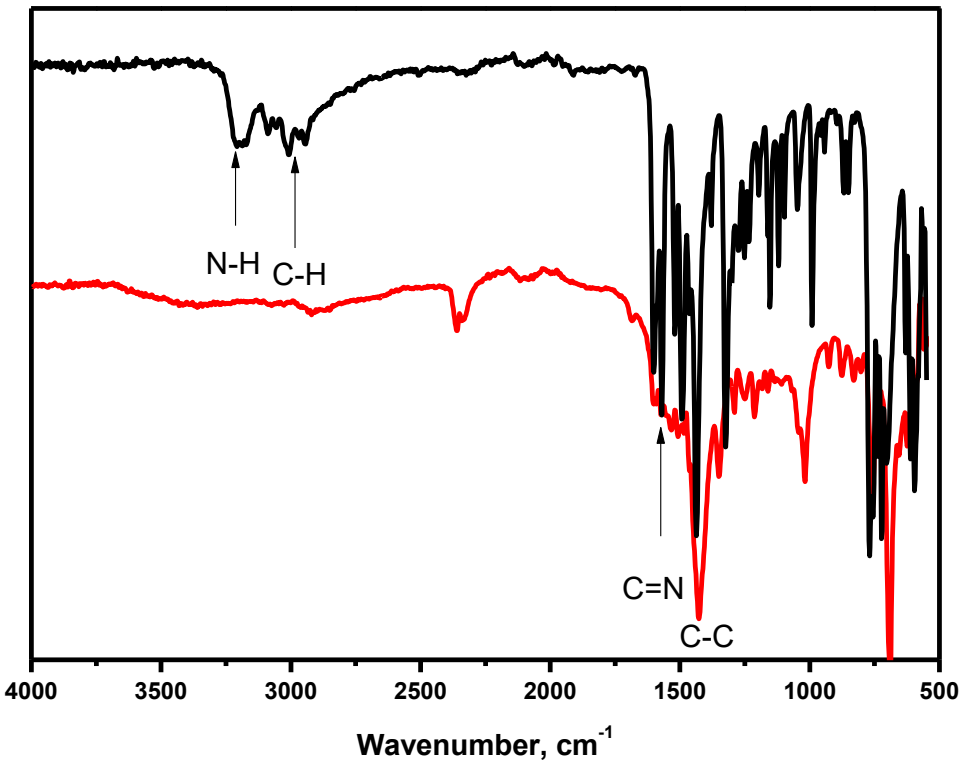


Figure 15x: FTIR spectrum of free ligand, H(2-Meap) and mixed-ligand diruthenium complex, $Ru_2(OAc)_3$(2-Meap)Cl.